Copy No. 121
RM No. L6J18a

~~CONFIDENTIAL~~

5-31-79

TECH LIBRARY KAFB, NM
0134900

# RESEARCH MEMORANDUM

## LOW-SPEED WIND-TUNNEL TESTS OF A PILOTLESS AIRCRAFT HAVING HORIZONTAL AND VERTICAL WINGS AND CRUCIFORM TAIL

By

N. Mastrocola and A. Assadourian

Langley Memorial Aeronautical Laboratory
Langley Field, Va.

~~CONFIDENTIAL~~

This document contains classified information affecting the National Defense of the United States within the meaning of the Espionage Act, USC 50:31 and 32. Its transmission or the revelation of its contents in any manner to an unauthorized person is prohibited by law. Information so classified may be imparted only to persons in the military and naval services of the United States, appropriate civilian officers and employees of the Federal Government who have a legitimate interest therein and to United States citizens of known loyalty and discretion who of necessity must be informed thereof.

## NATIONAL ADVISORY COMMITTEE FOR AERONAUTICS

WASHINGTON

August 19, 1947

~~CONFIDENTIAL~~

RM L6J18a
7072
21.1.18/.3

TECH LIBRARY KAFB, NM
0143900

NACA RM No. L6J18a ~~CONFIDENTIAL~~

NATIONAL ADVISORY COMMITTEE FOR AERONAUTICS

RESEARCH MEMORANDUM

# LOW-SPEED WIND-TUNNEL TESTS OF A PILOTLESS AIRCRAFT HAVING HORIZONTAL AND VERTICAL WINGS AND CRUCIFORM TAIL

By N. Mastrocola and A. Assadourian

## SUMMARY

Low-speed tests of a pilotless aircraft were conducted in the Langley propeller-research tunnel to provide information for the estimation of the longitudinal stability and control, to measure the aileron effectiveness, and to calibrate the radome and the Machmeter pitot-static orifices.

It was found that the model possessed a stable variation of elevator angle required for trim throughout the speed range at the design angle of attack. A comparison of the airplane with and without JATO units and with an alternate rocket booster showed that a large loss in longitudinal stability and control resulting from the addition of the rocket booster to the aircraft was sufficient to make the rocket-booster assembly unsatisfactory as an alternate for the JATO units.

Reversal of the aileron effectiveness was evident at positive deflections of the vertical wing flap indicating that the roll-stabilization system would produce rolling moments in a tight right turn contrary to its design purpose.

Vertical-wing-flap deflections caused large errors in the static-pressure reading obtained by the original static-tube installation. A practical installation point on the fuselage was located which should yield reliable measurement of the free-stream static pressure.

## INTRODUCTION

Low-speed wind-tunnel tests of a pilotless aircraft having horizontal and vertical wings and a cruciform tail were made at the Langley propeller-research tunnel. These tests were made to provide information for the estimation of the longitudinal stability and control, to measure the aileron effectiveness, and to calibrate the radome and the Machmeter pitot-static orifices.

The aircraft, powered by rockets located in the tail, is designed so that a Machmeter regulates the rocket thrust to maintain the flight speed at a Mach number of approximately 0.85. The airplane is intended to fly at zero angle of attack relying on pressure differentials set up at the radome orifices to effect proper changes in the control surfaces. The cruciform-tail control surfaces fulfill the function of both rudder and elevator. The horizontal wing flaps are used to provide lift control, whereas the vertical wing flaps are utilized for turns. Ailerons are also provided for roll stabilization.

The tests reported herein provide information for the estimation of the longitudinal stability and control of the model with and without JATO units. Similar tests were performed with a rocket-booster assembly as an alternate for the JATO units. Data are presented for tests made to evaluate the effects of components of the aircraft. Data relative to the aileron effectiveness, radome pressure-orifices calibration, and Machmeter pitot-static orifices calibration are also presented.

## SYMBOLS

$C_L$ lift coefficient $\left(\frac{L}{q_o S}\right)$

$C_D$ drag coefficient $\left(\frac{D}{q_o S}\right)$

$C_m$ pitching-moment coefficient with moment center at pivot point $\left(\frac{M}{q_o Sc}\right)$

$C_{m_{c.g.}}$ pitching-moment coefficient with moment center at design c.g. of configuration $\left(\frac{M_{c.g.}}{q_o Sc}\right)$

$C_l$ rolling-moment coefficient $\left(\frac{L'}{q_o Sb}\right)$

$C_{h_{f_H}}$ horizontal-wing-flap hinge-moment coefficient $\left(\frac{H}{q_o b_f c_f^2}\right)$

$\frac{p - p_o}{q_o}$ static-pressure coefficient

$\frac{H - p_o}{q_o}$ total-pressure coefficient

| | |
|---|---|
| $L$ | lift |
| $D$ | drag |
| $M$ | pitching moment about pivot point |
| $M_{c.g.}$ | pitching moment about design center of gravity of configuration (See table I.) |
| $L'$ | rolling moment |
| $H$ | hinge moment |
| $S$ | horizontal-wing area (10.9 sq ft) |
| $c$ | horizontal-wing chord (1.77 ft); also mean aerodynamic chord, M.A.C. |
| $b$ | horizontal-wing span (6.17 ft) |
| $b_f$ | horizontal-wing-flap span, total for two, (54.85 in.) |
| $c_f$ | horizontal-wing-flap chord (4.24 in.) |
| $q_o$ | free-stream dynamic pressure |
| $p_o$ | free-stream static pressure |
| $H$ | local total pressure |
| $p$ | local static pressure |
| $\alpha$ | angle of attack of fuselage center line, degrees |
| $\delta_{f_H}$ | horizontal-wing-flap deflection, positive when trailing edge is deflected downward, degrees |
| $\delta_{f_V}$ | vertical-wing-flap deflection, positive when trailing edge is deflected to the left, degrees |
| $\delta_e$ | elevator deflection, positive when trailing edge is deflected downward, degrees |

## APPARATUS AND TESTS

The airplane as installed in an inverted position for testing in the propeller-research tunnel is shown in the photographs of

figure 1. Figure 2 presents a three-view drawing giving the principal dimensions and characteristics of the model. Although the JATO units and rocket-booster assembly were not tested together nor are they intended to be used in conjunction with one another, they are shown mounted simultaneously for illustrative purposes. The test model was a full-scale production aircraft stripped of its operational and propulsive equipment. The fuselage was of flush-riveted sheet aluminum-alloy construction and the wings were aluminum-alloy extrusions. The aircraft had a production finish for these tests.

Some details of the control surfaces are given in figures 3 and 4. No aerodynamic balance is incorporated in the design of either the wing flaps or elevators and the gaps were unsealed. The tail control surfaces were deflected only as elevators during all the tests reported herein. The ailerons, consisting to two small lifting surfaces retractable into the tips of the vertical wing (figs. 5(a) and 5(c)), incorporated an NACA 16-209 airfoil section set at an incidence of 4° to the wing chord with the nose of the aileron to the left. These ailerons are part of the roll-stabilizing system of the aircraft and extend individually to counteract any rolling disturbance.

The model was inverted during tests to obtain the range of angle of attack desired and supported in ball bearings at fuselage station 78.2 on a single strut affixed to the six-component balance system of the propeller-research tunnel. The motion of the model in pitch was restrained by a "nose" wire (fig. 1(a)) which was attached to a scale to measure pitching moment. A "tail" wire (fig. 1(c)) was used for the same purpose during tests with the rocket-booster assembly attached. A measure of the rolling moments during the aileron-effectiveness tests was obtained by the use of wires from the horizontal wing tips. (See fig. 1(d).) Horizontal-wing-flap hinge moments were measured with electrical strain gages installed on the control linkages; excessive friction in the tail-surface bearings, however, prevented measurement of the elevator hinge moments.

Removal of the upper vertical wing during all tests was necessitated by mounting exigencies and the wing attachment fittings were covered with suitable fairings.

Pitot and static tubes were provided with the model (fig. 5); the pitot in the lower vertical wing and the static in the upper vertical wing. Since the upper vertical wing was removed during these tests, the static orifice was tested by replacing the lower with the upper vertical wing (aileron-effectiveness tests were also made with the model in this condition). The flush static-tube exit, modified to extend 1 inch aft of wing trailing edge (fig. 5(c)), was tested in an attempt to reduce the effects of flap deflection on the static-pressure measurement. A survey was made for the same purpose

to locate a suitable fuselage static-pressure orifice on a longitudinal line 45° from the fuselage-wing intersection.

To avoid separation that would occur in the absence of the rocket jet, due to the blunt fuselage tail, a fuselage tail cone (fig. 1) was installed.

The radome consists of four flush static orifices mounted on the nose of the fuselage. The distribution of the orifices which are part of the angle-of-attack control mechanism is indicated in figure 2.

A summary of the tests, all of which were made at a tunnel airspeed of approximately 100 miles per hour, is given in table I. The range of variables tested is as follows: angle of attack, $-6°$ to $10°$; wing-flap angle, $-55°$ to $55°$; and elevator angle, $-20°$ to $20°$.

## RESULTS AND DISCUSSION

The test data, corrected for jet-boundary and tare drag effects, are plotted as nondimensional coefficients based on a mean aerodynamic chord of 1.77 feet, a wing area of 10.90 square feet, and a wing span of 6.17 feet. Sign conventions relative to forces, moments, and surface deflections used throughout this report are given in figure 6 and apply to the model in the upright attitude. Throughout the following discussion, the model and its components are always referred to in the upright attitude.

### Longitudinal Stability and Control

In the following sections, data are presented for the estimation of the longitudinal stability and control of the airplane with and without JATO units. Similar data are presented for a rocket-booster assembly as an alternate to the JATO units.

Pitching-moment coefficients are presented about the pivot point and also about the design center of gravity for each configuration. (See fig. 2.) Faired values of $C_m$, $C_L$, and $C_D$ were used in the transfer of pitching moments to the center of gravity.

Because all tests were made with the upper vertical wing removed, a wing-tare test was made with the lower vertical wing in place and removed in order to evaluate the effects of one-half of the vertical wing on the aerodynamic characteristics. These data, presented in

figure 7, indicate that the lower vertical wing had practically no effect on the pitching-moment-coefficient curve but increased the drag coefficient by an amount ranging from 0 to 0.03. The drag-coefficient increment resulting from the absence of the upper vertical wing during all tests has not been corrected for since there does not appear to be a consistent variation of the increment with angle of attack or flap deflection.

Addition of the lower vertical wing produced a small increase of the lift coefficient for all flap angles and angles of attack. (See fig. 7(a).) It is uncertain, however, as to whether the increase in lift would be lost or doubled with both vertical wings in place, since the phenomena inducing the increase are not understood. For this reason and because the lift-coefficient increments are of the same magnitude as the test-point scatter, the lift data presented herein have not been corrected for the absence of the upper vertical wing during this investigation.

Complete model.- The aerodynamic characteristics of the airplane are shown in figures 8, 9, 10, and 11 for several horizontal-wing-flap and elevator deflections. (Several curves and test points were omitted when they were considered to be inconsistent with other results.) Several significant aerodynamic characteristics were determined from these data at the condition $\alpha = 0^\circ$, $\delta_{f_H} = 0^\circ$, and $\delta_e = 0^\circ$ and are tabulated below:

| | |
|---|---|
| Slope of lift curve, $dC_L/d\alpha$, figure 8(c) | 0.060 |
| Drag coefficient (minimum), figure 9(e) | 0.030 |
| Slope of pitching-moment curve, $dC_{mc.g.}/dC_L$ figure 11(c) | -0.36 |
| Elevator effectiveness, $dC_m/d\delta_e$, figure 10(c) | -0.039 |
| Horizontal-wing-flap effectiveness, $dC_L/d\delta_{f_H}$, figure 8(c) | 0.012 |

These characteristics, with the exception of drag coefficient, are essentially unaffected by horizontal-wing-flap or elevator deflection.

The variation of elevator deflection required for trim with lift coefficient for various horizontal-wing-flap deflections is shown in figure 12. A stable variation of elevator deflection is indicated throughout the speed range except for the highest lift coefficient with $\delta_{f_H} = 55^\circ$ where the slope is zero. It is also noted that the higher flap deflections ($\delta_{f_H} = \pm 55, 45$) tend to decrease the stable variation.

Model with JATO units.- Lift, drag, pitching-moment, and horizontal-wing-flap hinge-moment coefficients obtained with the JATO units attached

are presented in figure 13 as a function of angle of attack with horizontal-wing-flap deflection as a parameter at $\delta_e = 0^\circ$. Pitching-moment coefficients, transferred to the design center of gravity with two loaded JATO units, are presented in figure 14 plotted against lift coefficient.

A comparison of these data with those of figures 8, 9, 10, and 11 indicates that the addition of the JATO units to the airplane (at $\alpha = 0^\circ$ and $\delta_{f_H} = 0^\circ$) causes a decrease of 0.002 in the lift-curve slope, a decrease of 0.002 in the horizontal-wing-flap effectiveness and an increase of 0.048 in the minimum drag coefficient. The slope of the pitching-moment-coefficient curve $dC_{m_{c.g.}}/dC_L$ is also reduced from 0.36 to 0.14.

The value of $dC_{h_{f_H}}/d\delta_{f_H}$ measured at $\alpha = 0^\circ$ (fig. 13(c)) is $-0.0076$ with $dC_{h_{f_H}}/d\alpha$ at $\alpha = 0^\circ$ varying from 0.006 at $\delta_{f_H} = 0^\circ$ to $-0.0025$ at $\delta_{f_H} = 30^\circ$ and $-0.0020$ at $\delta_{f_H} = 55^\circ$. These values are in general agreement with those expected from a plain unbalanced control surface.

Model with rocket-booster assembly.- The results for the model with the rocket-booster assembly attached are given in figure 15, while data with the moment center transferred to the design center of gravity (251.4-percent mean aerodynamic chord aft of wing leading edge) are presented in figure 16.

A comparison of the data with rocket-booster installed, for $\alpha = 0^\circ$, $\delta_e = 0^\circ$, and $\delta_{f_H} = 0^\circ$, with those for the model with and without JATO units is given in the following table:

| | Without JATO or rocket booster | With JATO unit | With rocket booster |
|---|---|---|---|
| $dC_L/d\alpha$ | 0.060 | 0.058 | 0.064 |
| $C_D$ (minimum) | .030 | .078 | .234 |
| $dC_{m_{c.g.}}/dC_L$ | −.36 | −.14 | .36 |
| $dC_m/d\delta_e$ | −.039 | ---- | 0 |
| $dC_L/d\delta_{f_H}$ | .012 | .010 | .002 |

In view of the large loss in longitudinal stability and control resulting from the addition of the rocket-booster assembly, it is evident that the booster is aerodynamically unsatisfactory as an alternate for the JATO units.

The curves of pitching-moment coefficient about the design center of gravity (fig. 16) indicate an unstable variation is obtained for low and negative lift coefficients. This instability is mainly a result of the extreme rearward position of the center of gravity.

The horizontal-wing-flap effectiveness, the effect of flap deflection on trim, and the elevator effectiveness for the model with the rocket booster are compared to other model configurations in figures 17, 18, and 19, respectively. The decrease in wing-flap effectiveness caused by the rocket booster (fig. 17) is a result of adverse load on the large area of the rocket-booster assembly which is produced by the downwash from the wing. This effect not only reduces the flap effectiveness but also introduces large trim changes when the flaps are deflected. (See fig. 18.) The large decrease in elevator effectiveness (fig. 19) results from the adverse pitching moments produced by the downwash aft of the tail. This loss in elevator effectiveness combined with the excessive trim changes made it impossible to trim the aircraft with booster attached except possibly for small horizontal-wing-flap deflections.

Because of model symmetry the pitching-moment coefficient with the booster attached at $\alpha = 0$, $\delta_e = 0$, and $\delta_{f_H} = 0$ would be expected to be zero; however, the results in figure 16 show a large pitching-moment coefficient in this condition. It is believed that the method of model support and the relatively weak rocket-booster attachment fitting resulted in asymmetry between the model and booster.

## Effects of Components

Model with tail removed.- The aerodynamic characteristics of the model with the vertical wing and tail assembly removed are given in figure 20 for several horizontal-wing-flap deflections. These data for $\delta_{f_H} = 0^\circ$ are replotted in figure 21 to show the contribution of the tail to the aerodynamic characteristics. The data for the configuration with wings and tail removed are also presented in this figure for comparison. The tail assembly contributes an increase of 0.007 to the lift-curve slope and a decrease of 0.045 to the pitching-moment curve slope ($dC_m/d\alpha$).

The role of the tail in reducing the trim changes resulting from horizontal-flap deflection is indicated in figure 18. The downwash changes at the tail, which bring about this reduction in trim changes, also cause the over-all effectiveness of the wing flaps to be reduced. (See fig. 17.)

Effect of tail cone.- Lift, drag, and pitching-moment coefficients for the fuselage alone with and without the fuselage tail cone fairing (figs. 1(f) and 1(g)) are given in figure 22 as a function of angle of attack. These data indicate changes in the aerodynamic characteristics which would result when the main rocket power is expended. The most significant of these changes is the increase in minimum drag coefficient amounting to 0.015. There is no lift change but a slight decrease in instability.

## Aileron Effectiveness

Rolling-moment coefficients for various wing-flap and aileron deflection combinations are shown in figure 23. Aileron effectiveness, determined as the difference in rolling-moment coefficient with the aileron retracted and extended, is shown in figure 24 as a function of vertical-wing-flap angle. Since some difficulty was encountered in measuring these small values of aileron effectiveness, care should be exercised in the quantitative use of these data. Scatter of the test and check points (fig. 23) indicate an accuracy in rolling-moment coefficient of approximately $\pm 0.002$. Reversal of aileron effectiveness, however, is always evident at positive deflections of the vertical wing flap. This would indicate that the roll-stabilization system in a tight right turn would produce rolling moments contrary to its design purpose. A consideration of the flow at the wing tip as effected by the vertical wing flap provides a qualitative check of the data.

## Pitot-Static Calibration

The design purpose of the Machmeter is to regulate the aircraft speed by controlling the rocket thrust. It is important, therefore, that the Machmeter pitot-static tubes accurately measure the free-stream total and static pressures under all conditions.

Original installation.- Total-pressure coefficients obtained with the wing pitot tube are shown in figure 25 and the static-pressure coefficients obtained with the wing static tube are shown in figure 26. The total-head coefficient does not attain the full value of $q_0$ due to the slight variation of total head across the

tunnel air stream. The variation of total head with angle of attack, however, is less than 0.01 $q_o$.

It can be noted in figure 26 that the vertical-wing-flap deflections caused large undesirable changes in the static-pressure readings: from $-0.515\ q_o$ to $0.175\ q_o$ at $\alpha = 0^\circ$. Measurements made with the modified wing-static-tube exit (included in fig. 26) show that the modification did not sufficiently remove the exit from the influence of the vertical wing flap.

Fuselage static-pressure survey.- Because the original static-pressure orifice installation was shown to be unsuitable for its design purpose, a survey was made to locate a position on the fuselage which would yield a more reliable measure of the free-stream static pressure. The variation of static-pressure coefficient, measured at several fuselage stations, with angle of attack are shown in figure 27 for various combinations of vertical- and horizontal-flap deflections. The maximum variation of these pressure coefficients for the range of variables tested is given in figure 28 plotted against fuselage station. It is noted that the variation decreases as the distance forward of the wing increases, that is, as the influence of the wing and wing flaps decreases. The smallest maximum variation was observed at station 54.82 inches from the fuselage nose and is only 0.05 $q_o$, indicating that such a static-tube location would yield a fairly reliable measure of the free-stream static pressure under all conditions tested. With a view toward providing a practical installation point on the service aircraft, measurements were obtained at fuselage station 52.91 and are shown in figure 29. The maximum variation of static-pressure coefficient at this point, about 0.035 $q_o$, is in accord with the above and therefore should also yield reliable measurement of the free-stream static pressure.

Fuselage stations farther forward may provide still smaller maximum variations in static pressure readings. It appears, however, that the permissible distance is very limited because the radius of curvature of the fuselage is decreasing toward the nose.

## Radome Calibration

The calibration of the radome pressure orifices is given in figure 30(a) plotted against angle of attack and the pressure differential available for the angle-of-attack control mechanism is presented in figure 30(b). The curves are fairly linear. There is no apparent reason for the difference between the two curves of pressure differential; it is believed, however, that small manufacturing irregularities on the surface in the region of the orifices may be responsible.

## CONCLUSIONS

1. The airplane possesses a stable variation of elevator angle required for trim throughout the speed range at the design angle of attack.

2. The comparison of the model with and without JATO units and with the alternate rocket-booster assembly showed that the loss in longitudinal stability and control resulting from the addition of the booster to the aircraft is sufficient to make the rocket-booster assembly aerodynamically unsatisfactory as an alternate for the JATO units.

3. Reversal of the aileron effectiveness was evident at positive deflections of the vertical wing flap indicating that roll-stabilization system in a tight right turn would produce rolling moments contrary to its design purpose.

4. Vertical-wing-flap deflections caused large changes in the static-pressure reading obtained by the original static-tube installation.

5. A practical installation point on the fuselage at station 52.91 was located which should yield reliable measurement of the free-stream static pressure.

Langley Memorial Aeronautical Laboratory
National Advisory Committee for Aeronautics
Langley Field, Va.

TABLE I.- SUMMARY OF TESTS

~~CONFIDENTIAL~~

| Tests | Configuration | | | | | Variables | | | Center-of-gravity position, percent M.A.C. (2) | | Figure references |
|---|---|---|---|---|---|---|---|---|---|---|---|
| | Lower vertical wing | Horizontal wing | Tail assembly | JATO units | Rocket-booster assembly | Vertical wing flap angle (deg) | Horizontal-wing-flap angle (deg) | Elevator angle (deg) | Aft wing leading edge | Below fuselage $\bar{c}_L$ | |
| Wing tare | Off | On | On | Off | Off | ---- | -55 to 55 | 0 | ---- | ---- | 7 |
| Longitudinal stability and control | On | On | On | Off | Off | 0 | -55 to 55 | -20 to 20 | 19.8 | 0 | 8 through 12 |
| | On | On | On | On | Off | 0 | 0 to 55 | 0 | 19.8 | 16.7 | 13, 14 |
| | On | On | On | Off | On | 0 | 0 to 55 | -20 to 20 | 251.4 | 0 | 15, 16 |
| Contribution of components | Off | On | Off | Off | Off | ---- | -55 to 55 | ---- | 19.8 | 0 | 20 |
| | Off | Off | Off | Off | Off | ---- | ---- | ---- | 19.8 | 0 | 22 |
| Aileron effectiveness | (1) | On | On | Off | Off | -55 to 55 | -60 to 60 | 0 | ---- | ---- | 23, 24 |
| Pitot calibration | On | On | On | Off | Off | 0 | 0 | 0 | ---- | ---- | 25 |
| Static calibration | (1) | On | On | Off | Off | -60 to 60 | 0 | 0 | ---- | ---- | 26 through 29 |
| Radome calibration | On | On | On | Off | Off | 0 | 0 | 0 | ---- | ---- | 30 |

~~CONFIDENTIAL~~

[1]Lower vertical wing replaced with upper vertical wing.
[2]Center-of-gravity position given is furthest aft for each configuration.

NATIONAL ADVISORY
COMMITTEE FOR AERONAUTICS

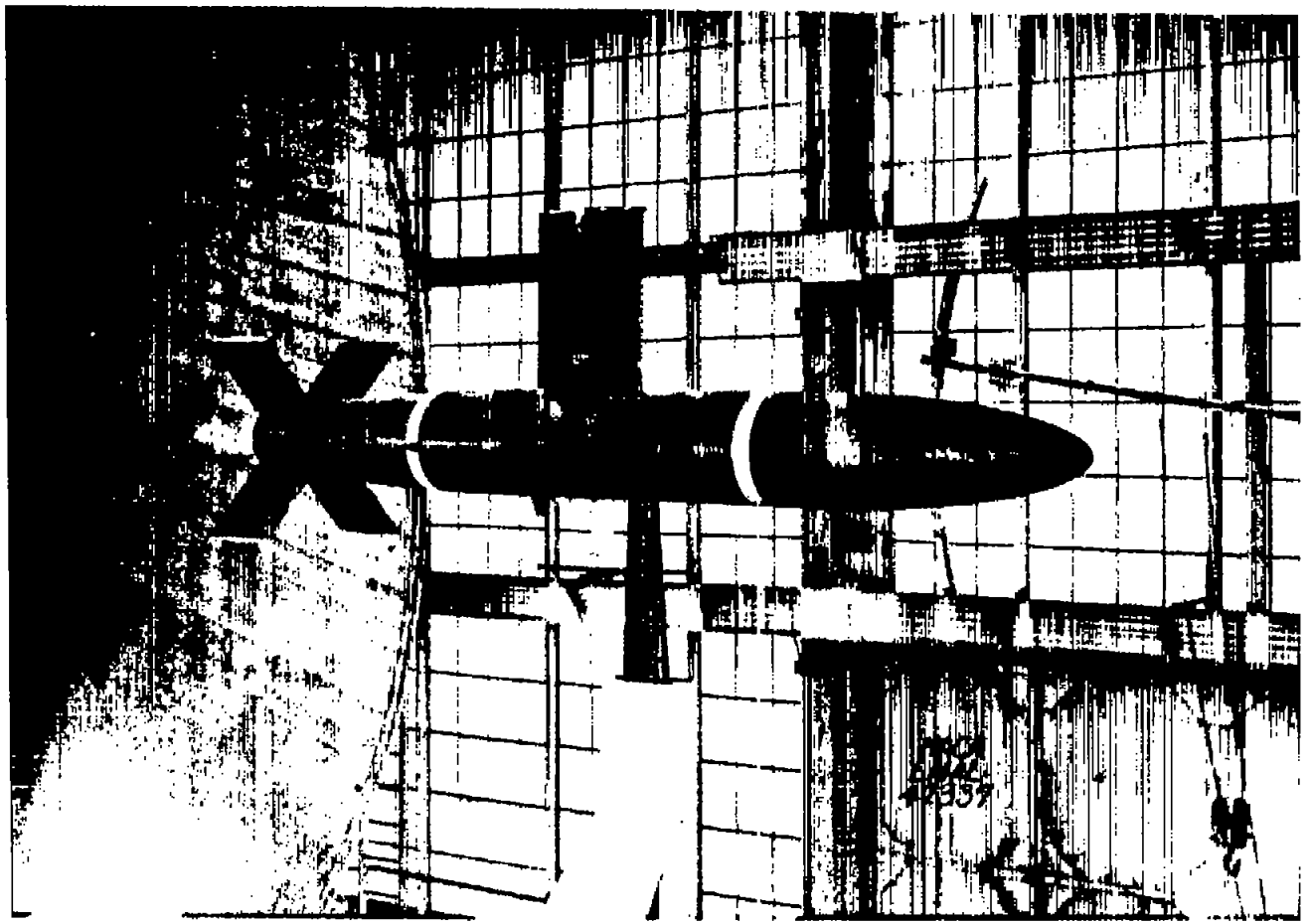



(a) Complete model.

Figure 1.- The airplane mounted in the Langley propeller-research tunnel, inverted and with the upper vertical wing removed.

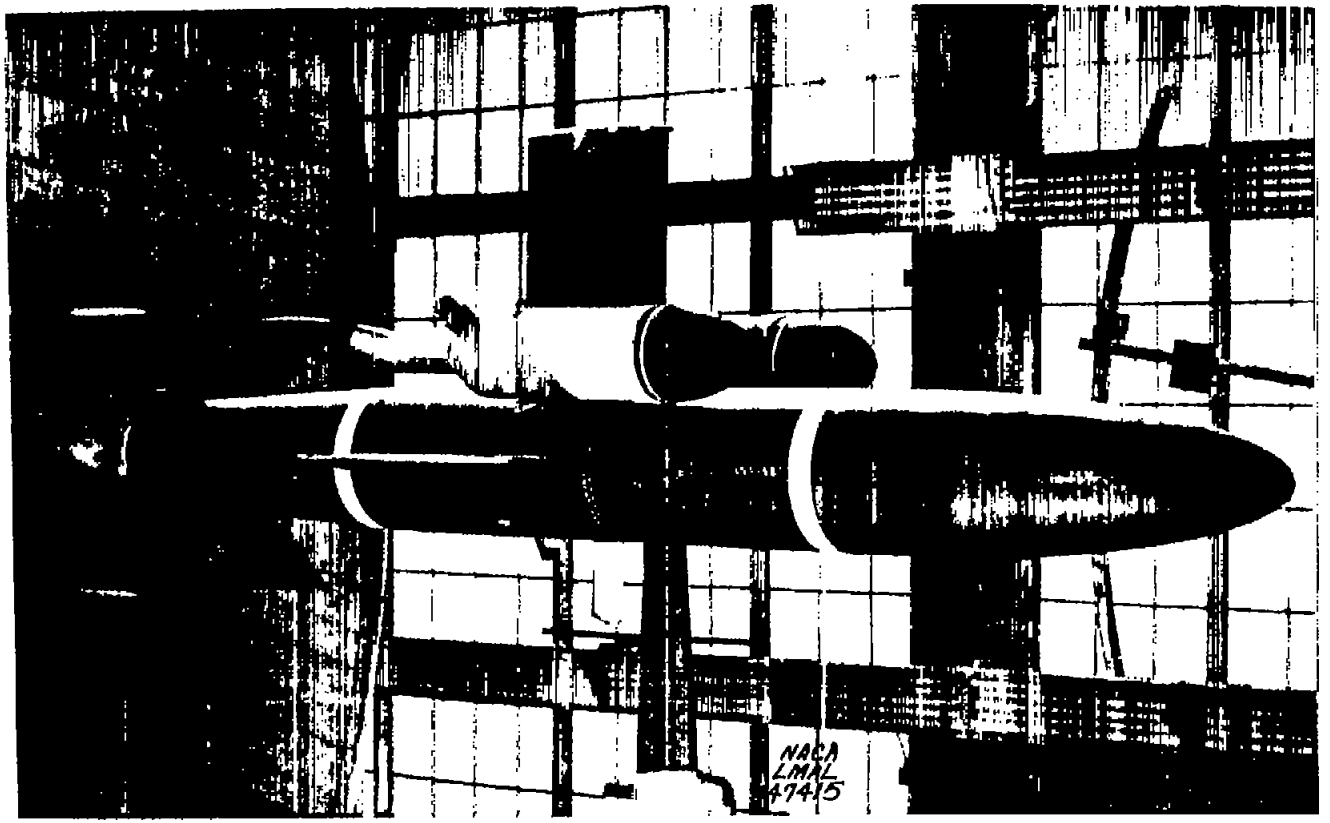


(b) JATO units attached.



Figure 1.- Continued.

CONFIDENTIAL

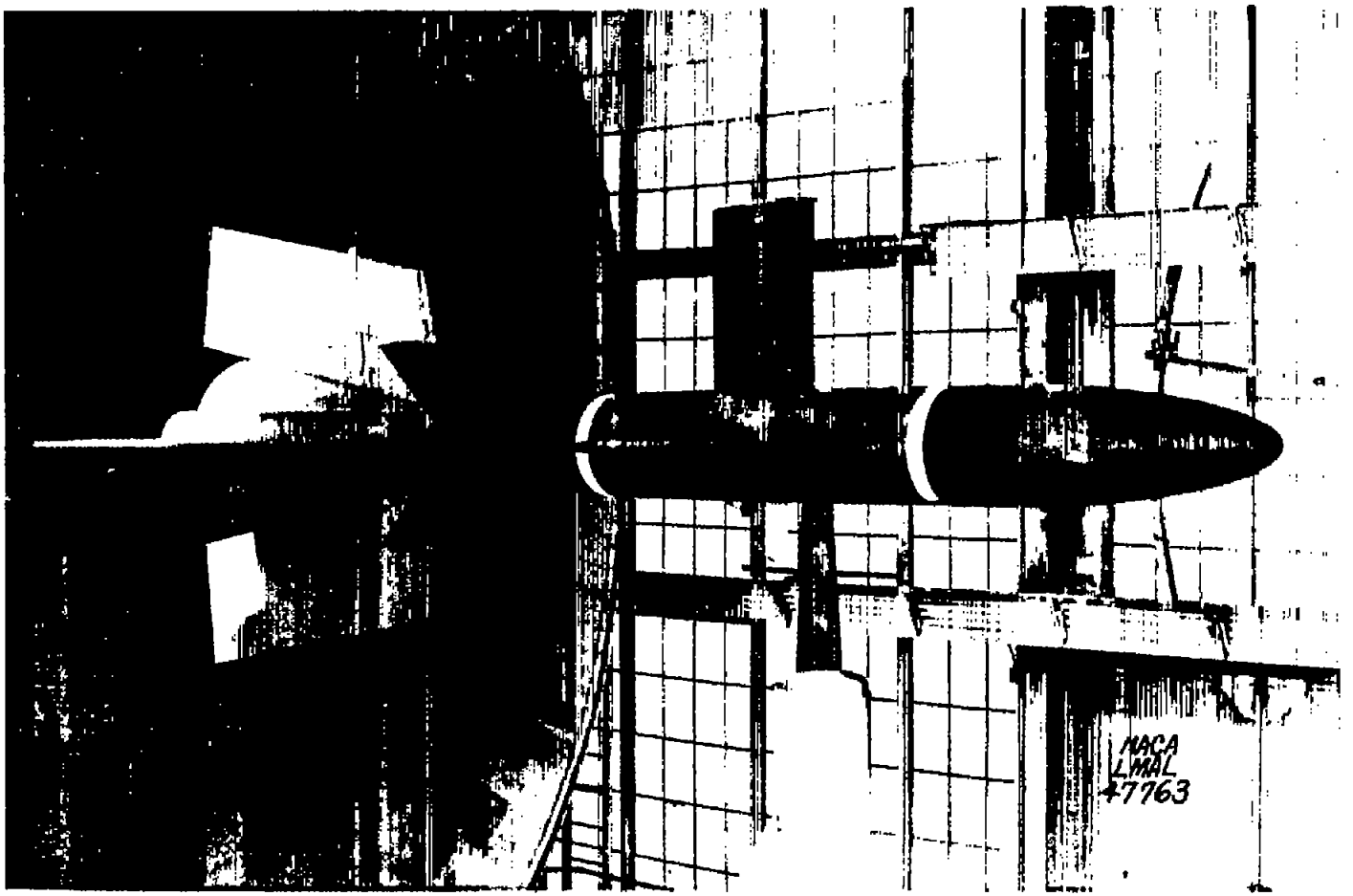


CONFIDENTIAL

(c) Rocket-booster assembly attached.

Figure 1.- Continued.

Fig. 1d

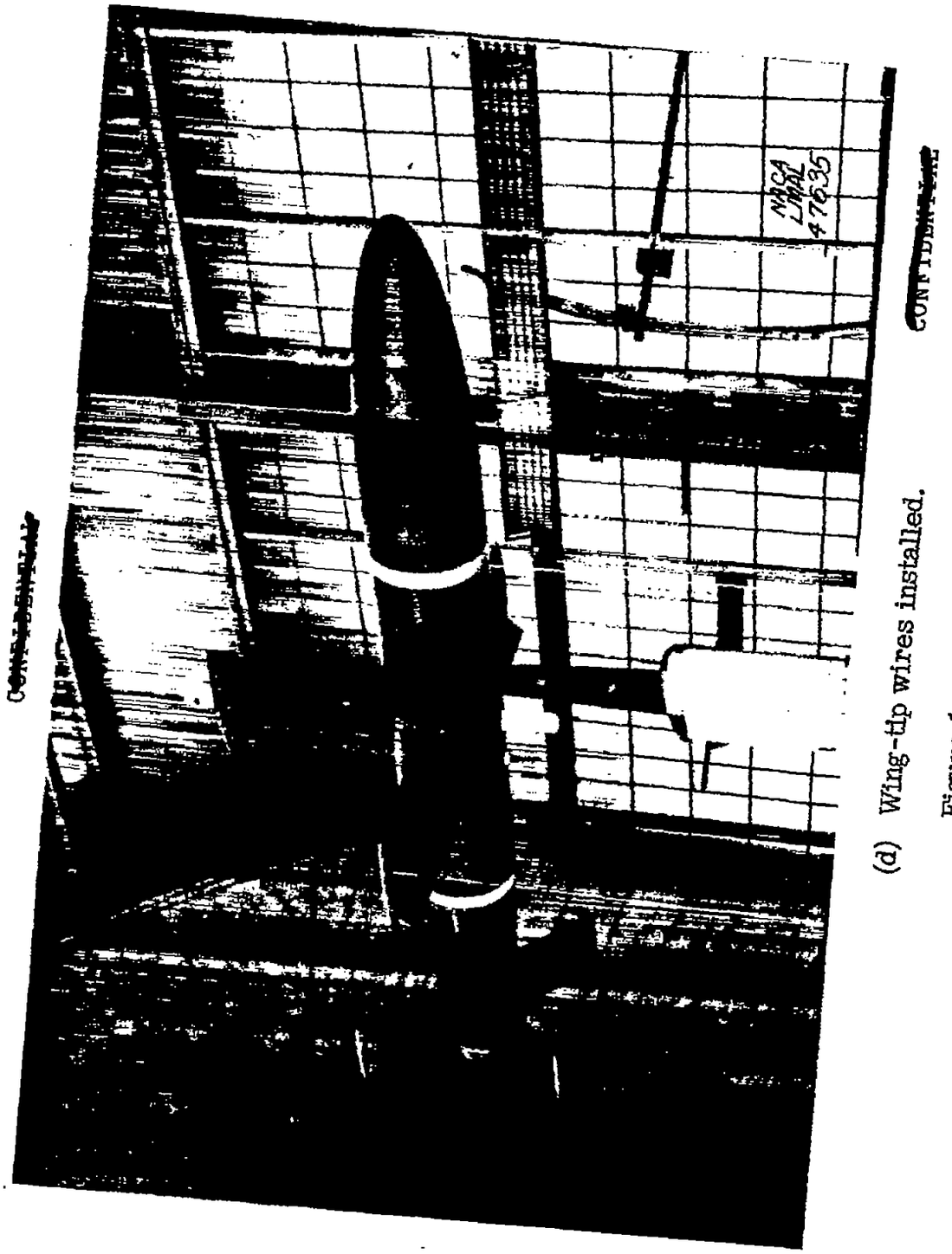


(d) Wing-tip wires installed.

Figure 1.- Continued.

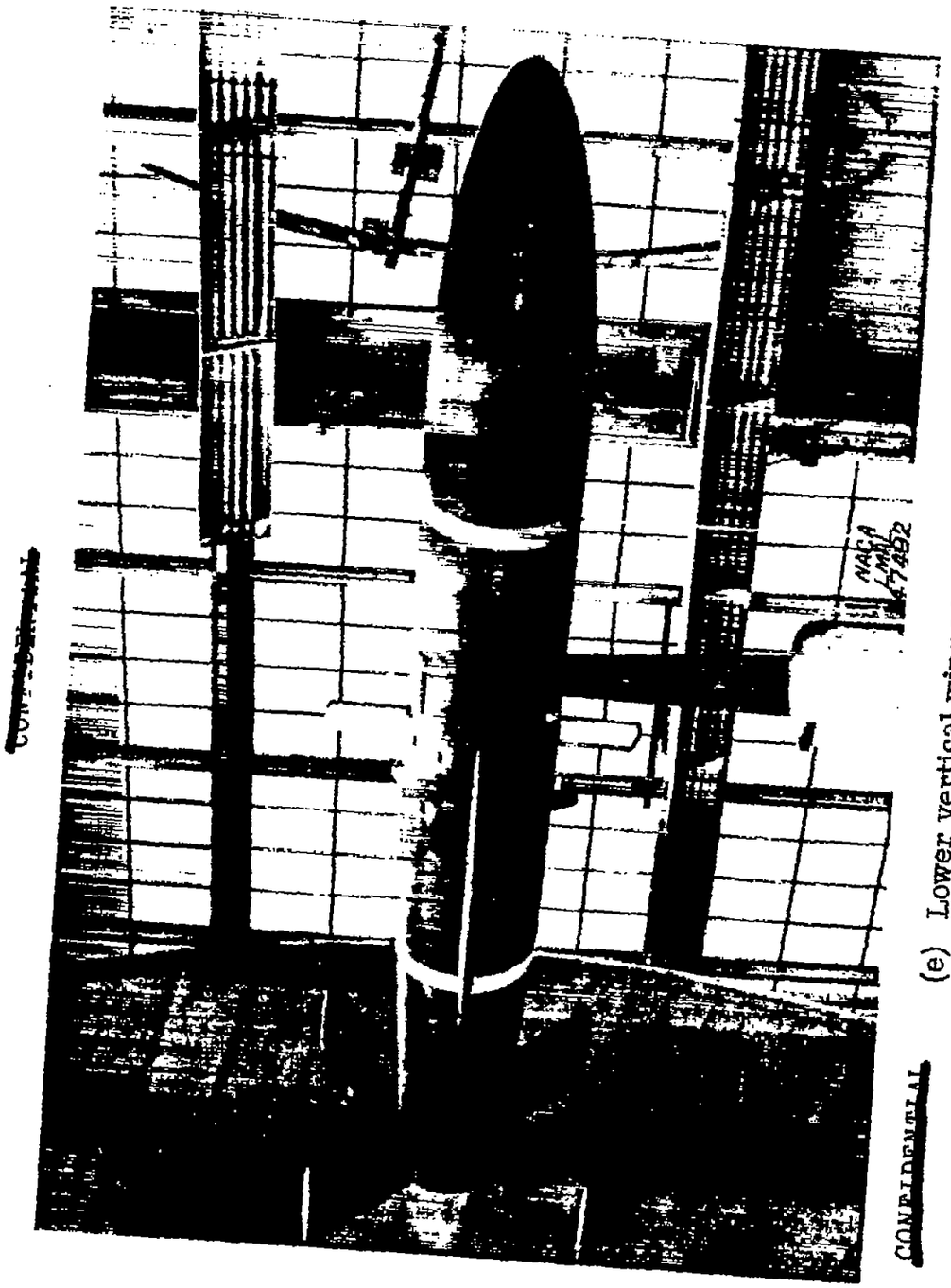


(e) Lower vertical wing removed.

Figure 1.- Continued.

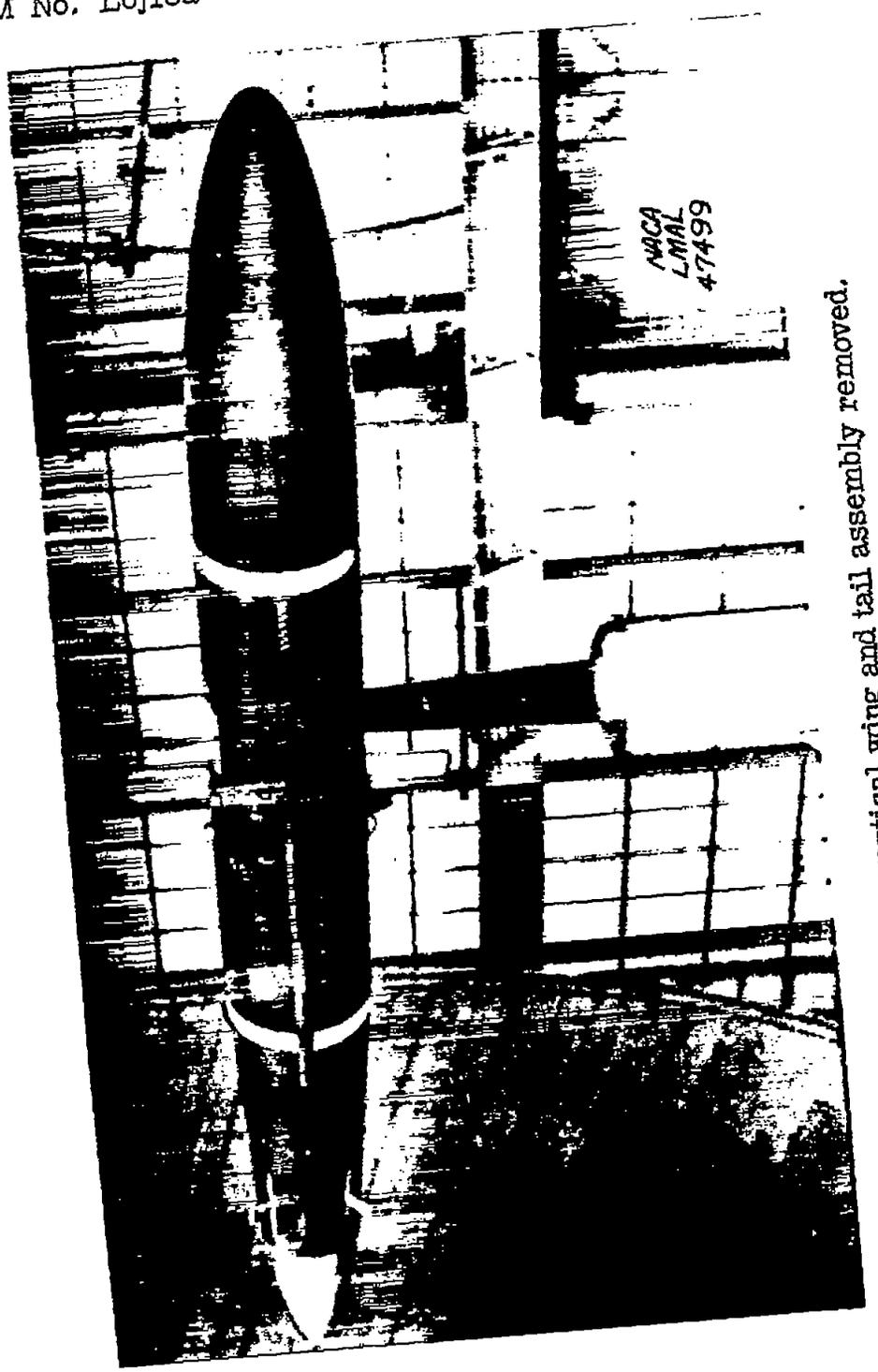


(f) Lower vertical wing and tail assembly removed.

Figure 1.- Continued.

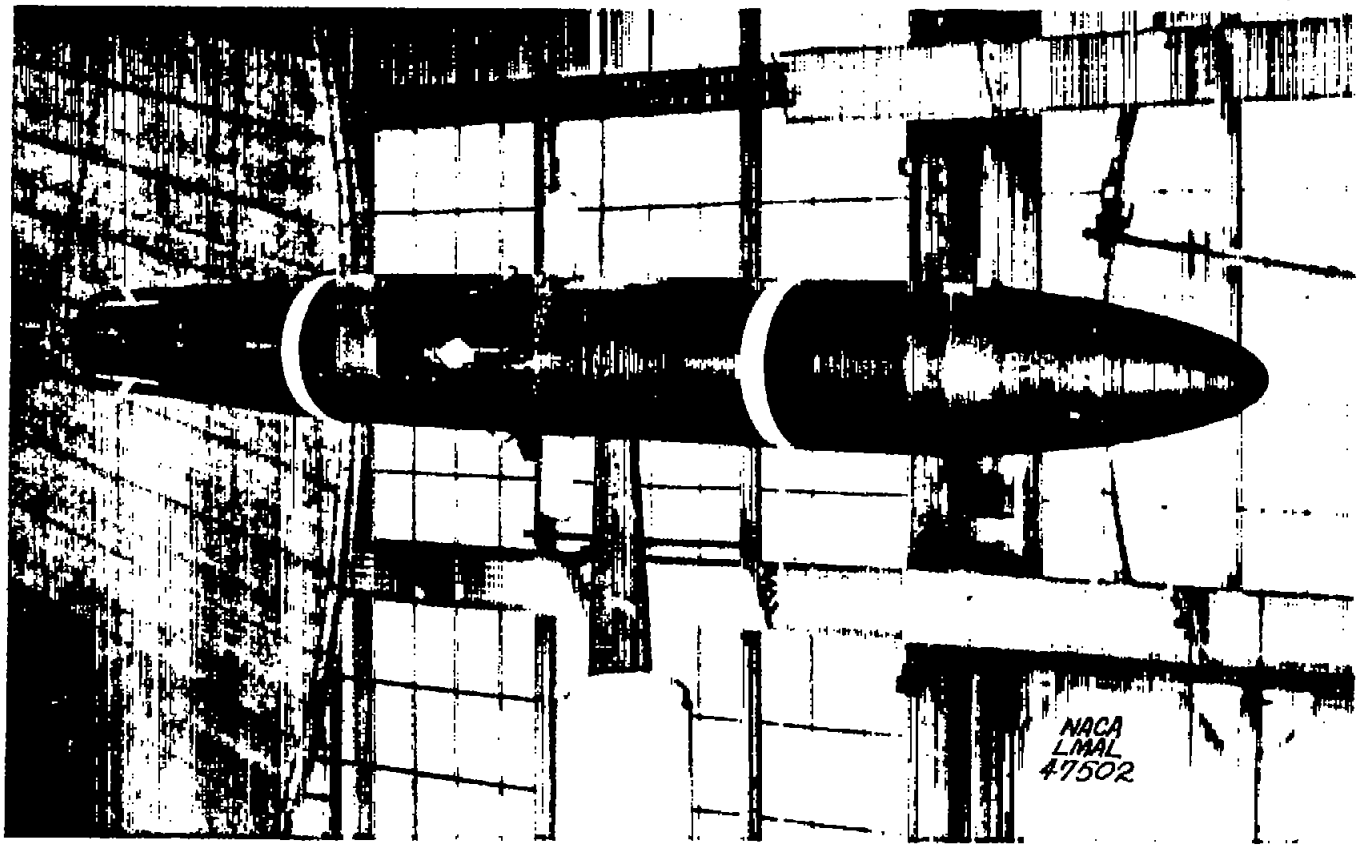


(g) Lower vertical wing, horizontal wing, tail assembly, and fuselage tail cone removed (fuselage alone).

Figure 1.- Concluded.

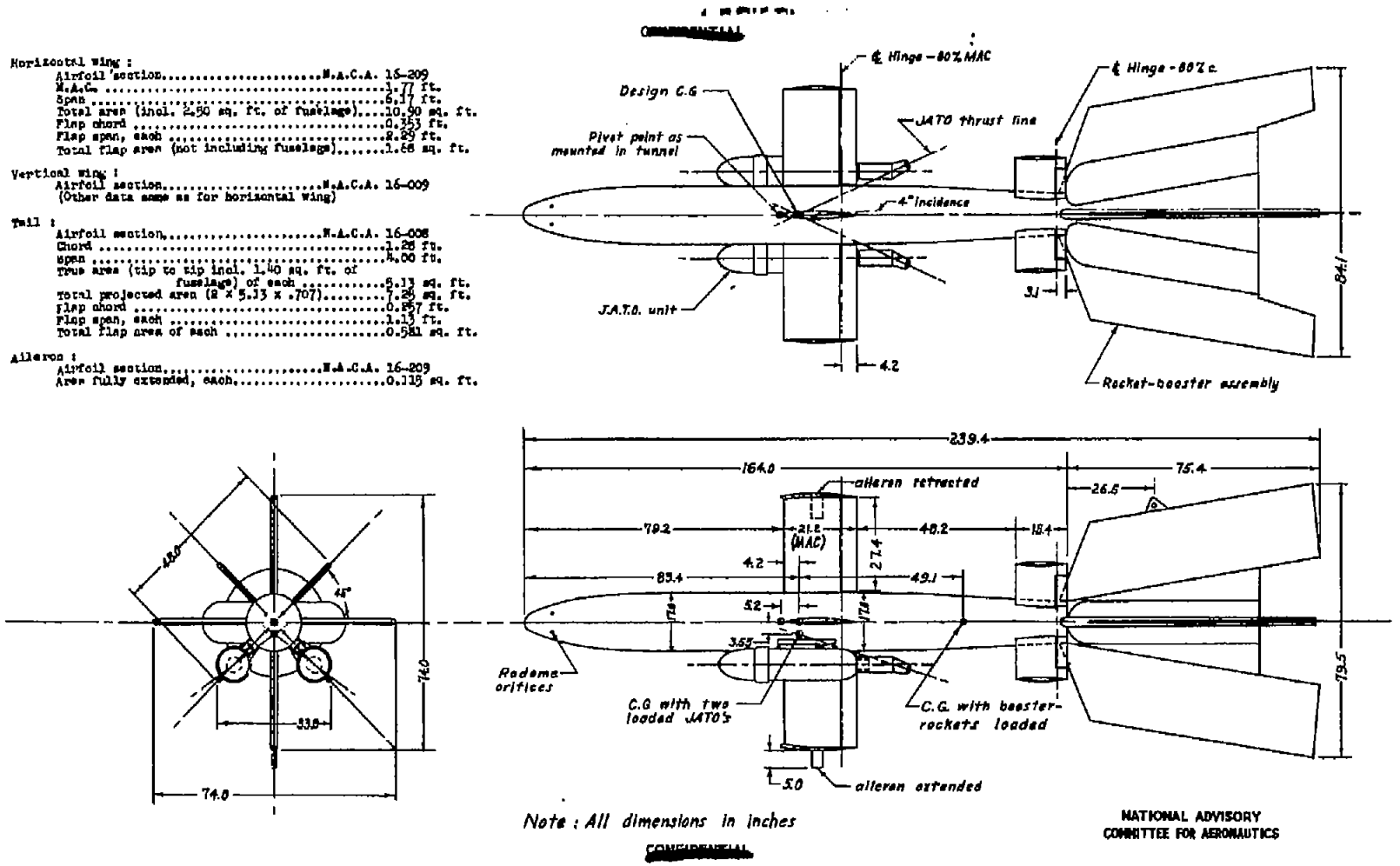


Figure 2.- Principal dimensions and general arrangement of the airplane used in the present investigation.

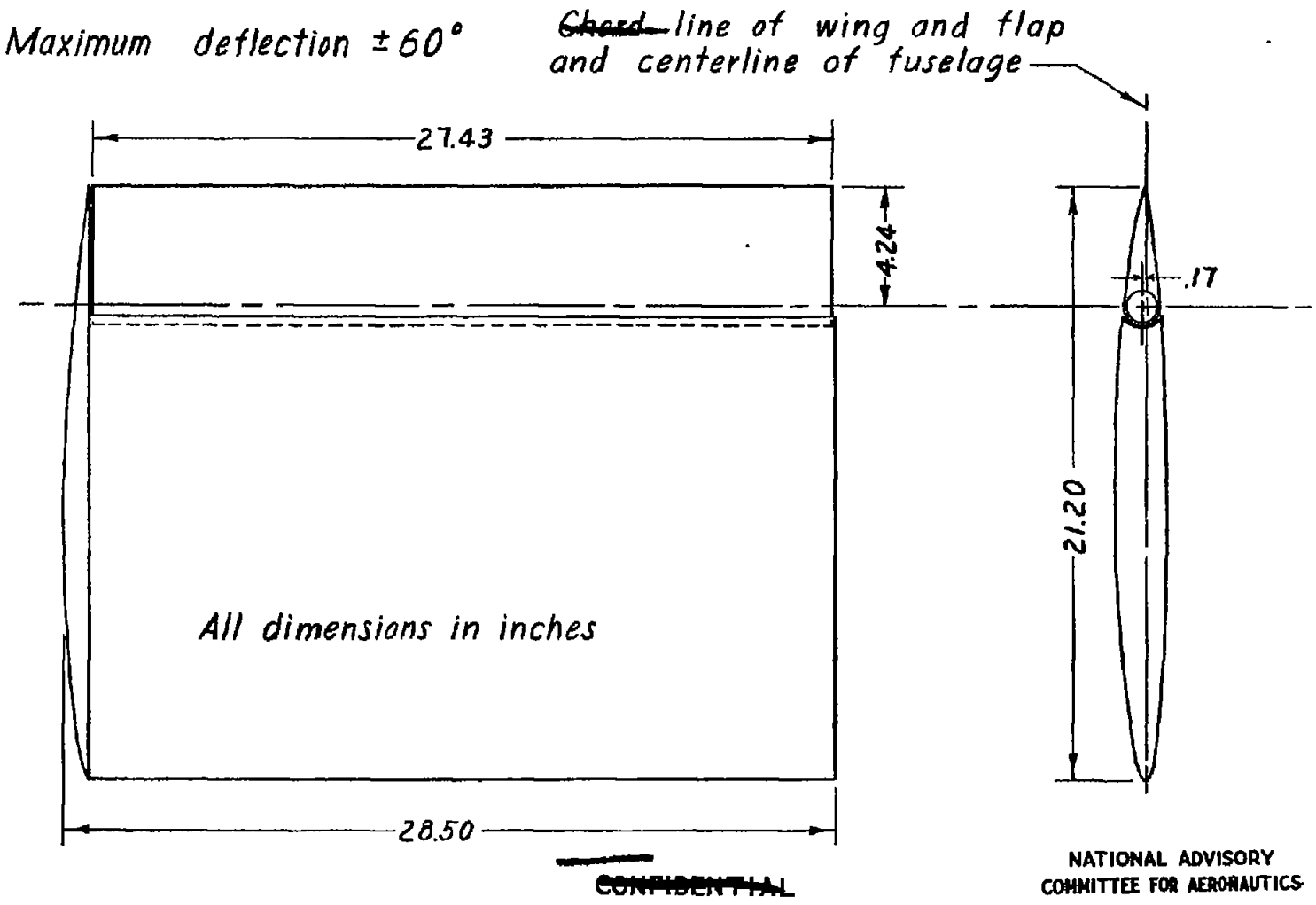


Figure 3.- Details of the horizontal wing flap.

~~CONFIDENTIAL~~

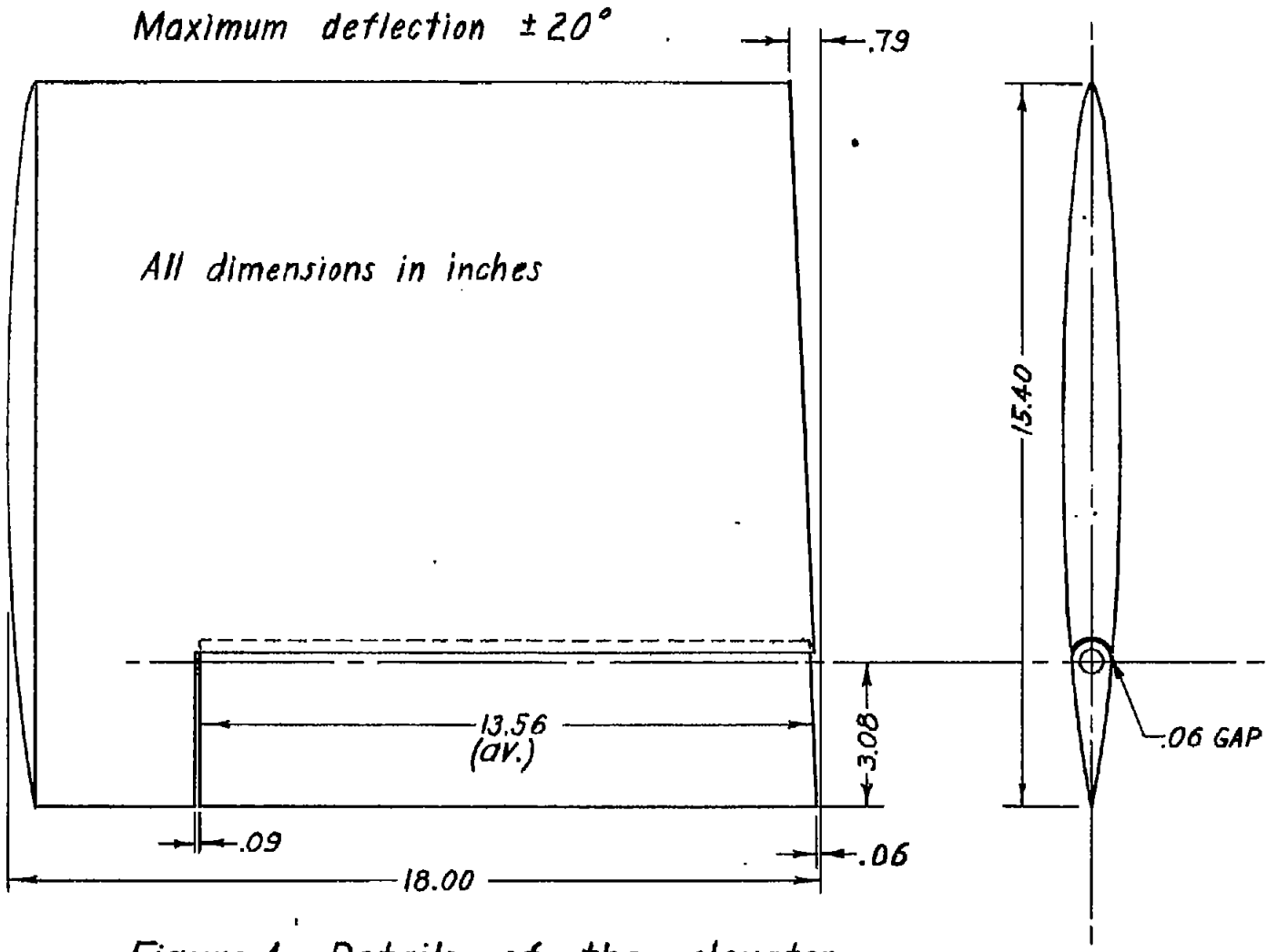


Figure 4.—Details of the elevator.

~~CONFIDENTIAL~~

~~CONFIDENTIAL~~




(a) Static-pressure tube exit and aileron (extended) in upper vertical wing.

Figure 5.- Details of machmeter orifices and aileron.

~~CONFIDENTIAL~~

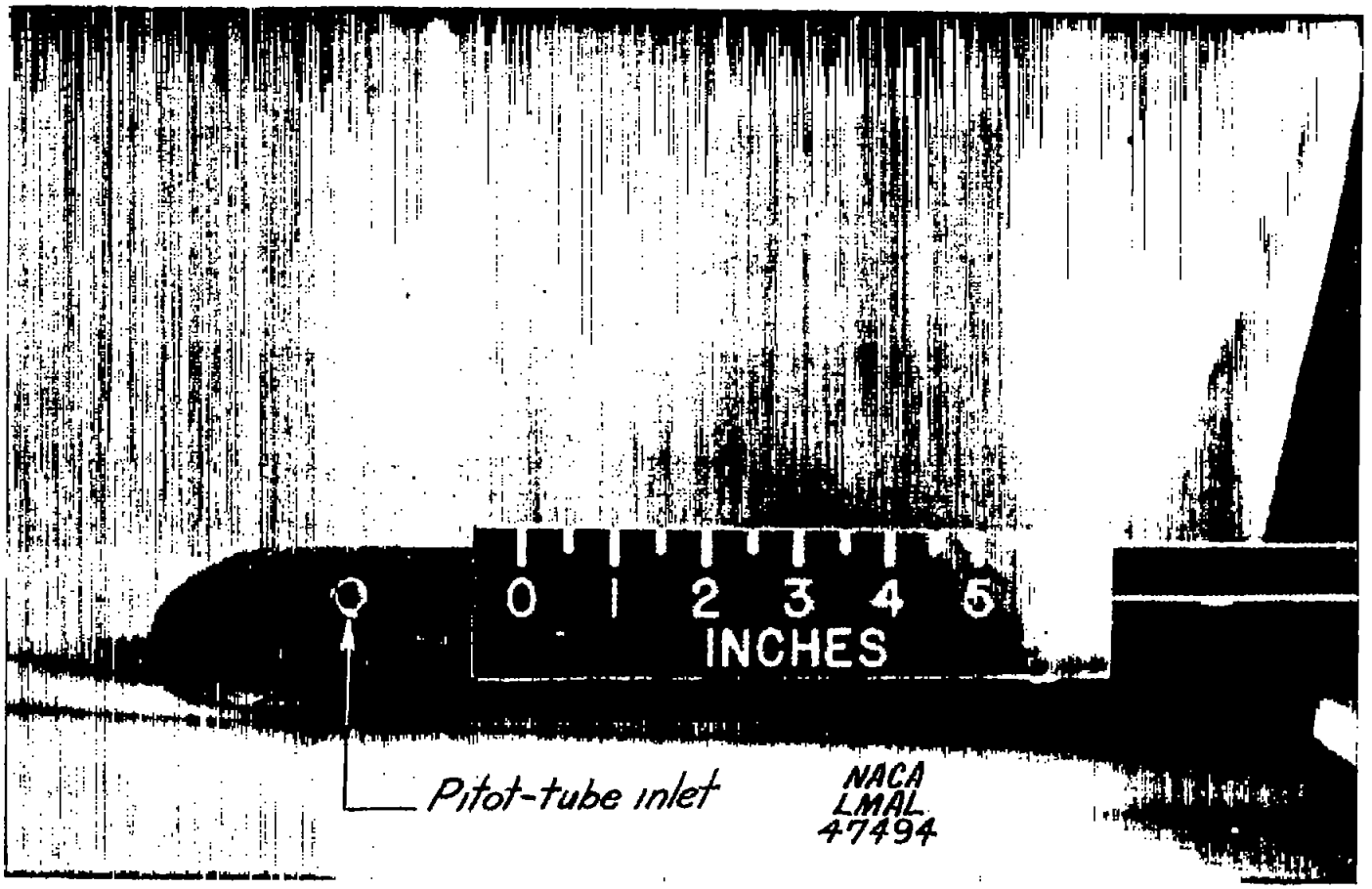


(b) Total-pressure (pitot) tube inlet in lower vertical wing (static-pressure tube inlet similar).

Figure 5.- Continued.

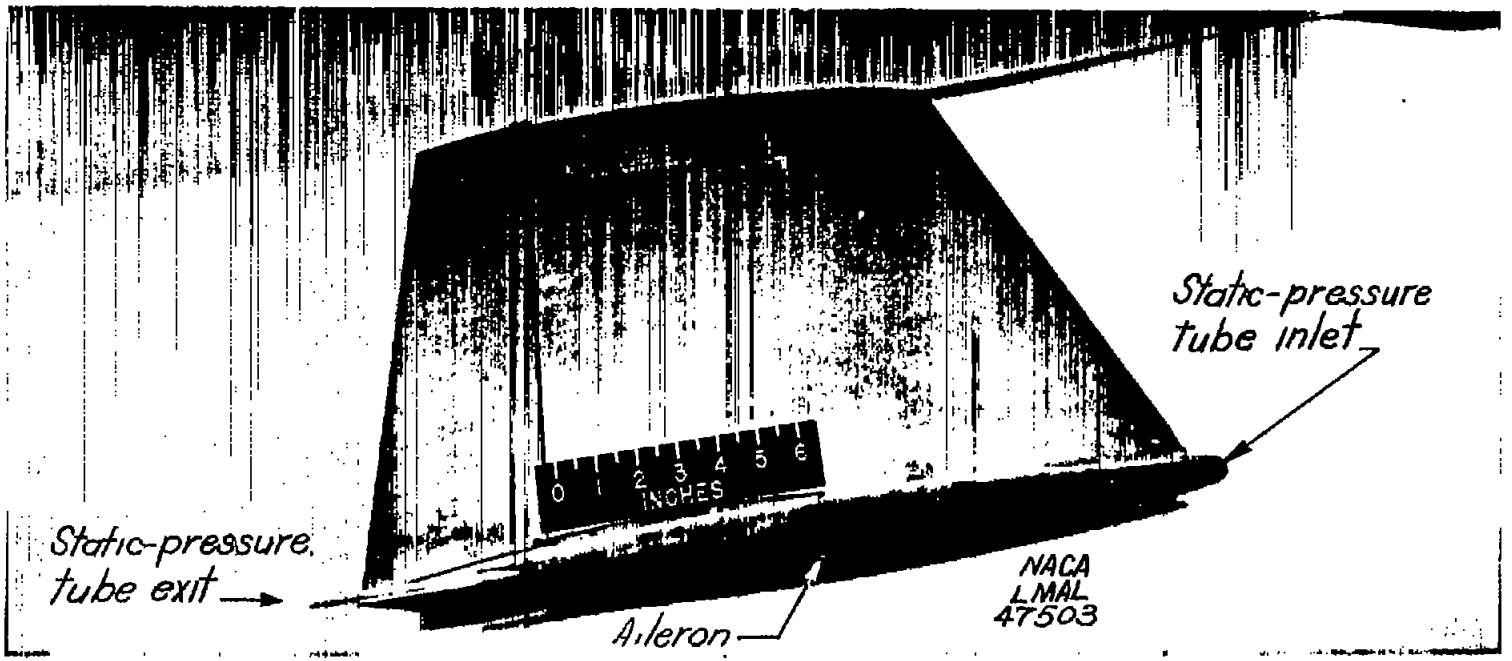


(c) Modified static-pressure tube exit and aileron (retracted) in upper vertical wing.

Figure 5.- Concluded.

CONFIDENTIAL

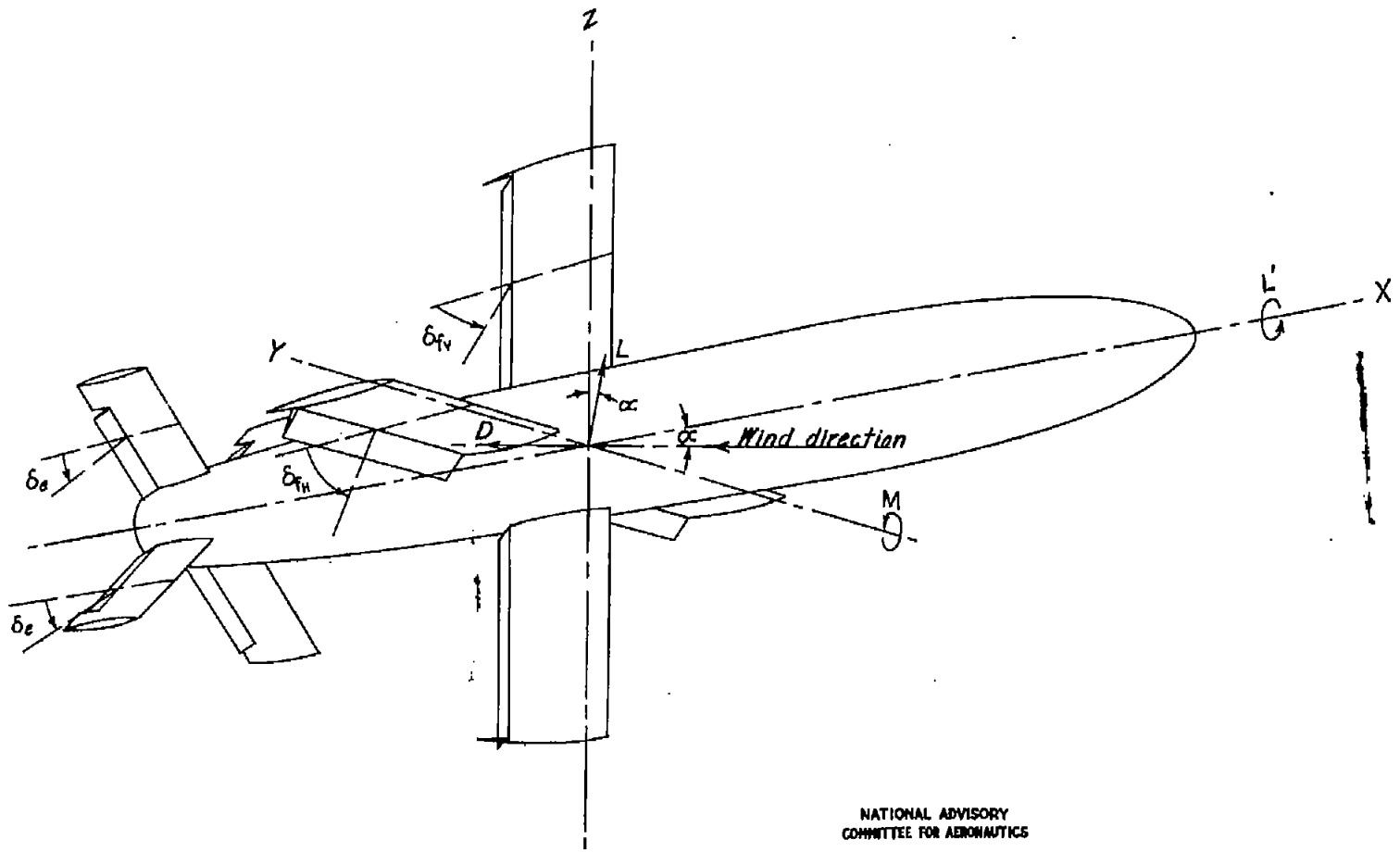


Figure 6.- Positive directions of forces and moments and control surface deflections.

CONFIDENTIAL

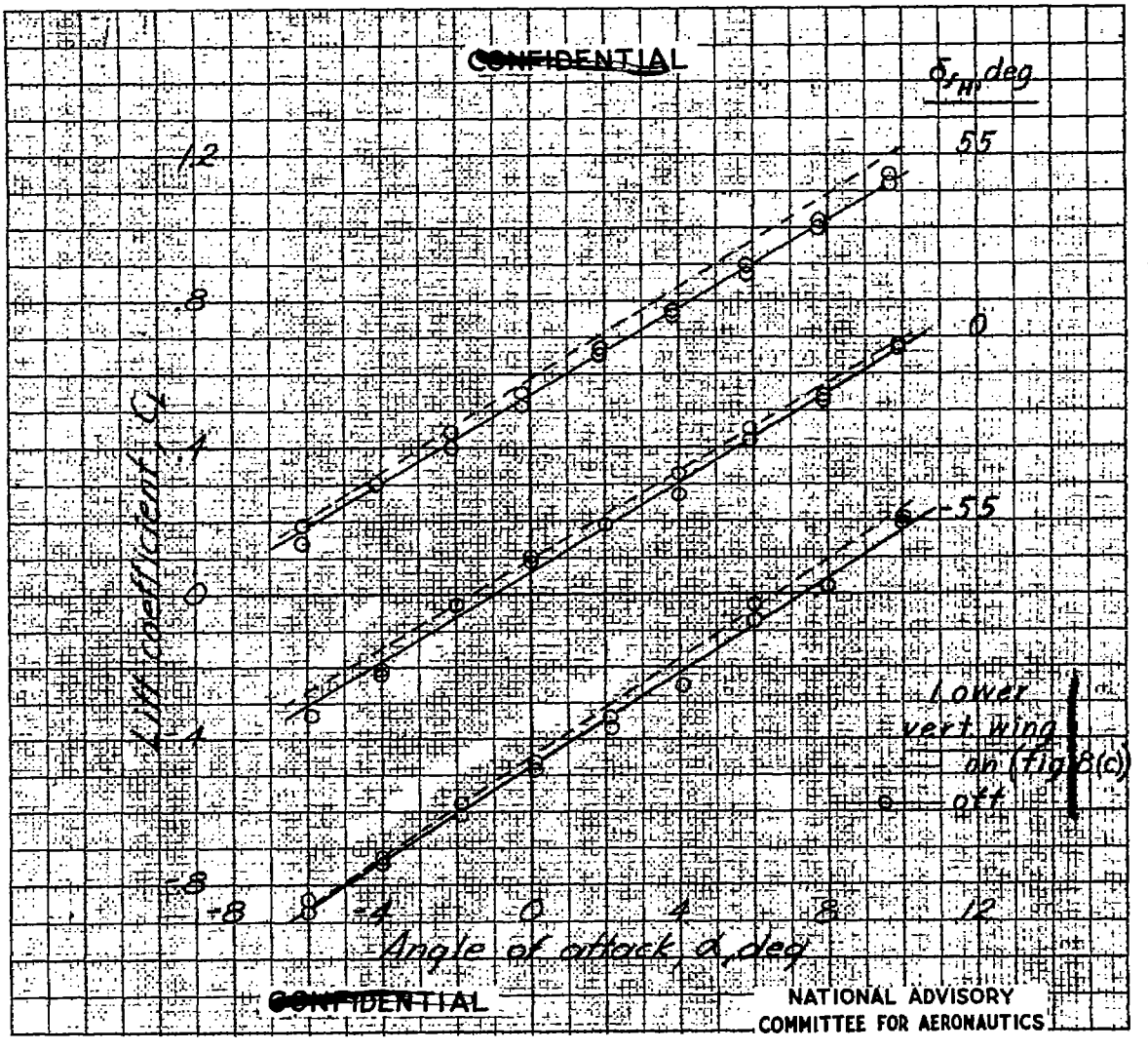


(a) Lift coefficients.

Figure 7.- Effect of the lower vertical wing on the aerodynamic characteristics of the airplane. $\delta_e = 0^\circ$. Moment center at the pivot point.

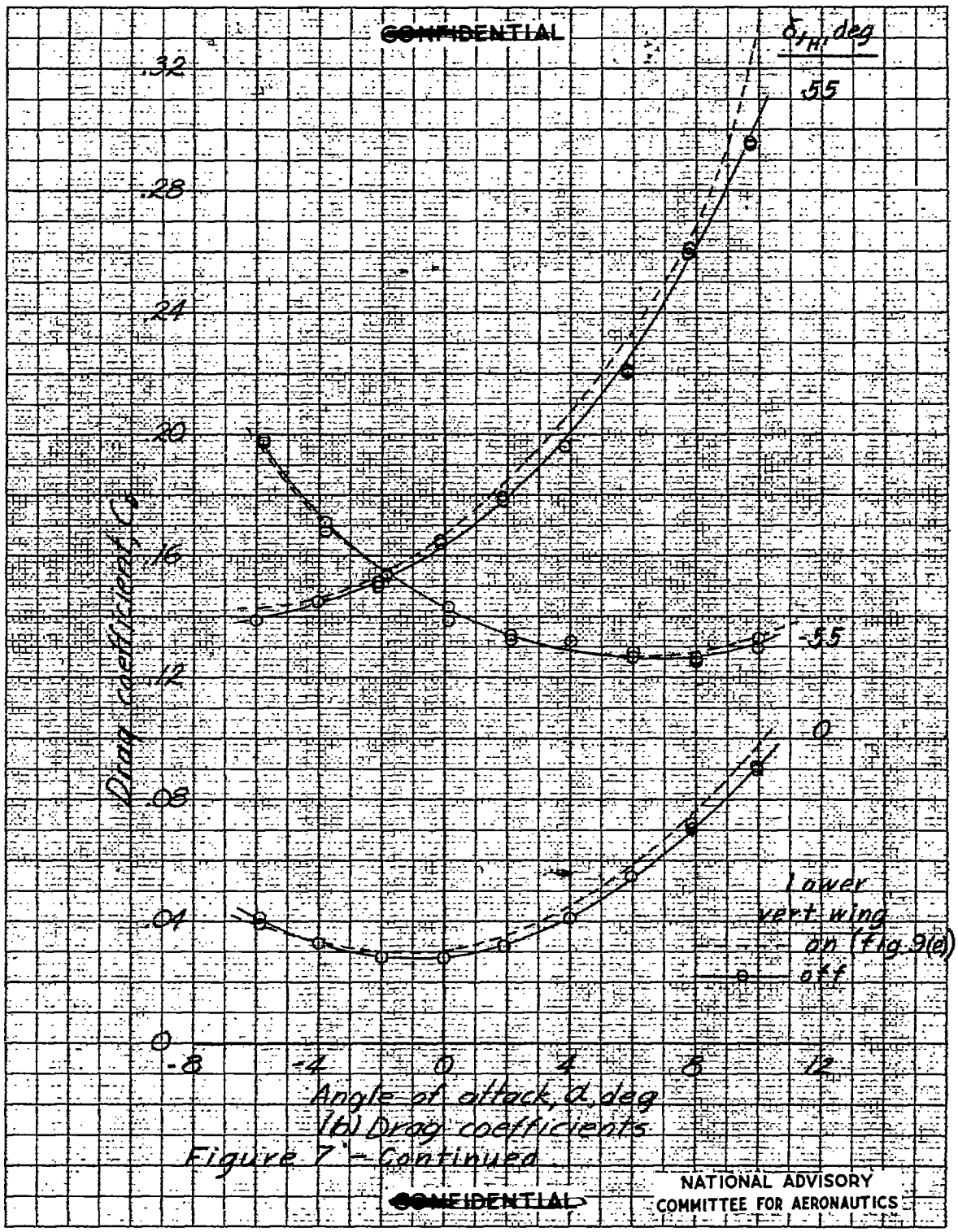


(b) Drag coefficients.

Figure 7.- Continued.

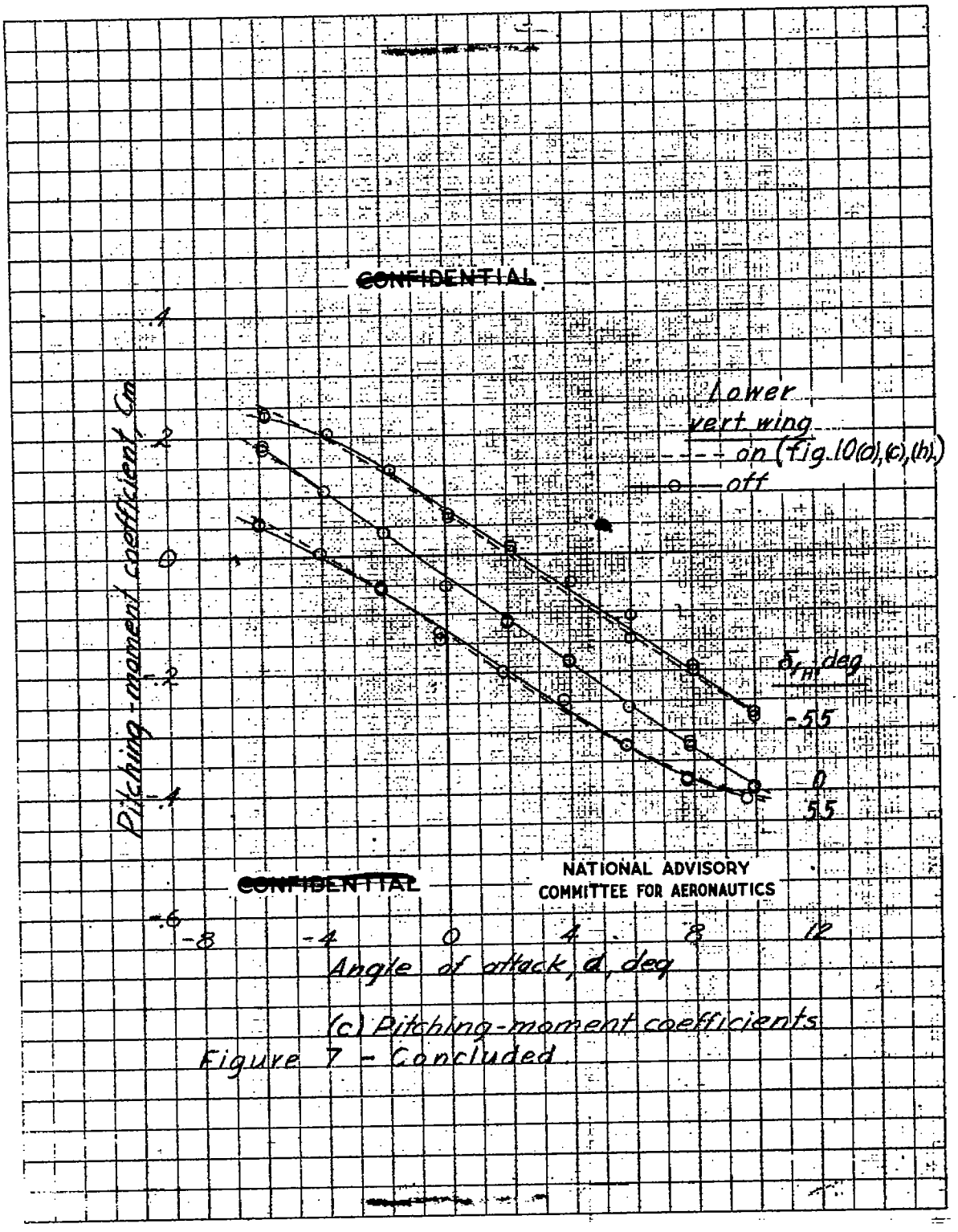


(c) Pitching-moment coefficients.

Figure 7 - Concluded.

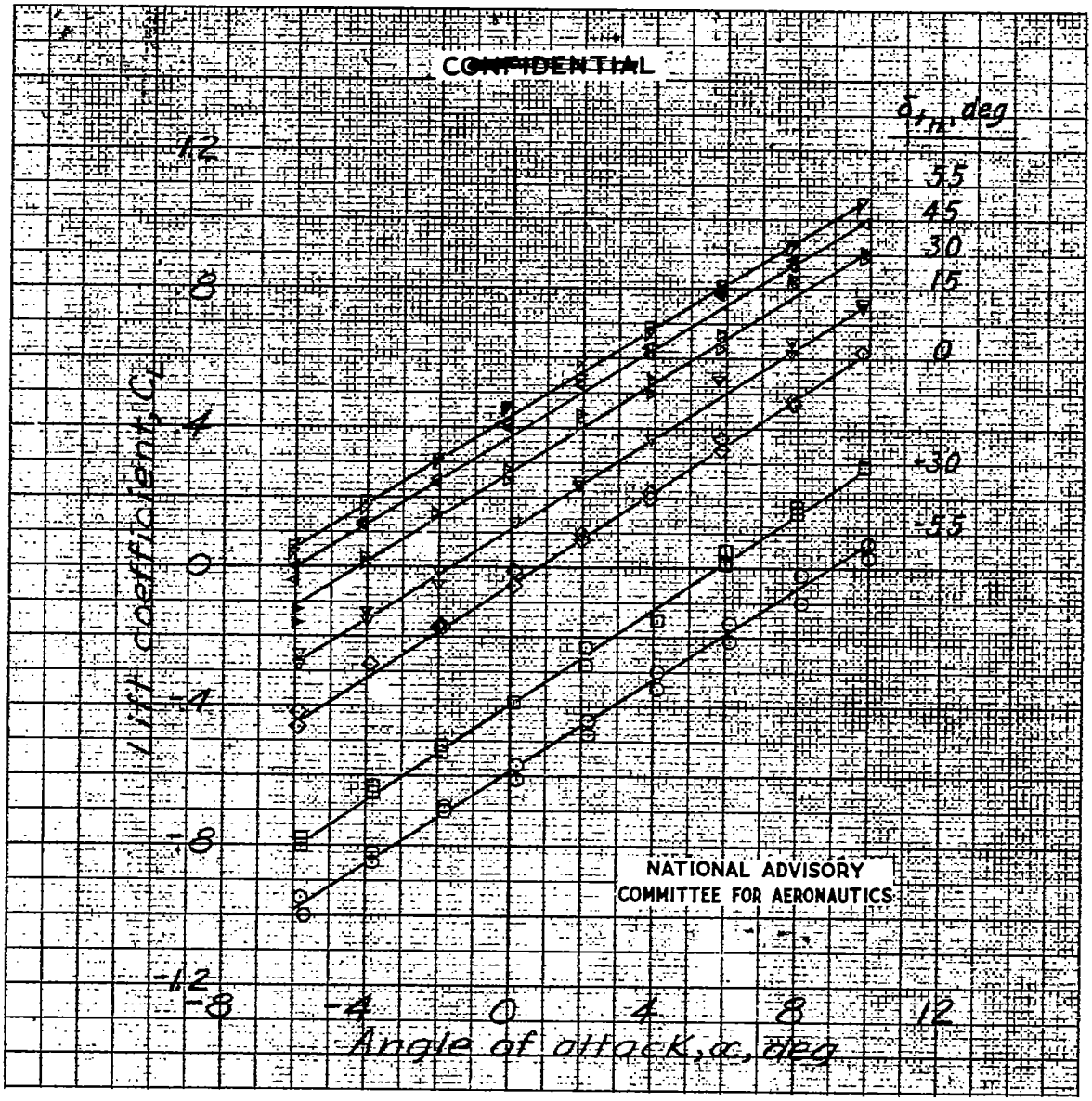


CONFIDENTIAL

(a) $\delta_e = -15^\circ$.

Figure 8.- Variation of lift coefficient with angle of attack for various horizontal flap and elevator deflections.

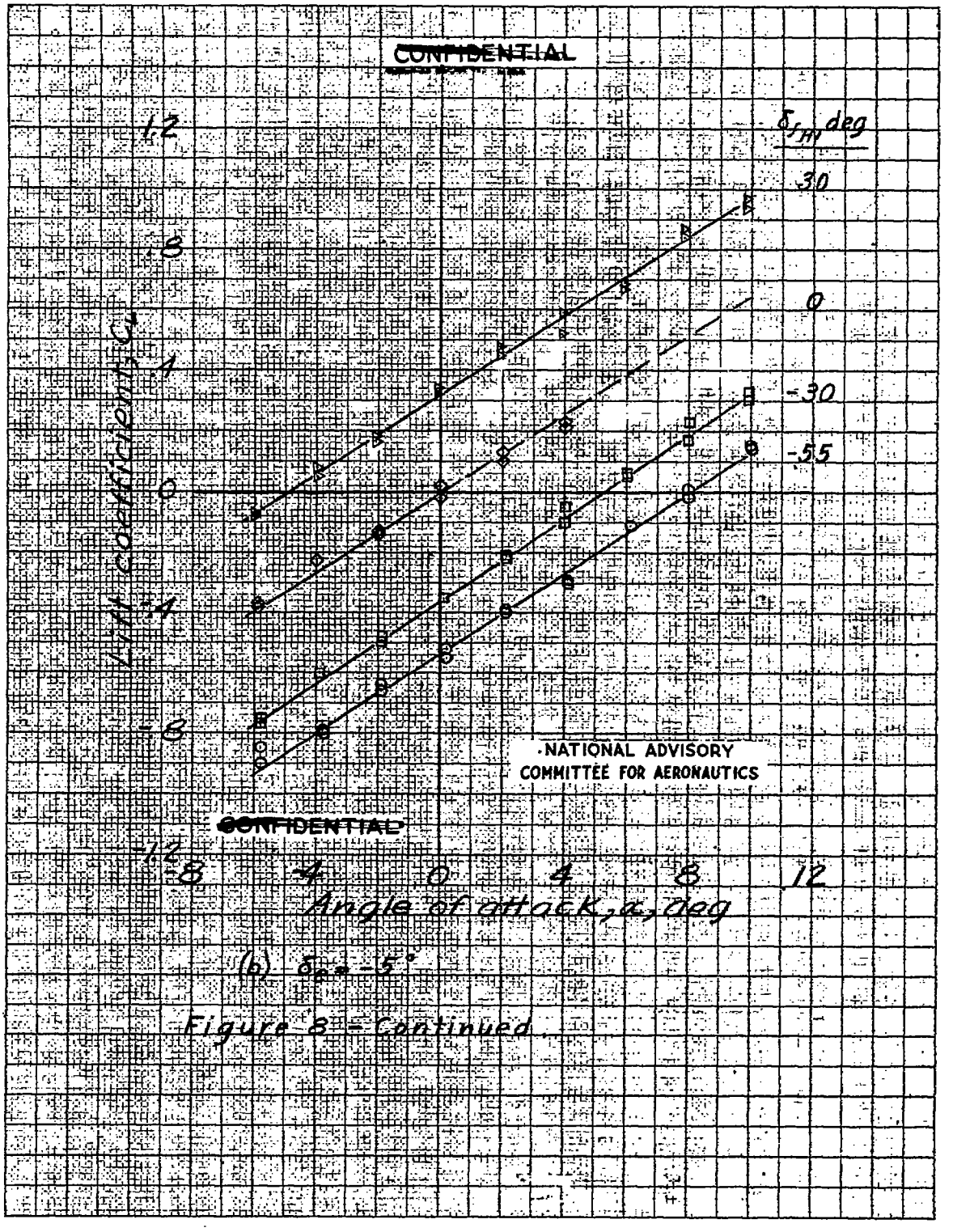


(b) $\delta_e = -5°$

Figure 8 - Continued

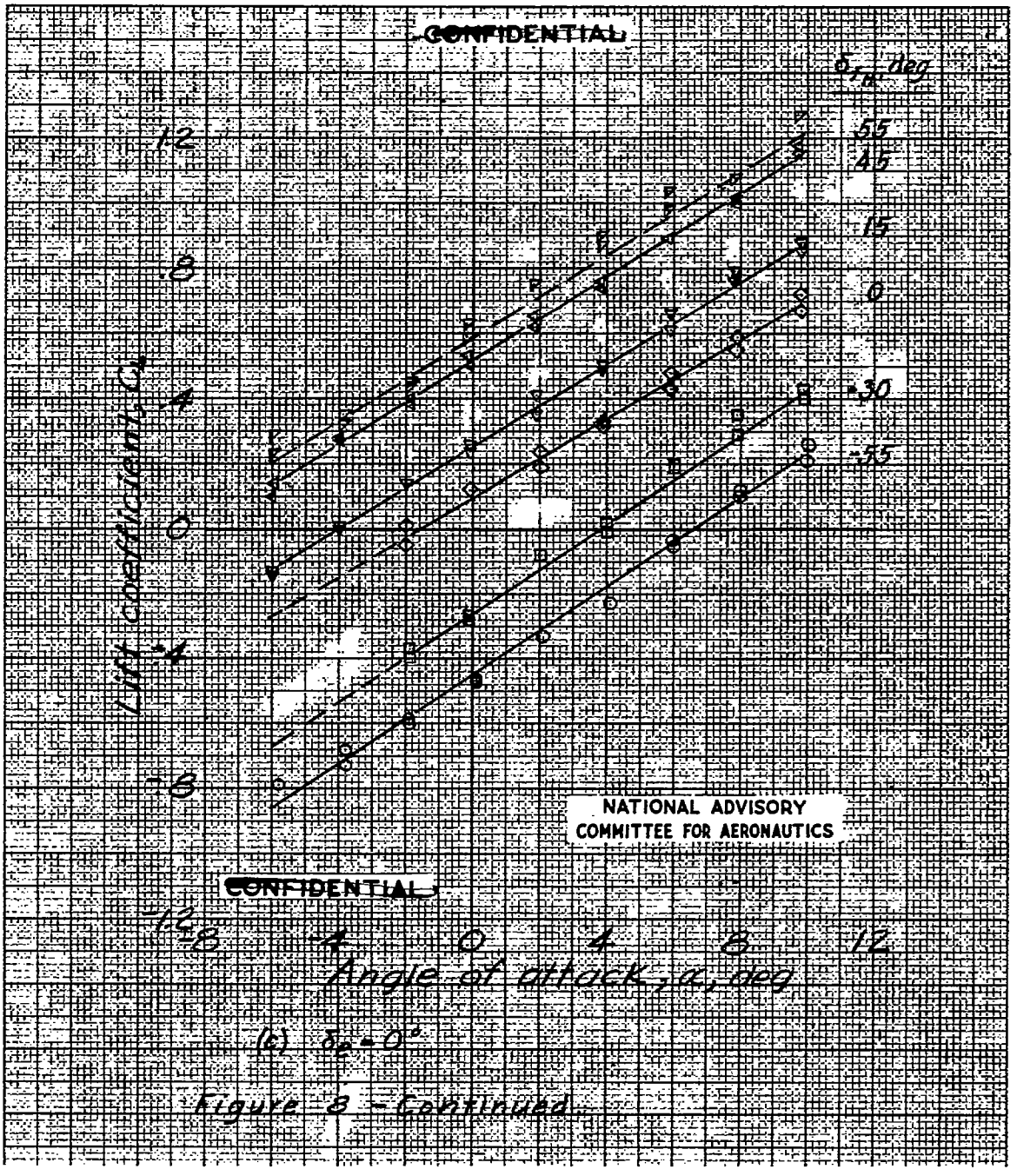


(c) $\delta_e = 0°$

Figure 8 - Continued

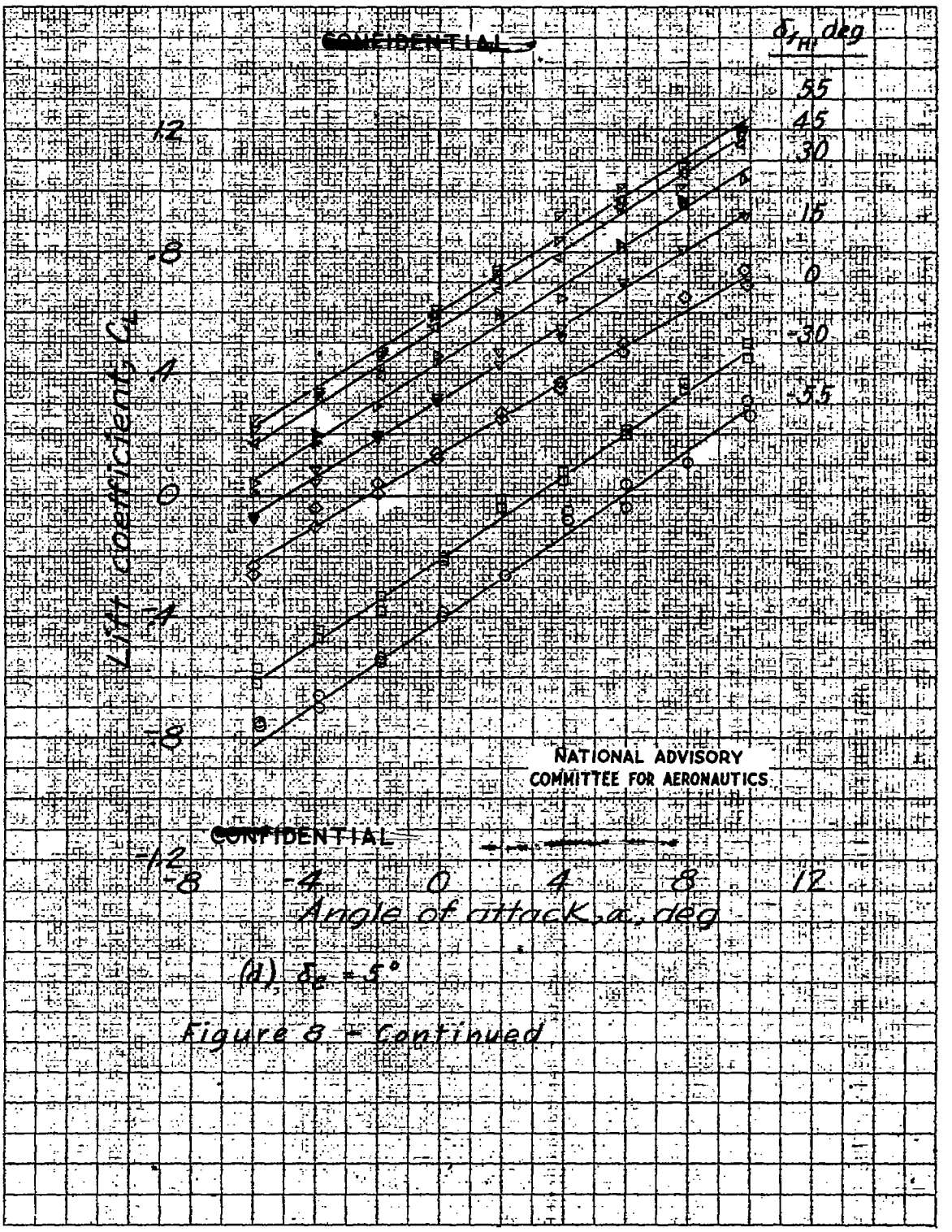


(d) $\delta_e = -5°$

Figure 8 - Continued

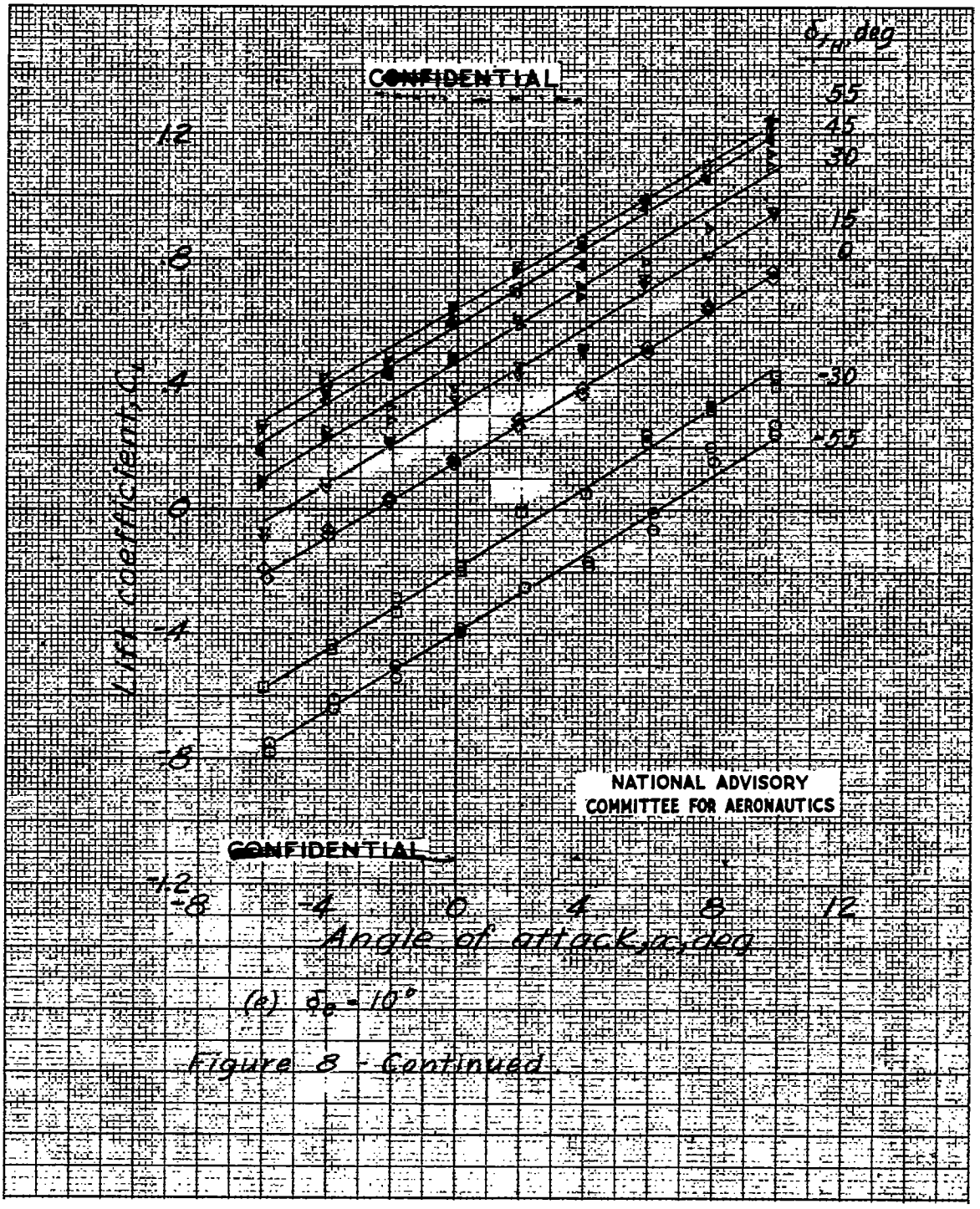


(e) $\delta_e = 10°$

Figure 8 - Continued

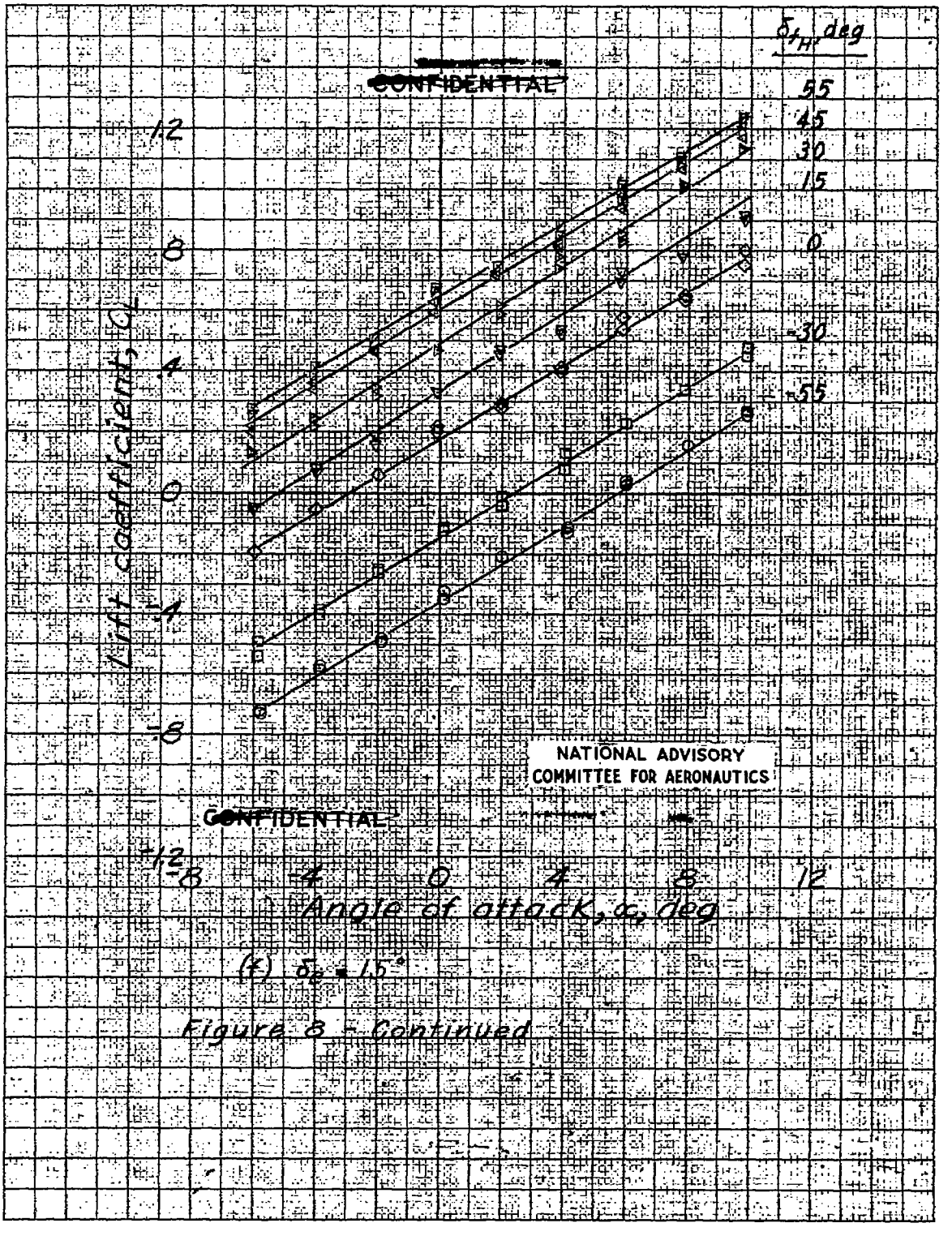


(f) $\delta_e = 15°$

Figure 8 - Continued

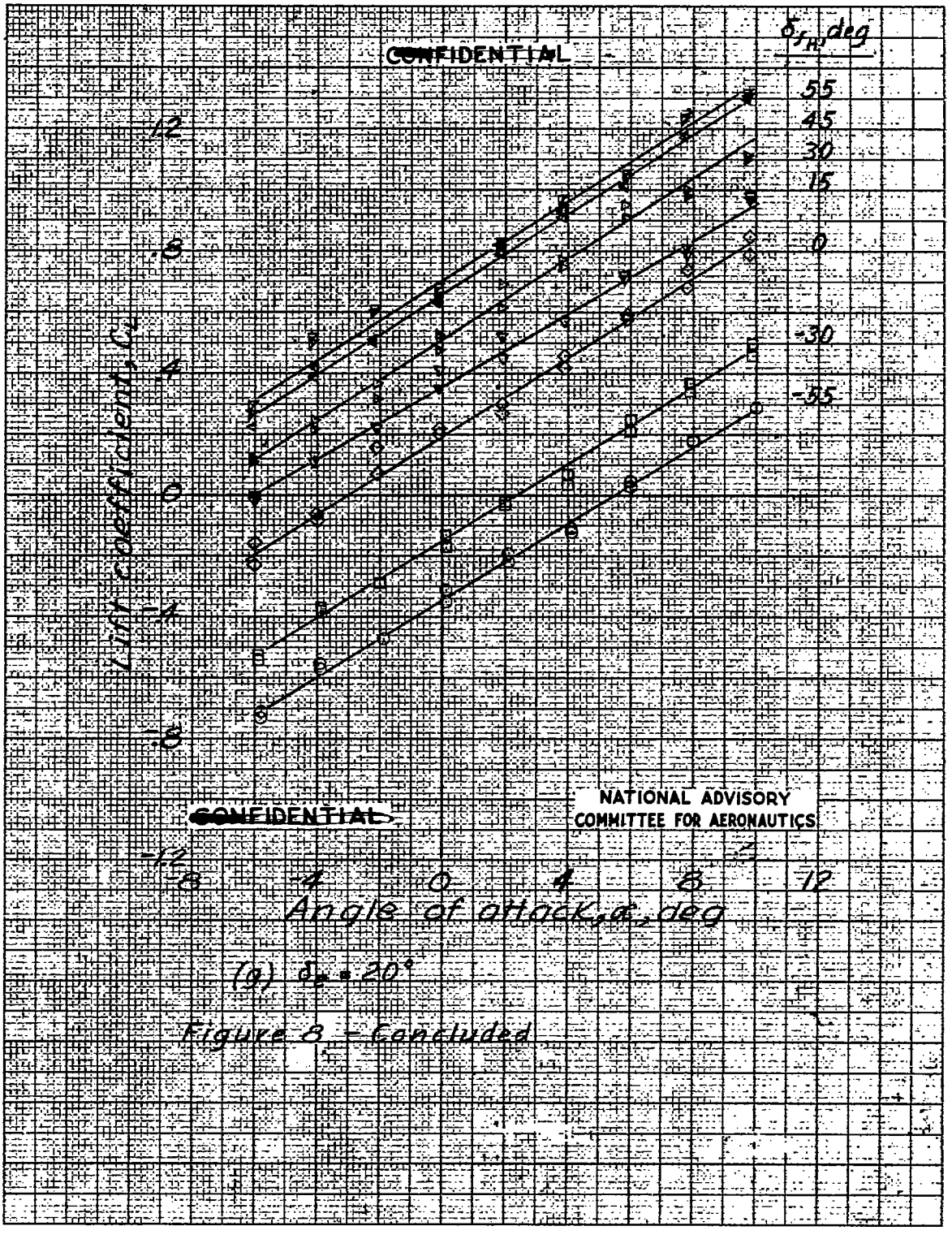


(g) $\delta_e = 20°$

Figure 8.- Concluded.

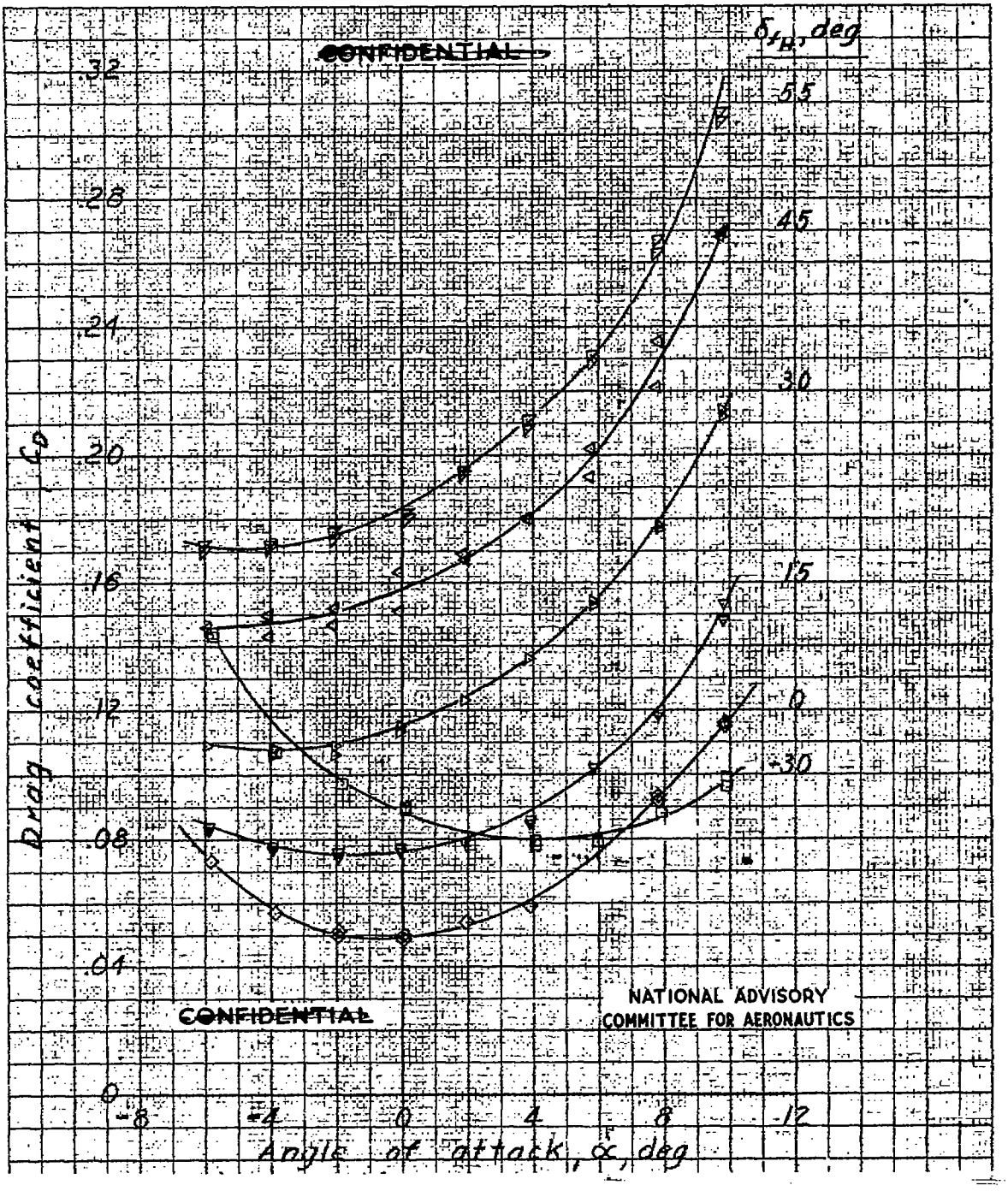


(a) $\delta_e = -20^\circ$.

Figure 9.- Variation of drag coefficient with angle of attack for various horizontal flap and elevator deflections.

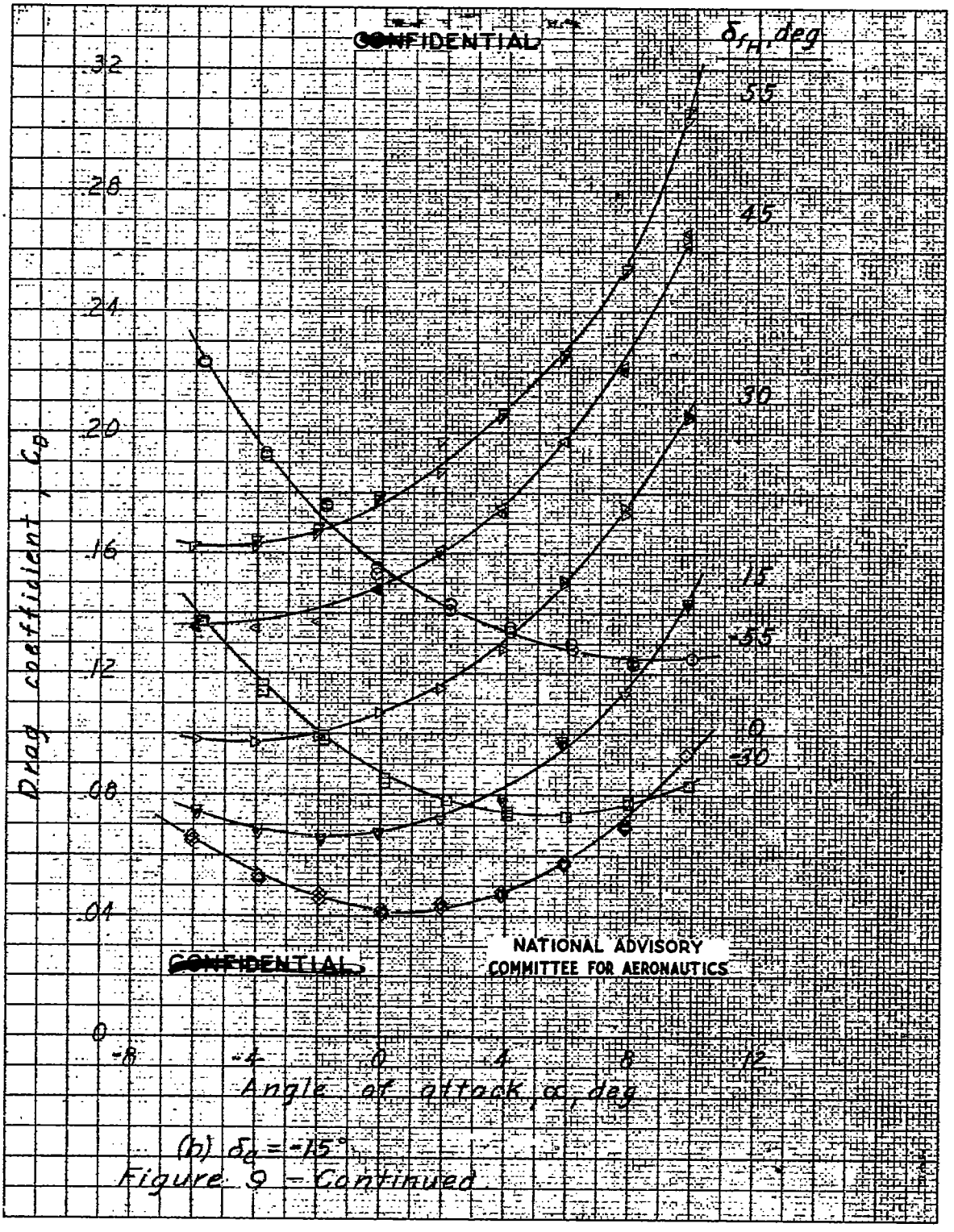


(b) $\delta_a = -15°$

Figure 9 - Continued

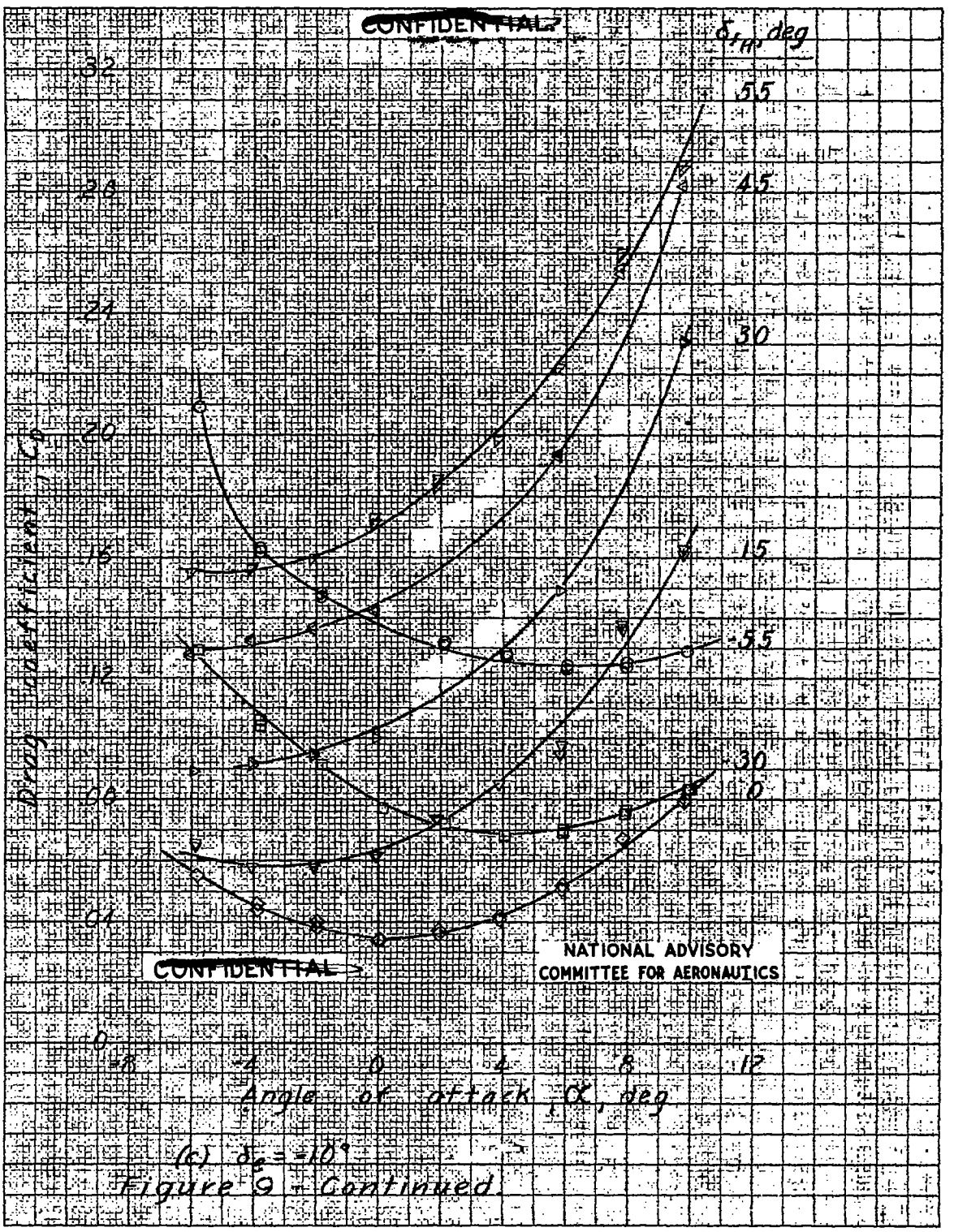


(c) $\delta_e = -10°$

Figure 9 - Continued.

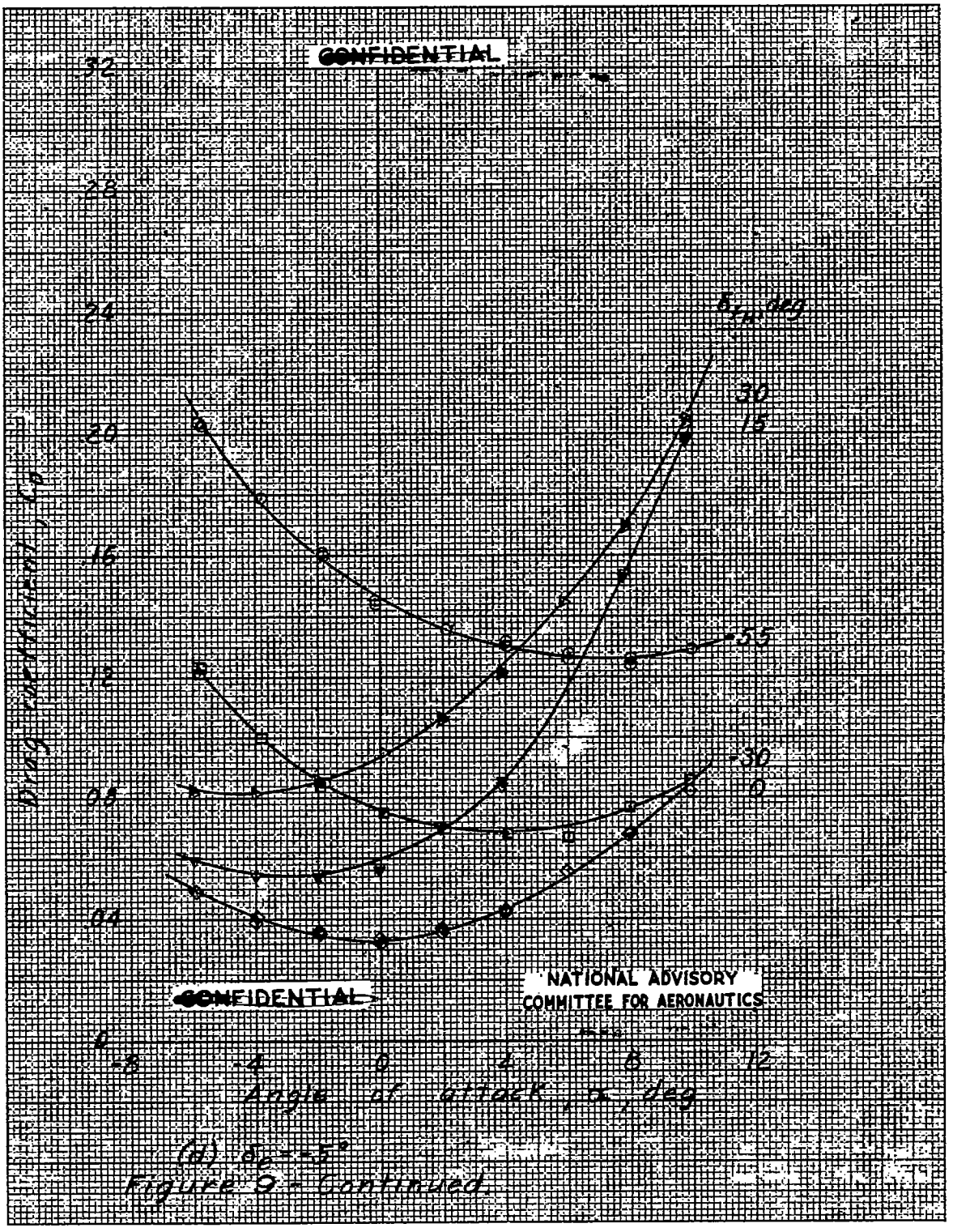


(d) $\delta_e = -5°$

Figure 9 - Continued

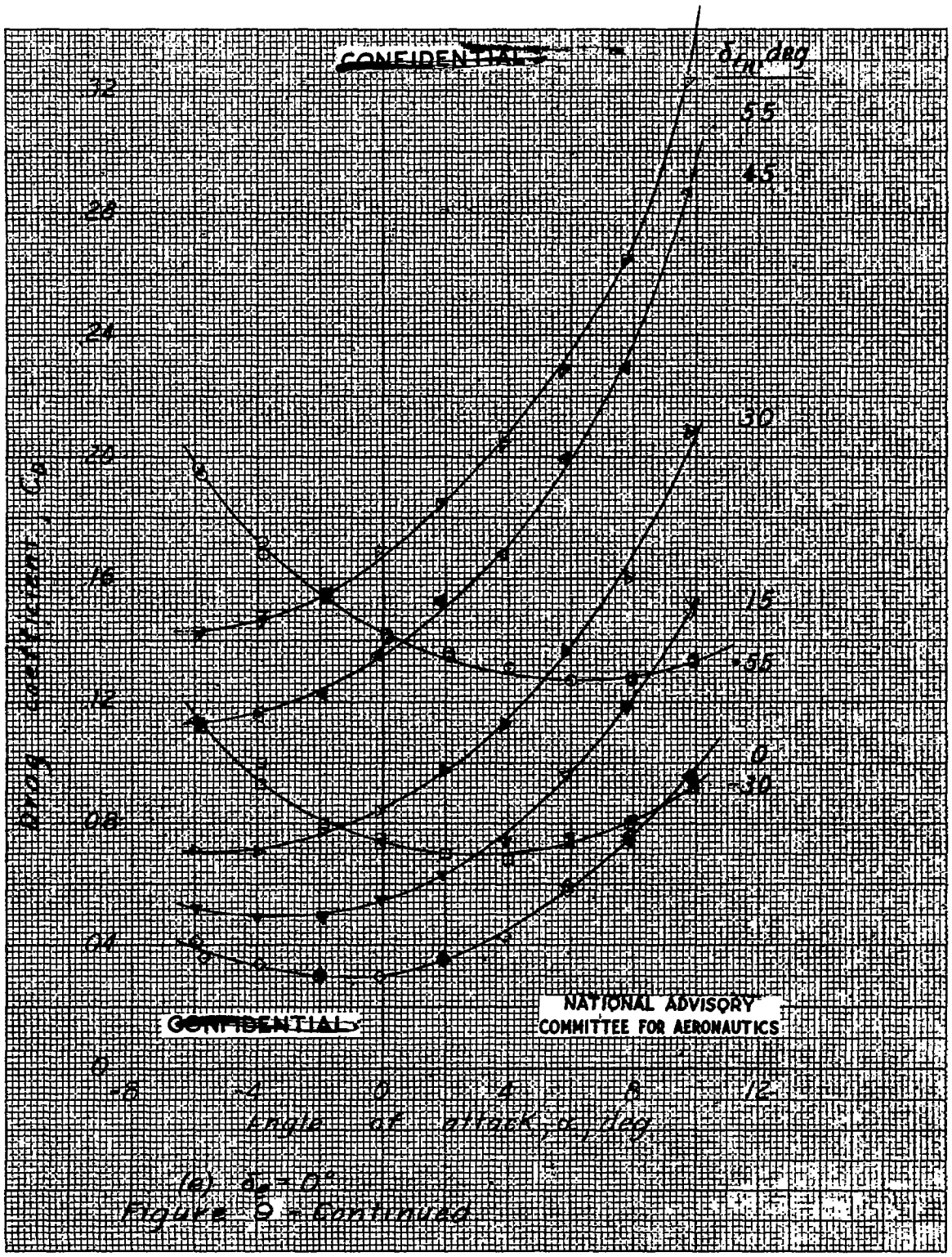


(e) $\delta_E = 0°$

Figure 9.- Continued

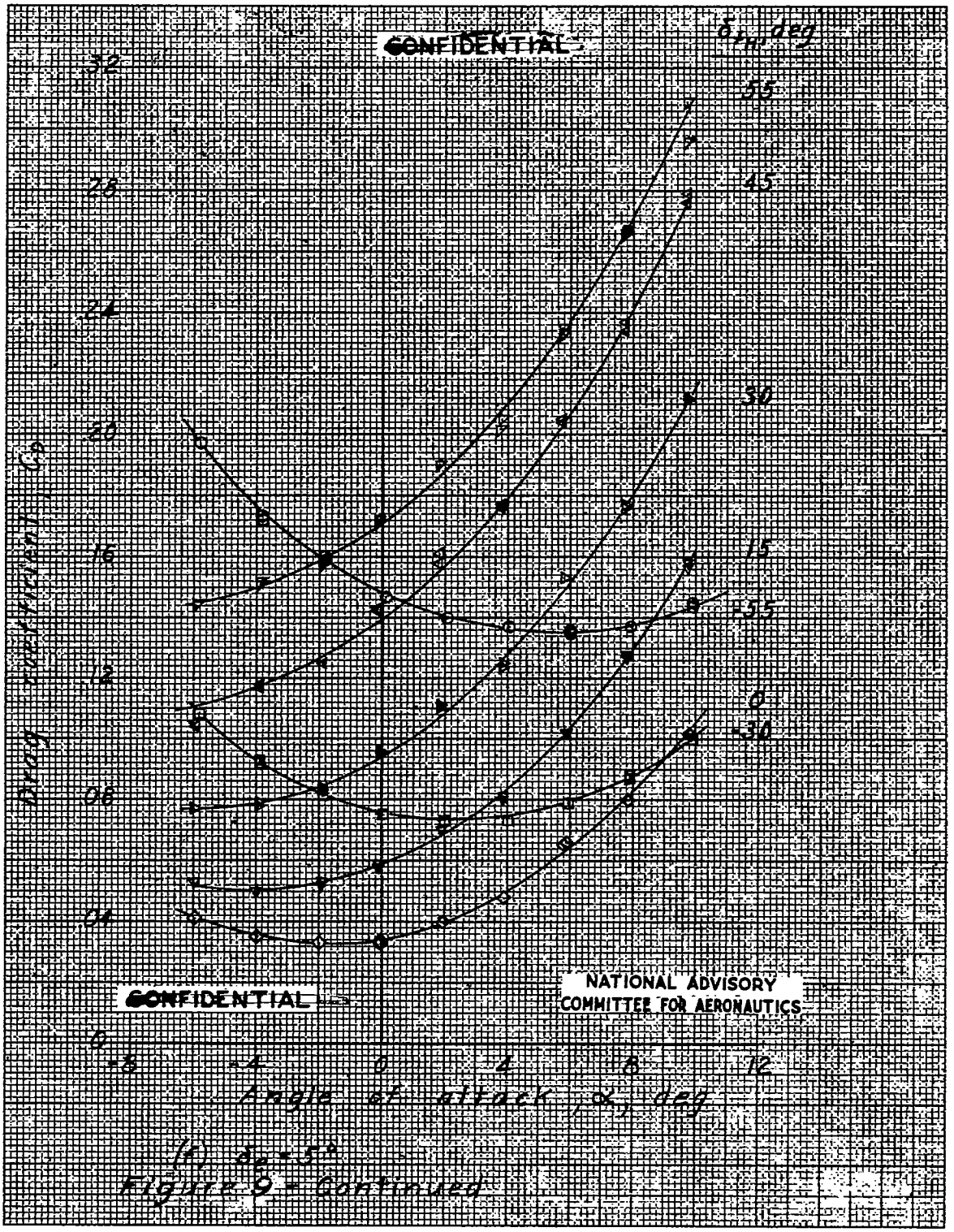


(h) $\delta_e = 5°$

Figure 9.- Continued

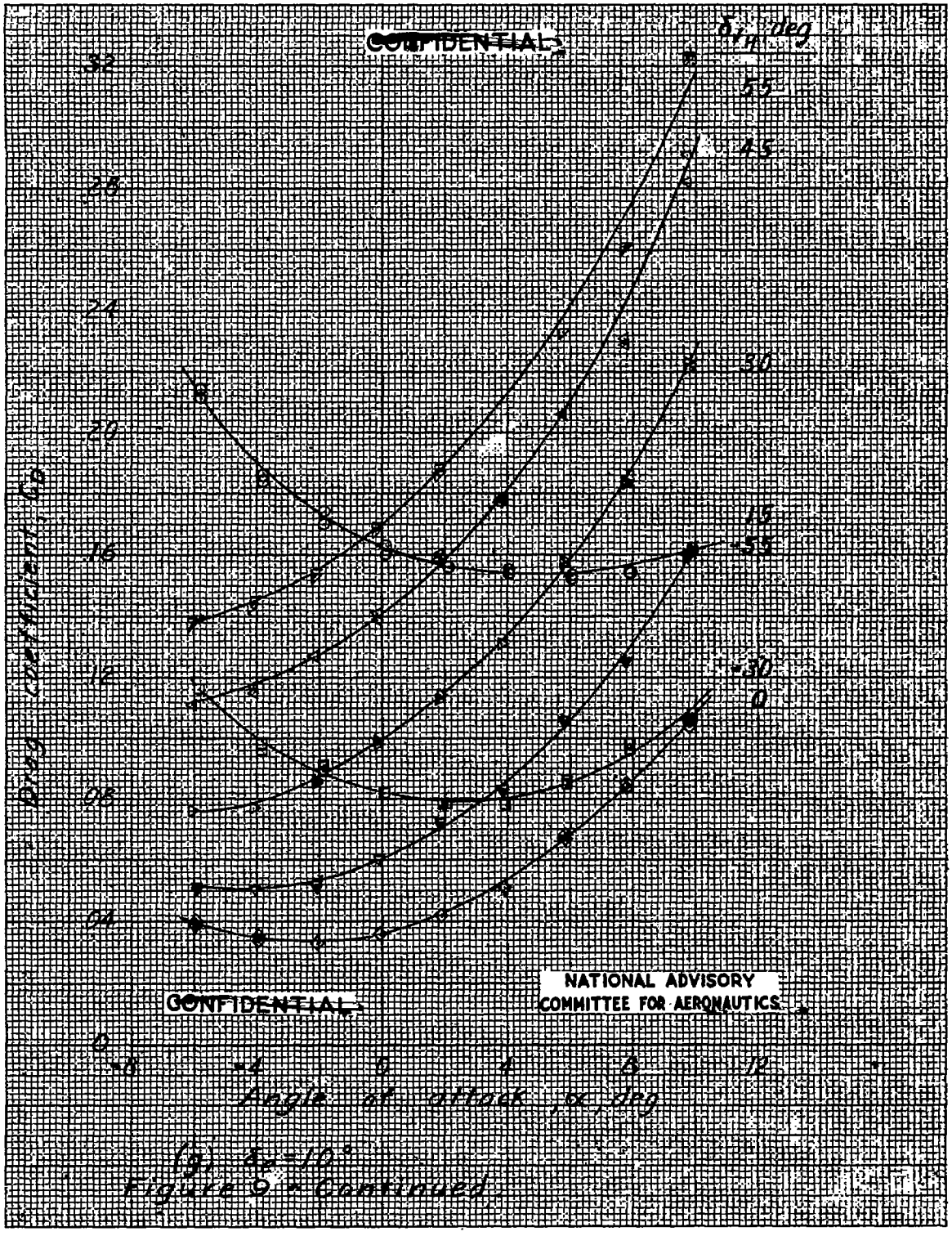


(g) $\delta_e = 10°$

Figure 9.- Continued.

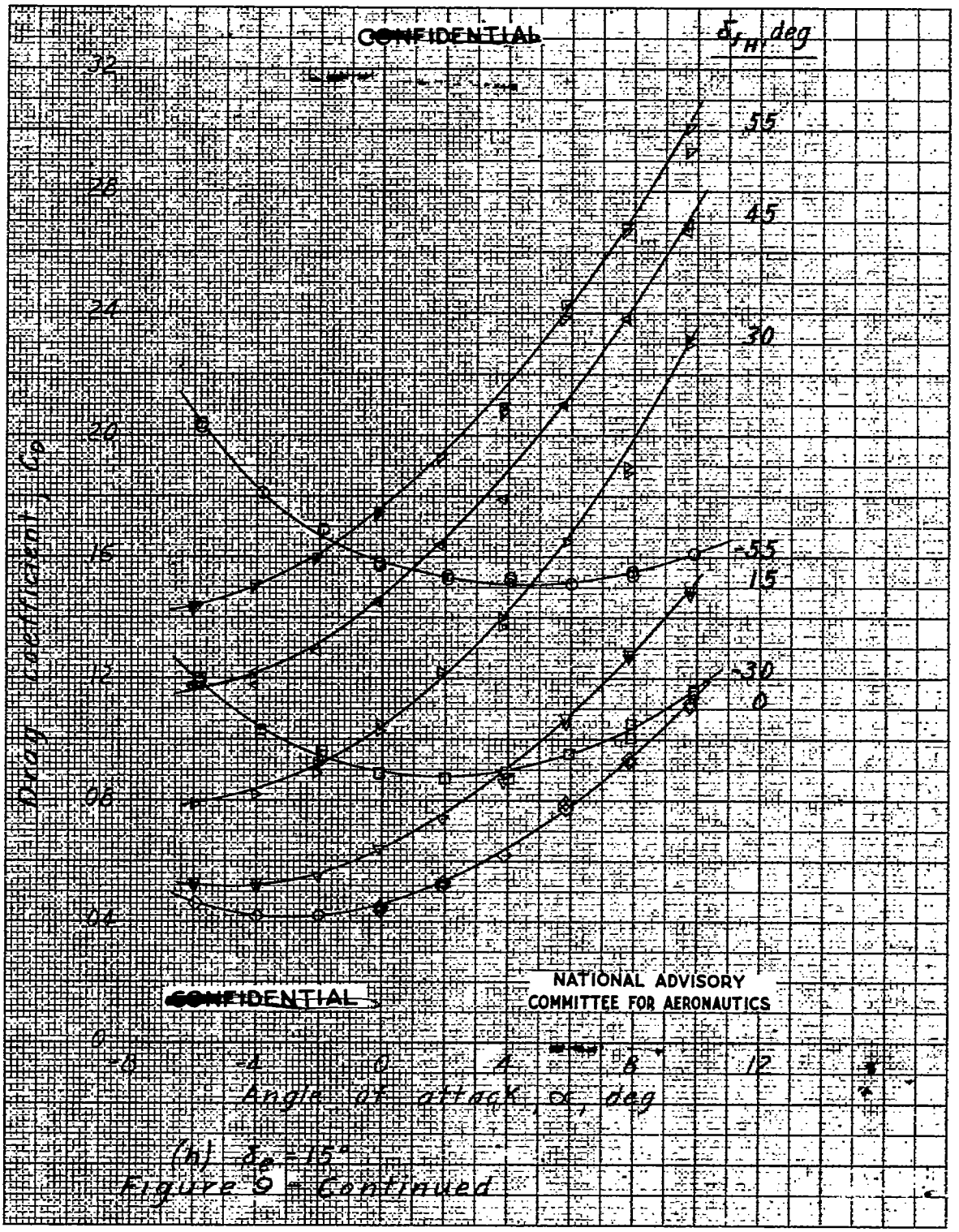


(h) $\delta_e = 15°$

Figure 9 - Continued

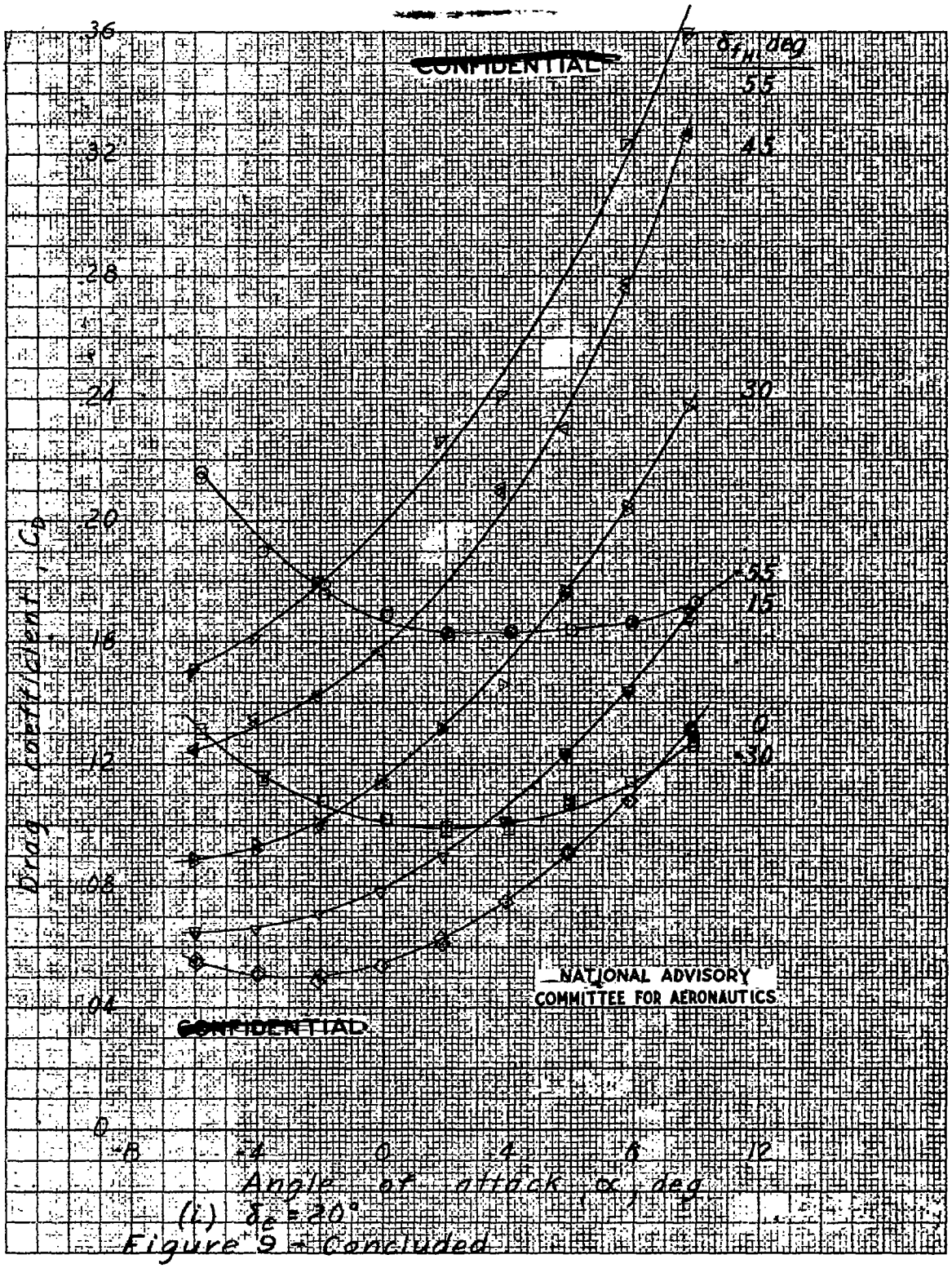


(i) $\delta_e = 20°$

Figure 9 - Concluded

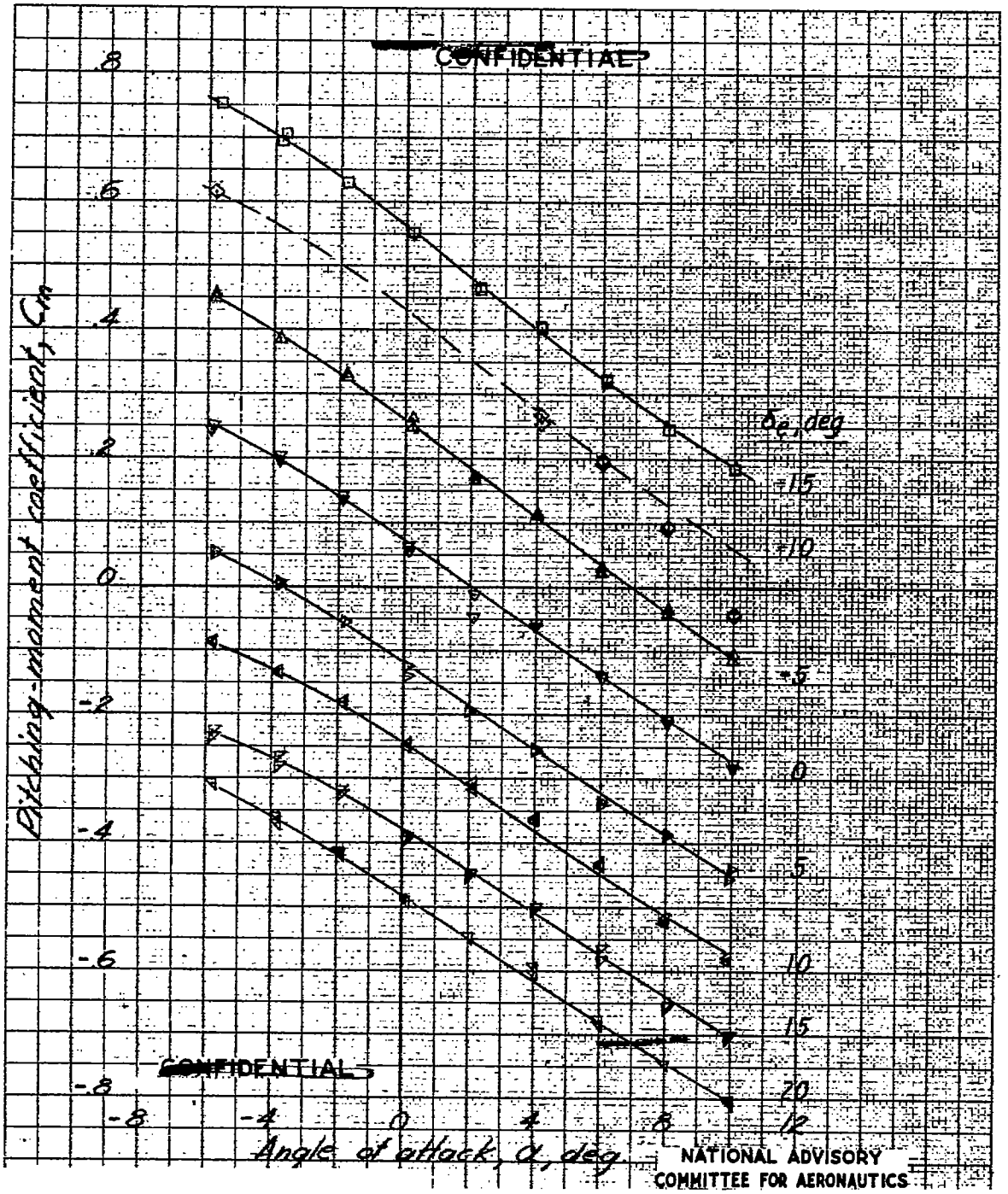


(a) $\delta_{f_H} = -55^\circ$.

Figure 10.- Variation of pitching-moment coefficient with angle of attack for various horizontal flap and elevator deflections. Moment center at pivot point.

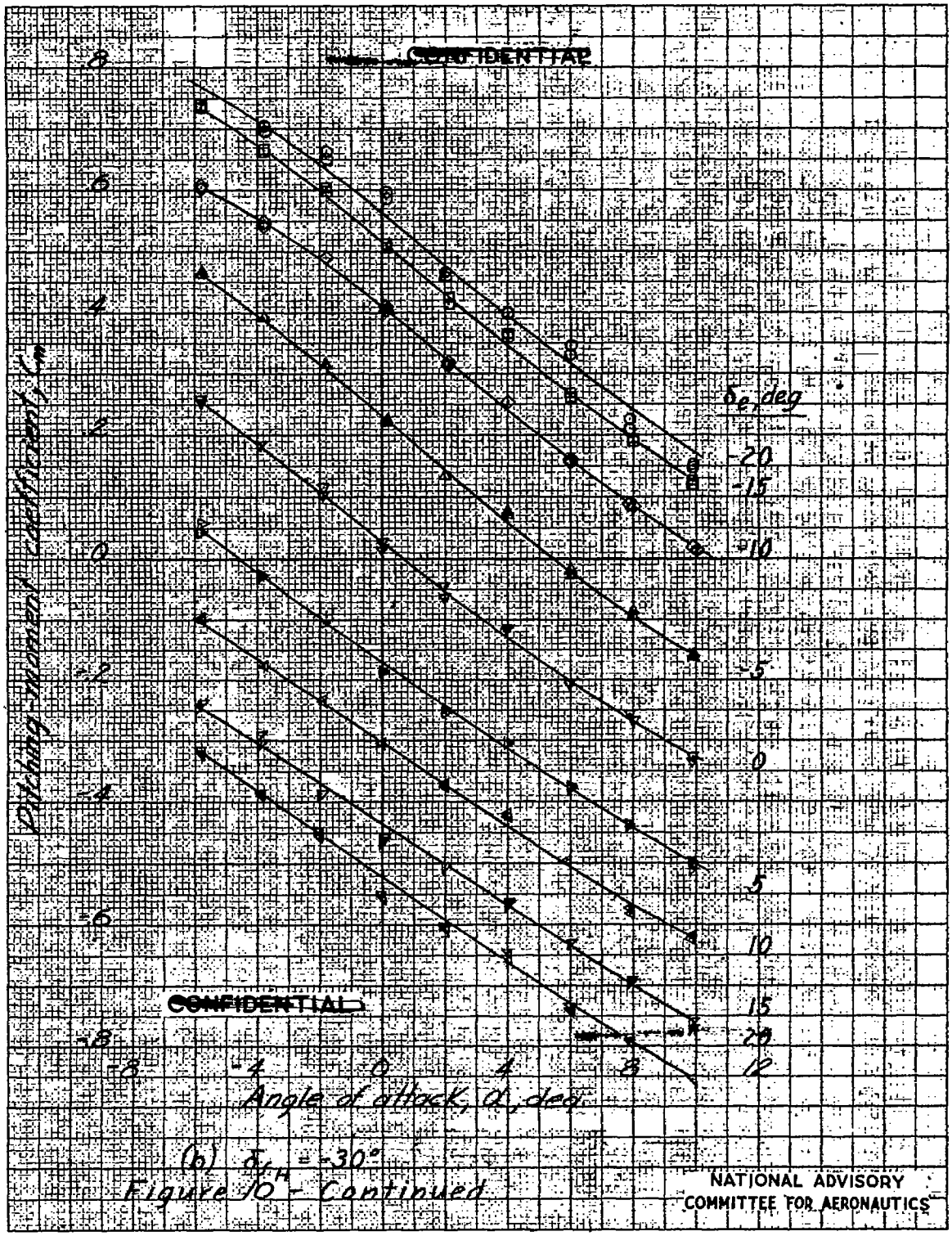


(b) $\delta_{f,H} = -30°$

Figure 10 - Continued

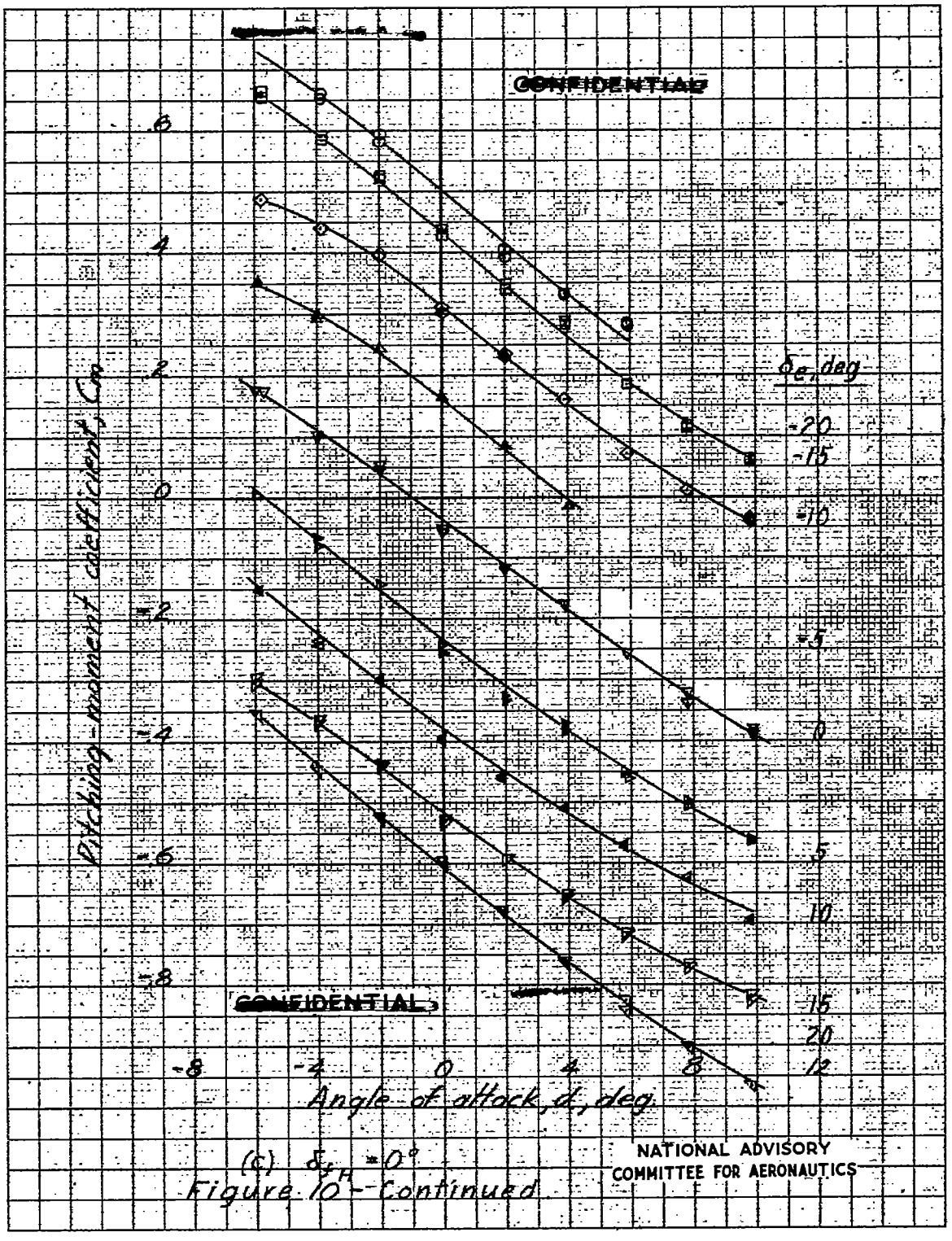


(c) $\delta_{f_H} = 0°$

Figure 10 - Continued

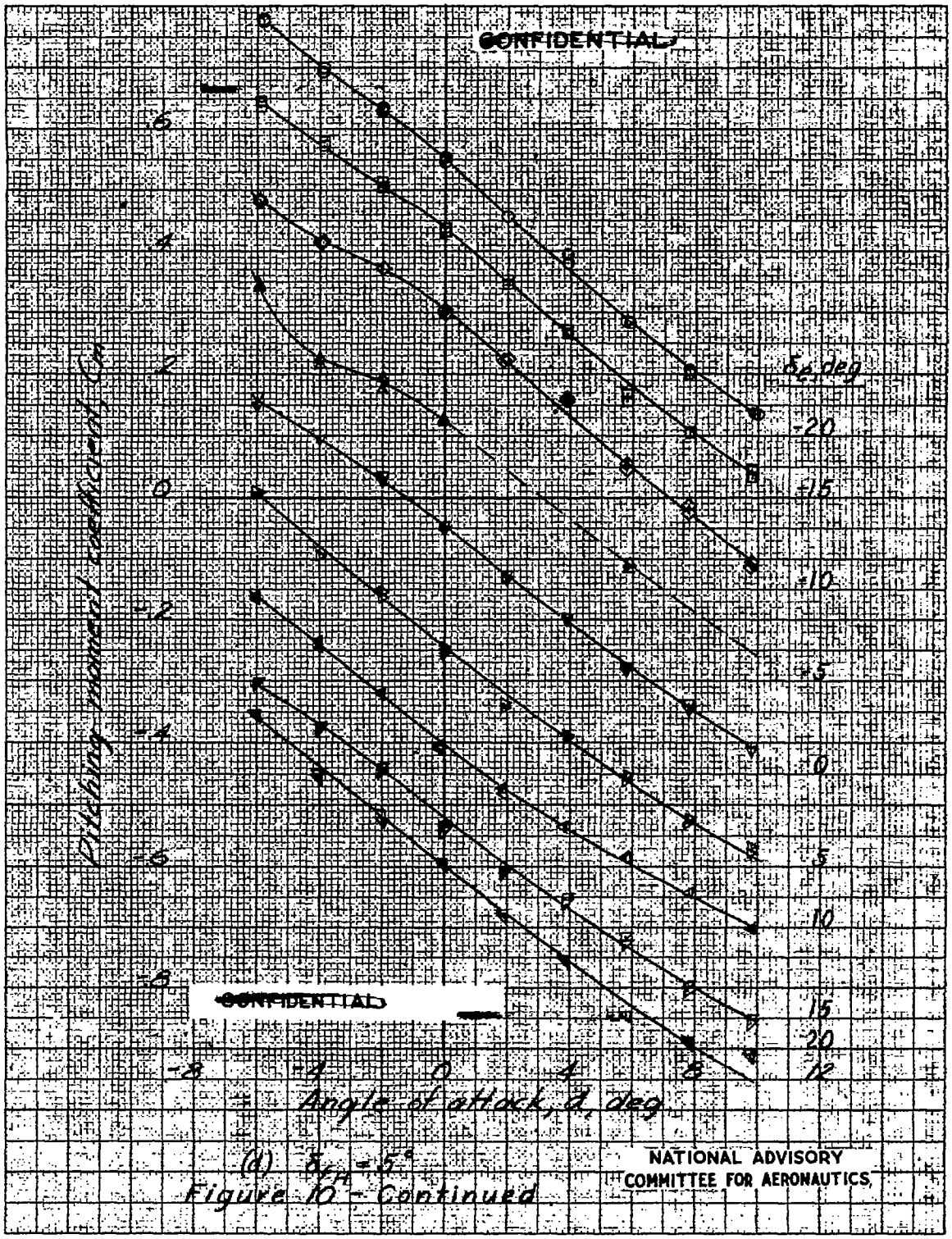


(d) $\delta_{e_A} = 5°$

Figure 10 - Continued

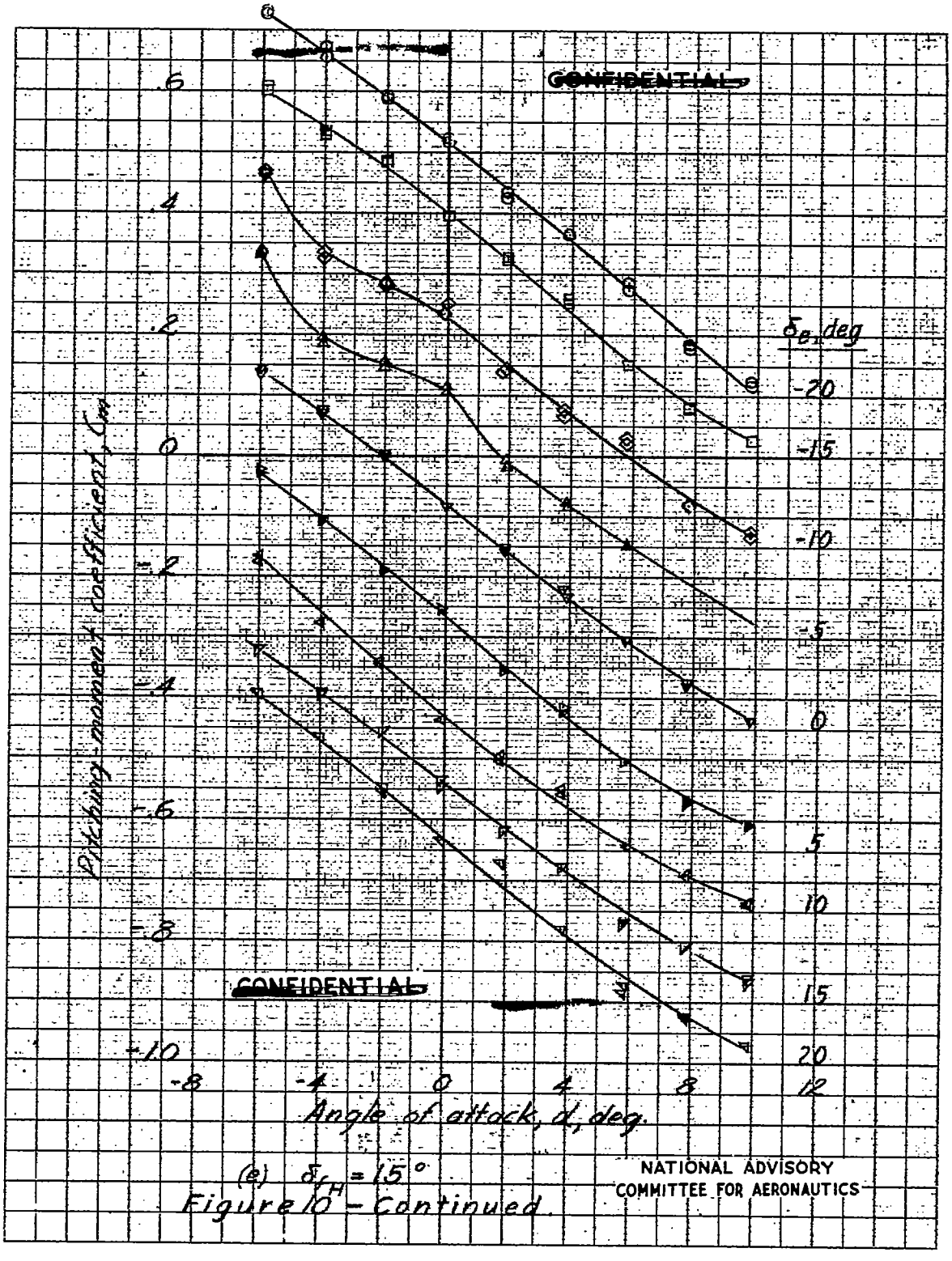


(e) $\delta_{f_H} = 15°$

Figure 10 - Continued.

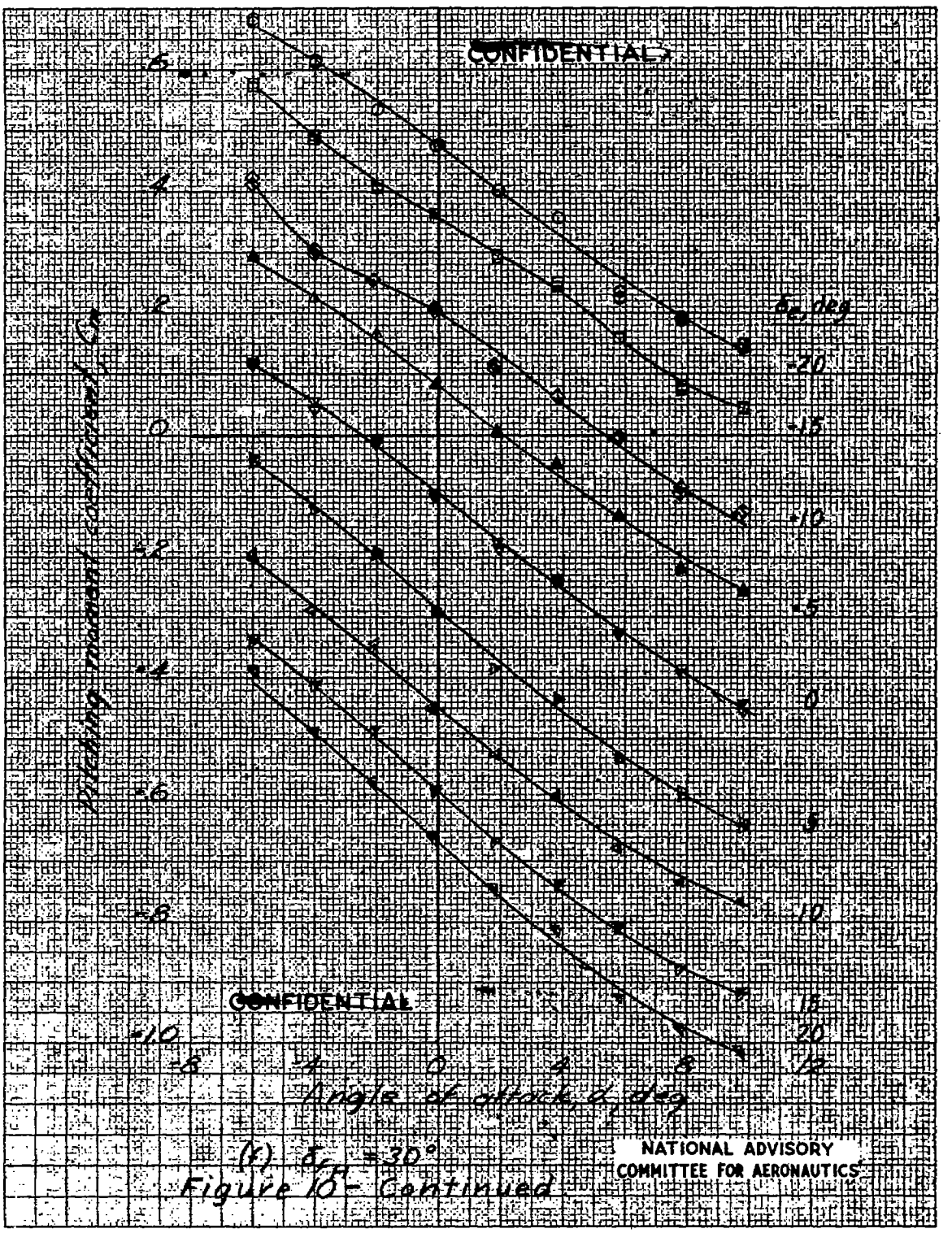


(f) $\delta_{f_1} = 30°$

Figure 10- Continued

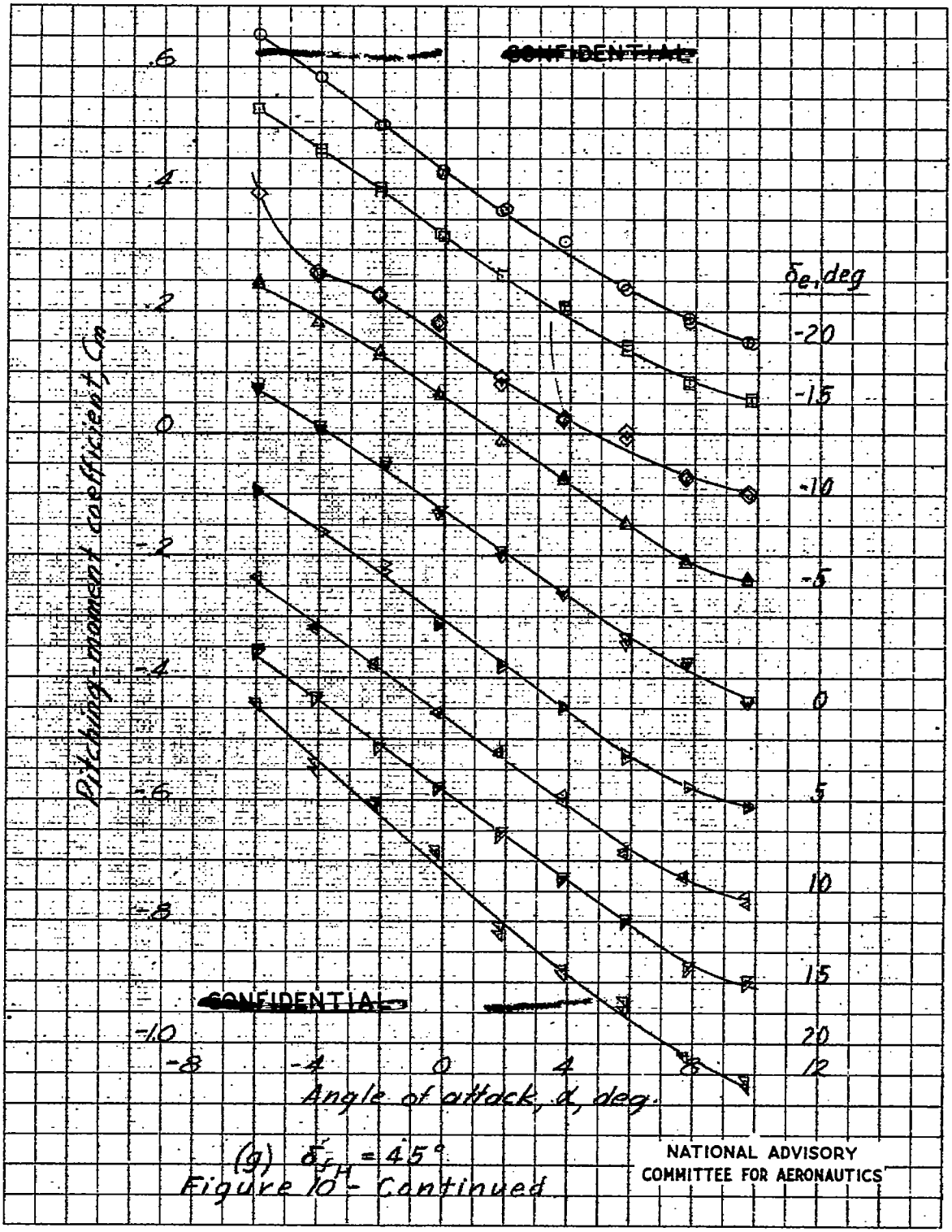


(g) $\delta_{f_H} = 45°$

Figure 10 - Continued

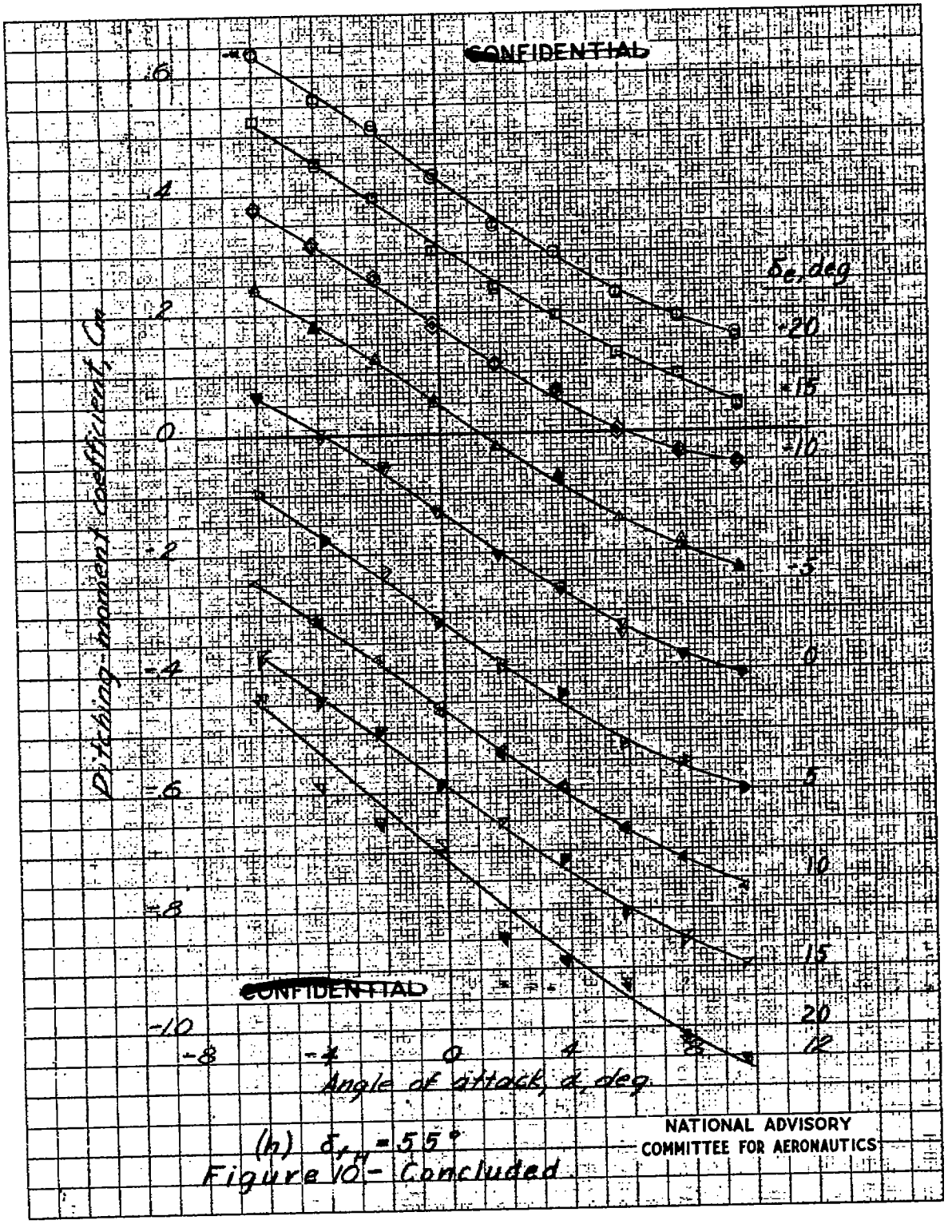


(h) $\delta_{f,H} = 55°$

Figure 10- Concluded.

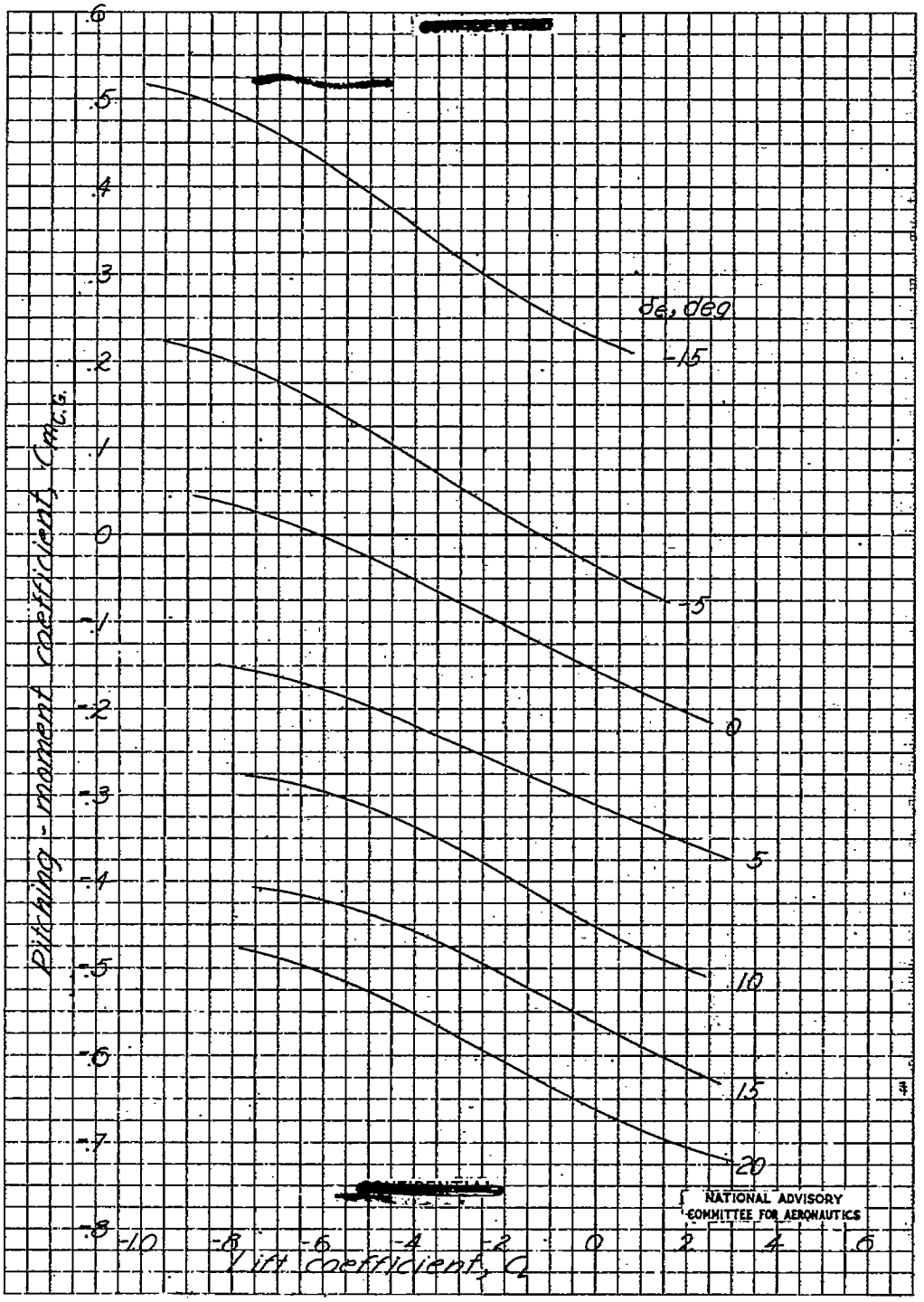


(a) $\delta_{f_H} = -55^\circ$.

Figure 11.- Variation of pitching-moment coefficient with lift coefficient for various horizontal-wing flap and elevator deflections. Moment center at 19.8 percent M.A.C. aft of wing leading edge.

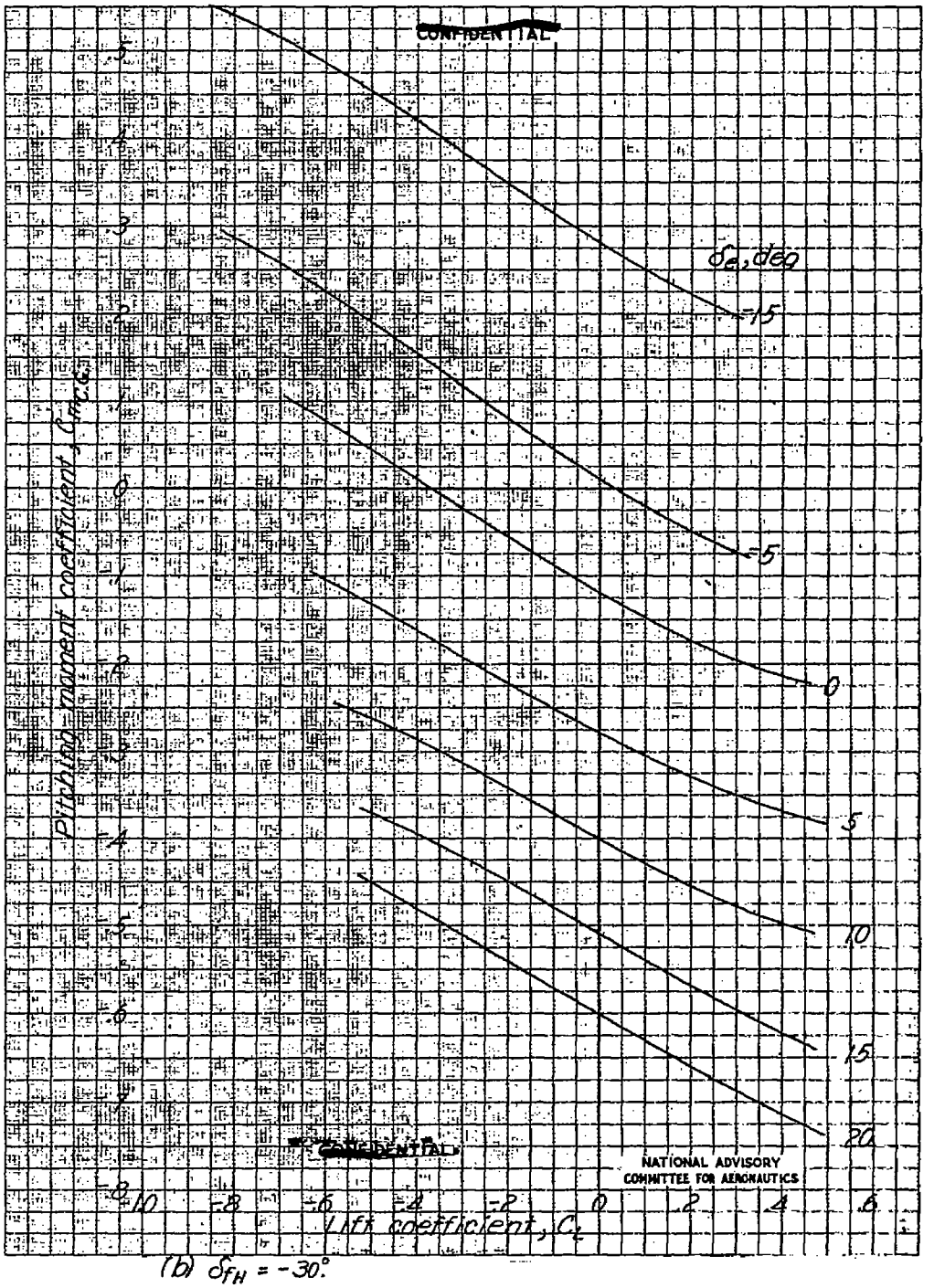


(b) $\delta_{FH} = -30°$

Figure 11.- Continued.

(c) $\delta_{f_H} = 0°$.

Figure 11 .- Continued.

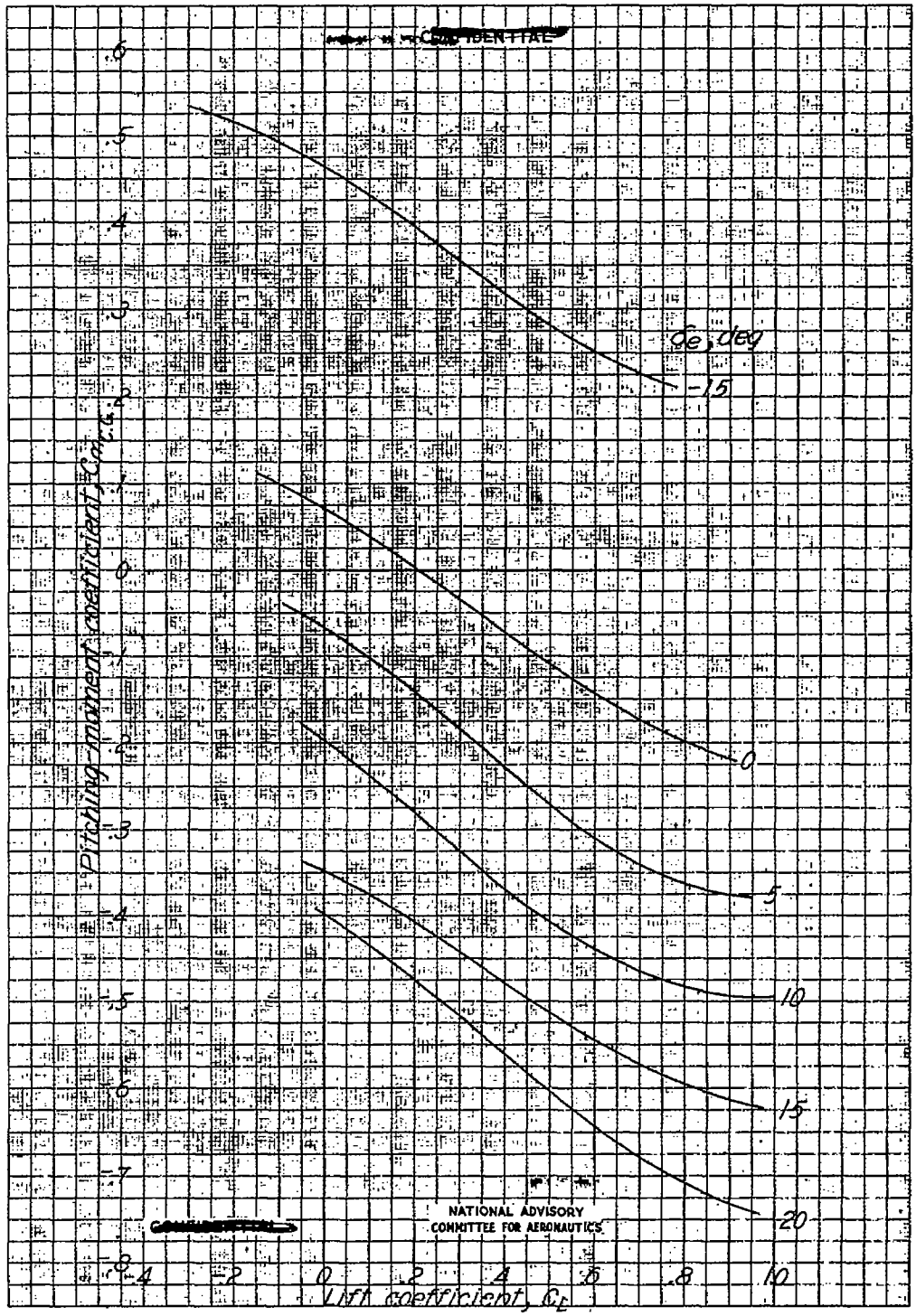


(d) $\delta_{tH} = 15°$.

Figure 11. - Continued.

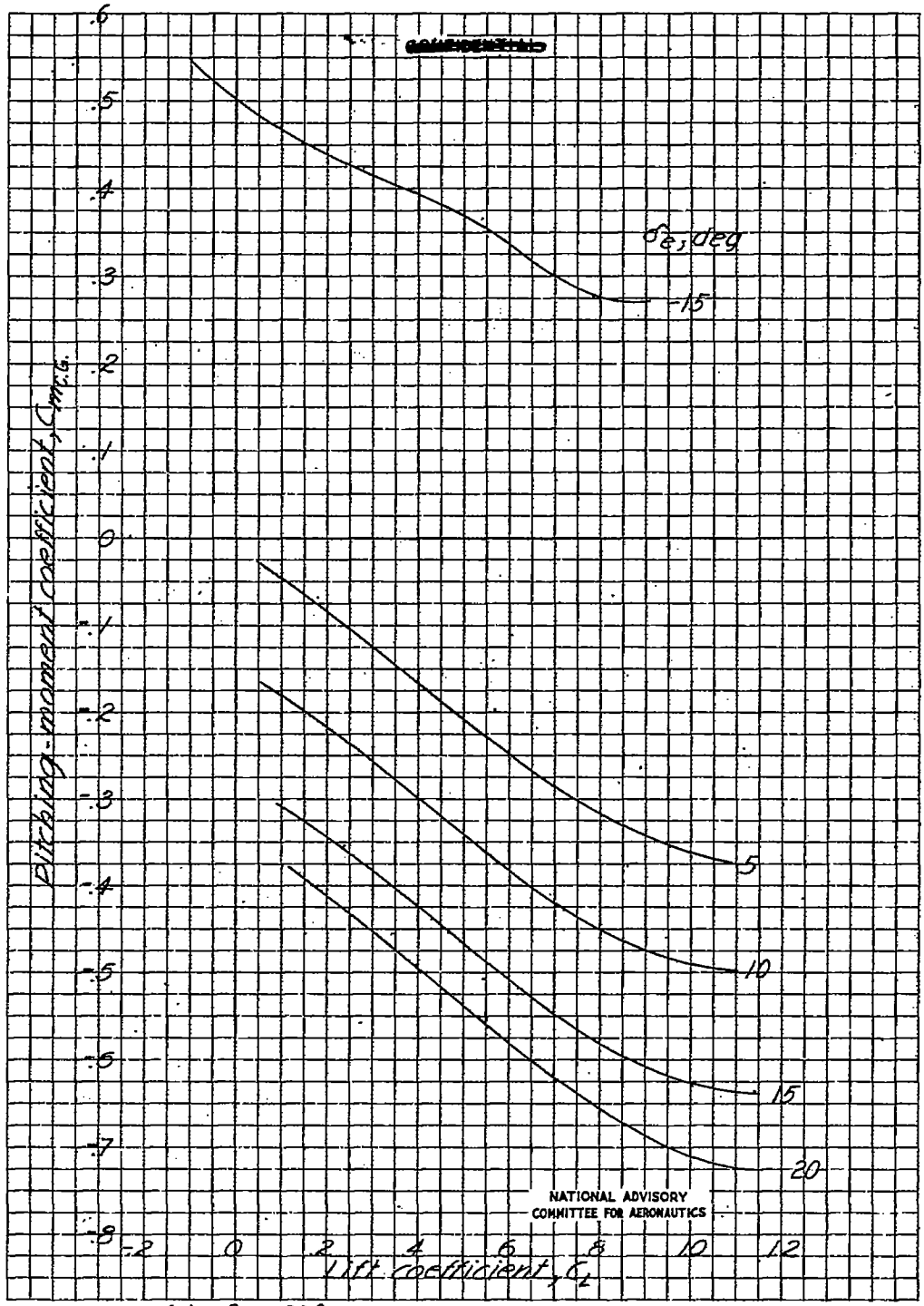


(e) $\delta_{f_H} = 30°$.

CONFIDENTIAL

Figure 11. - Continued.

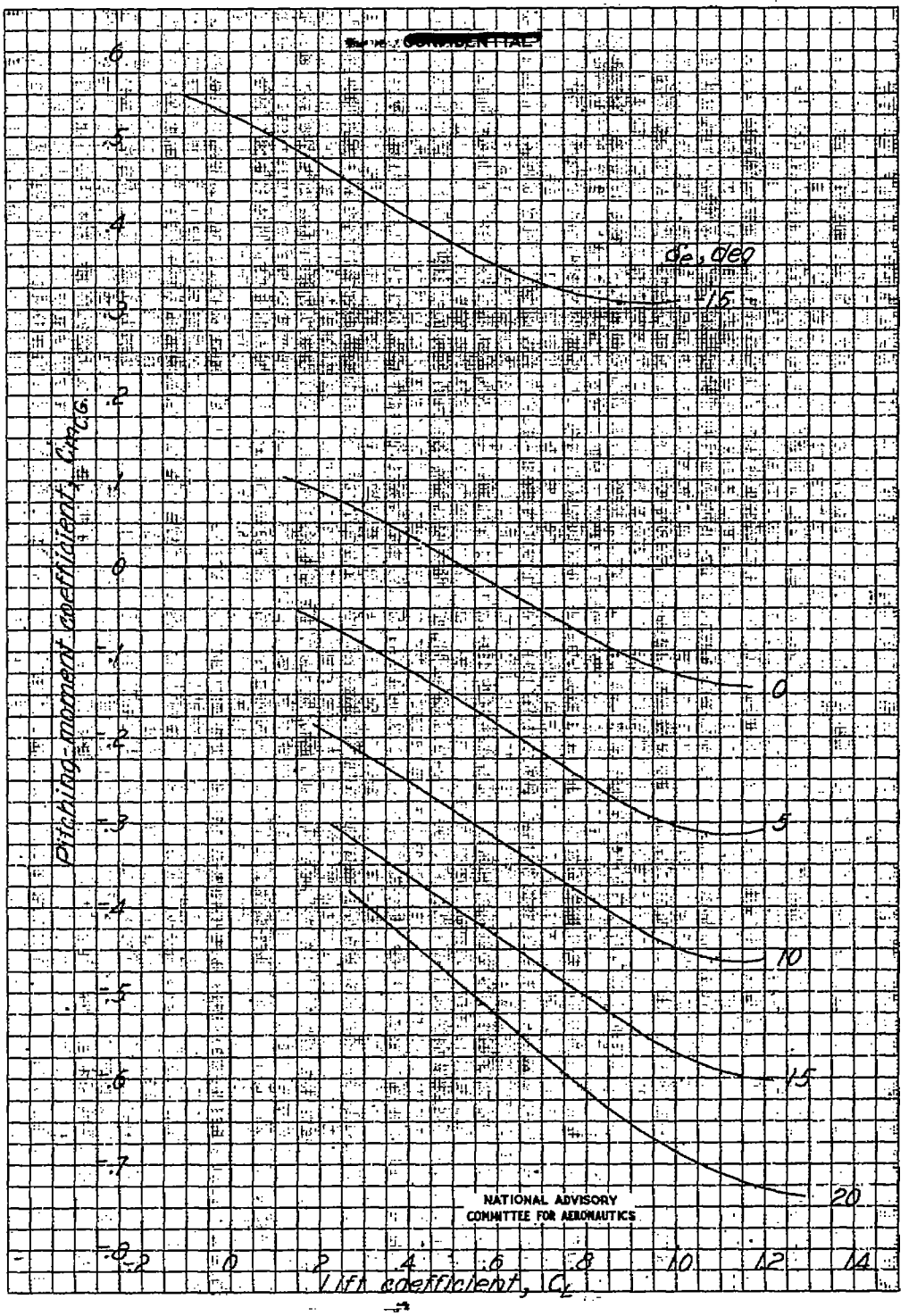


(f) $\delta_{f_H} = 45°$

Figure 11.- Continued.

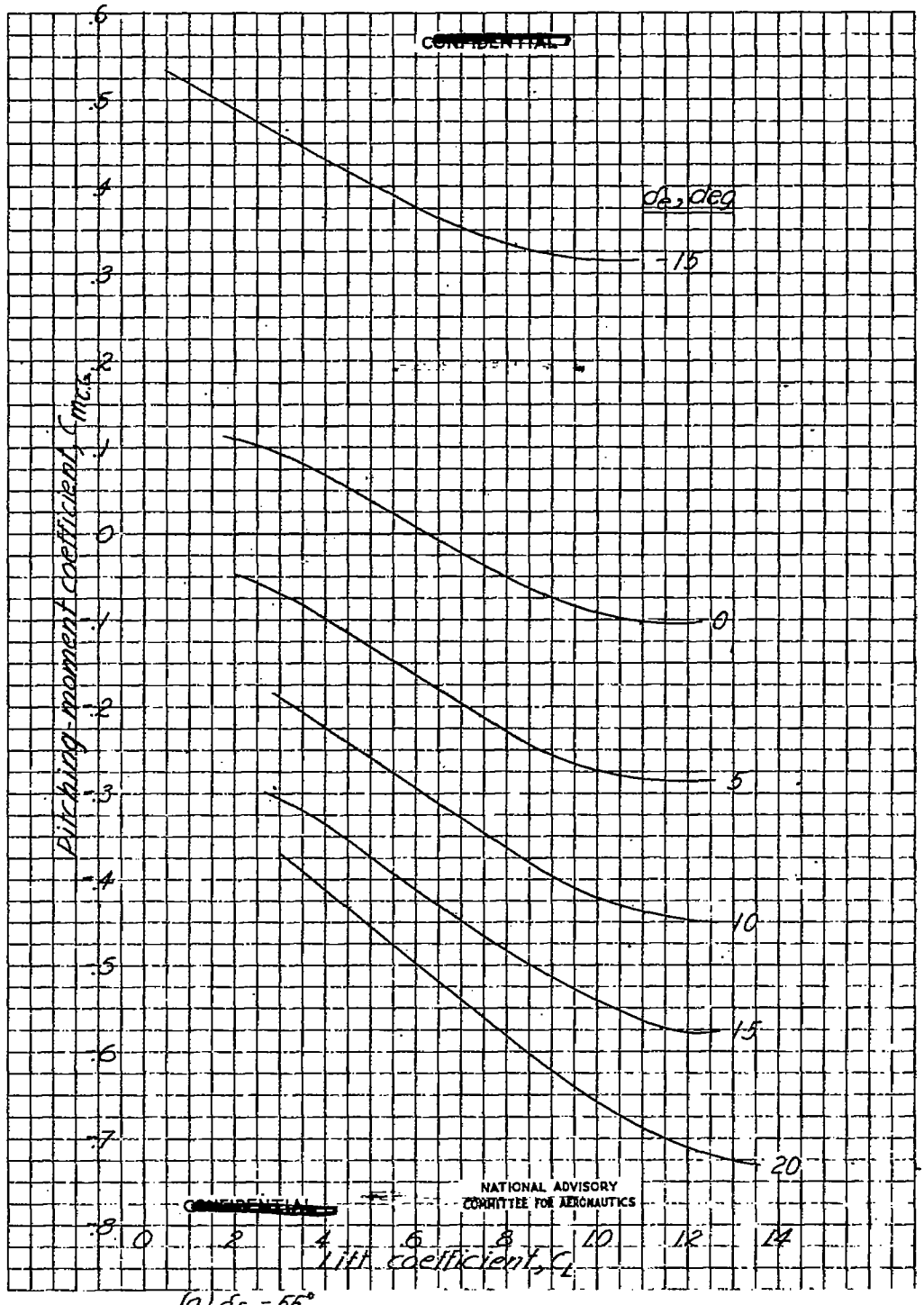


(g) $\delta_{F_H} = 55°$.

Figure 11.-Concluded.

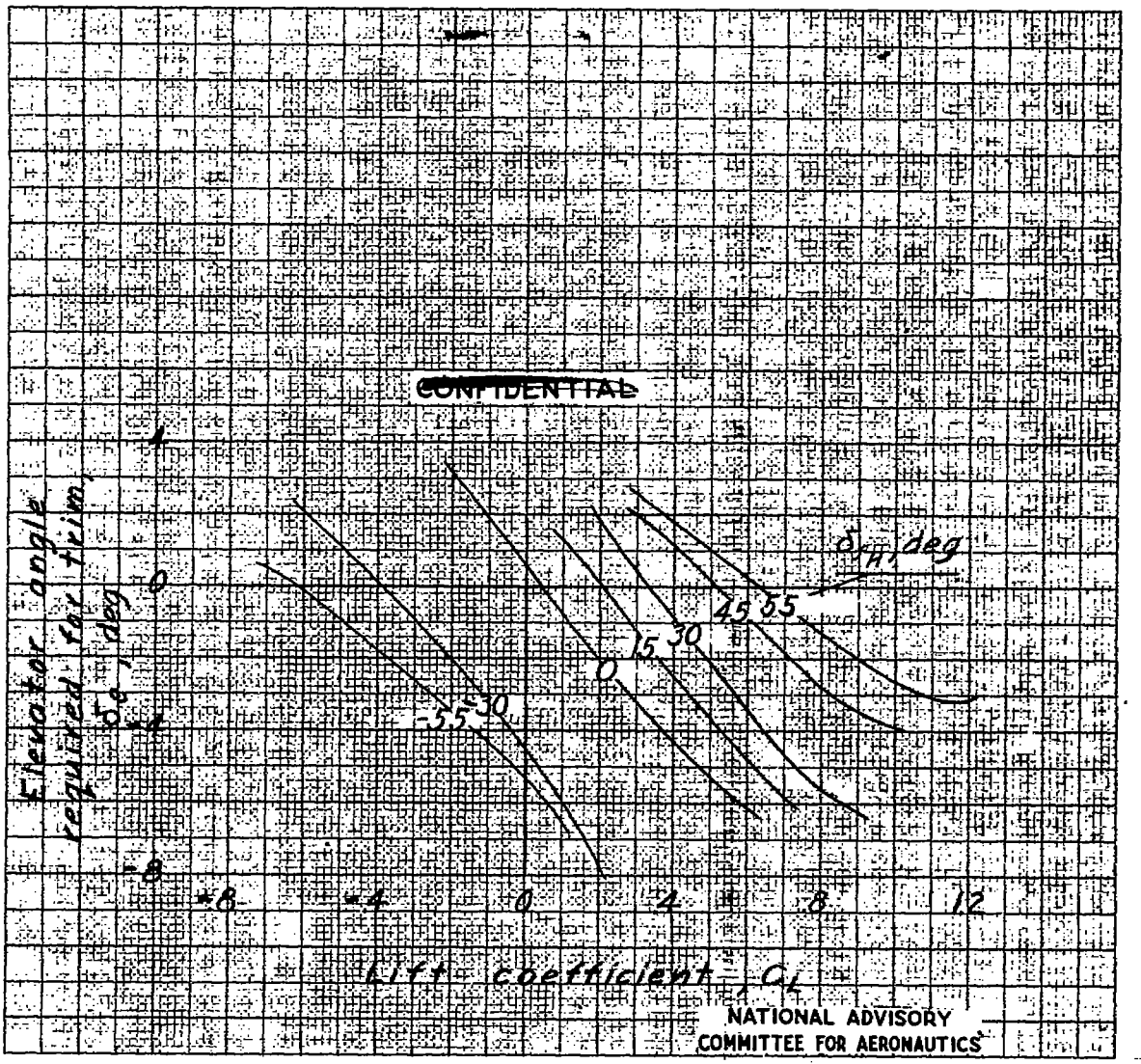


Figure 12.- Variation of elevator trim setting with lift coefficient for several horizontal-wing-flap deflections. Moment center at 19.8 percent M.A.C. aft of wing leading edge.

CONFIDENTIAL

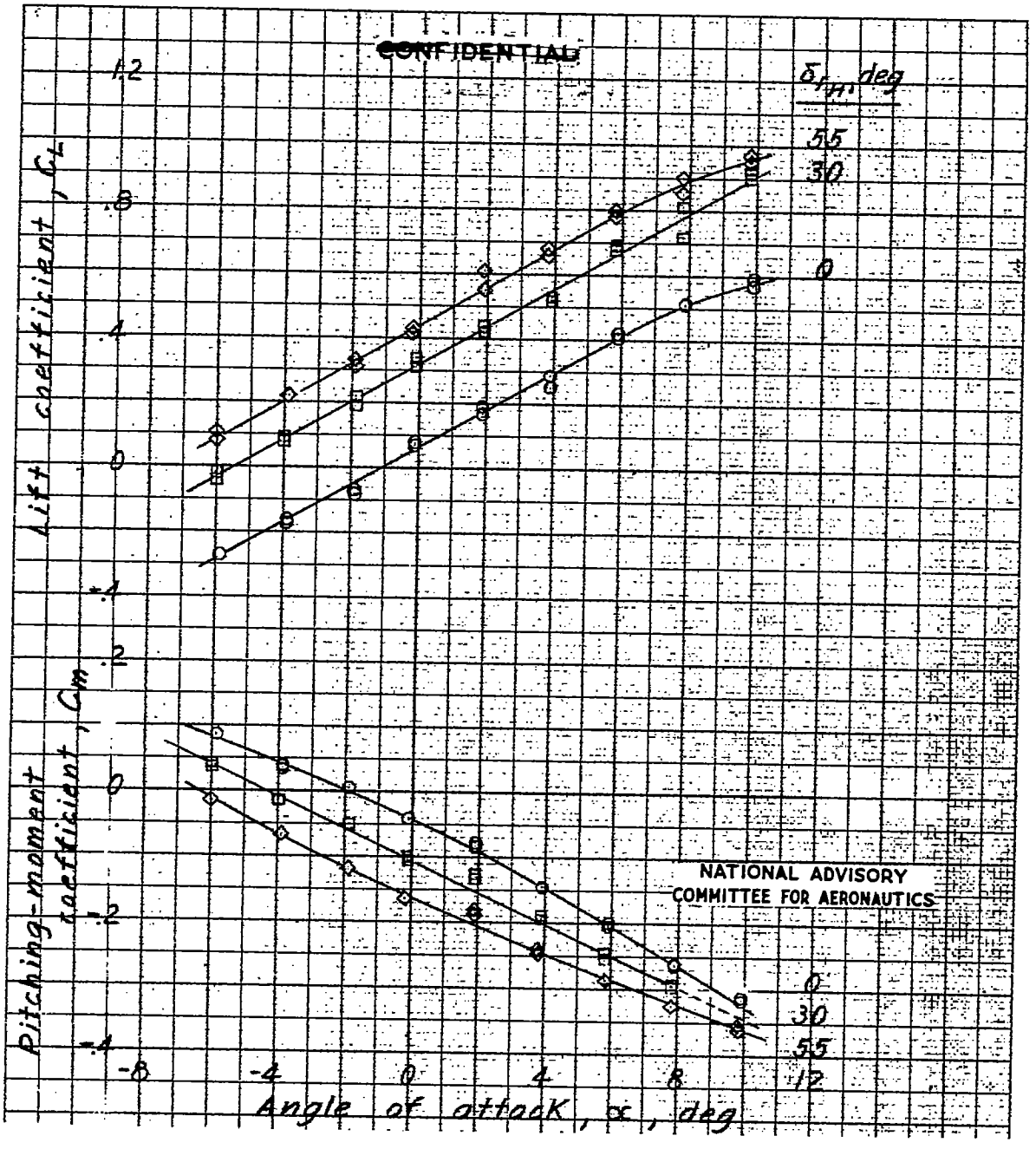


(a) Lift and pitching-moment coefficients.

Figure 13.- Aerodynamic characteristics of the airplane with JATO units attached. $\delta_e = 0^\circ$. Moment center at pivot point.

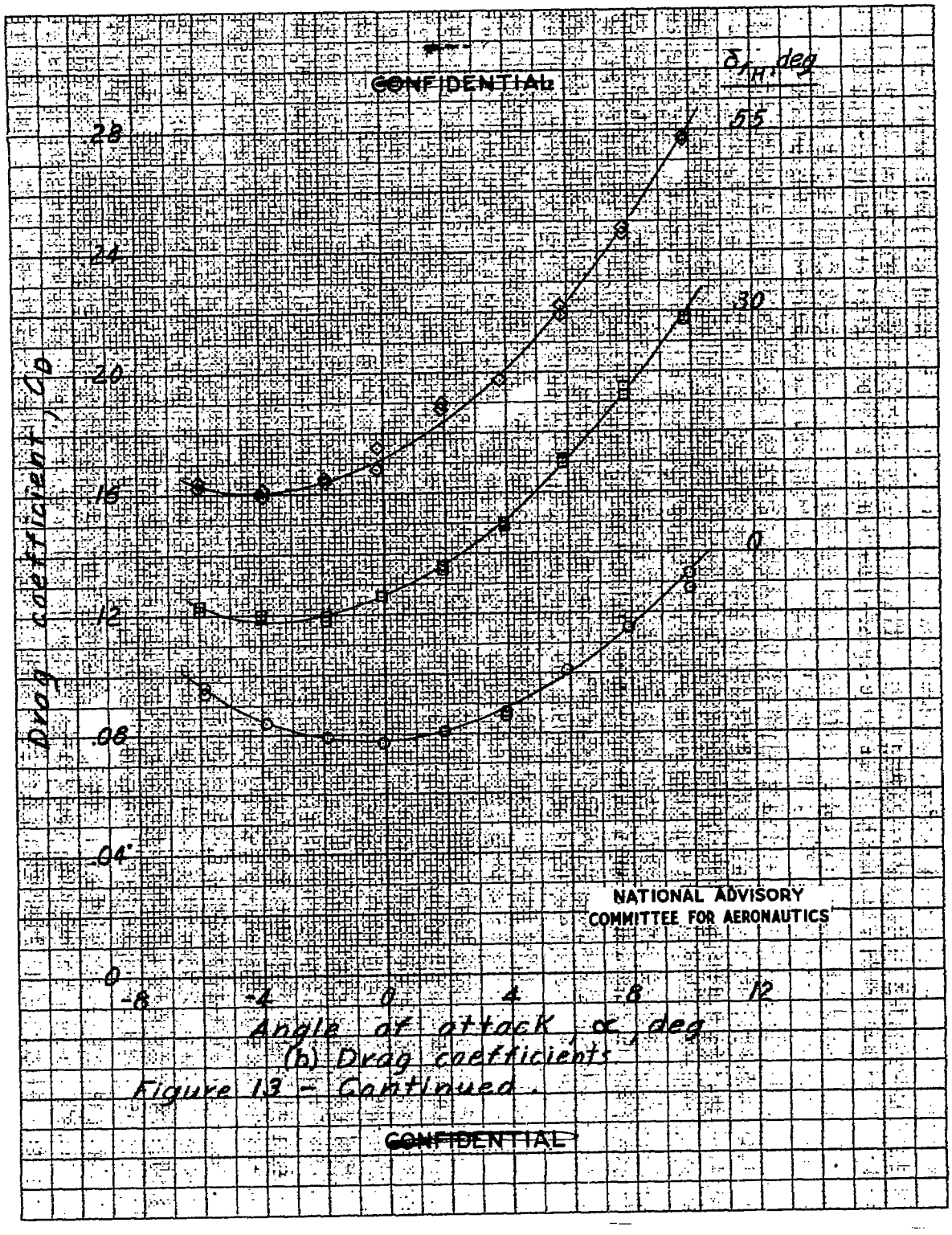


(b) Drag coefficients.

Figure 13 - Continued.

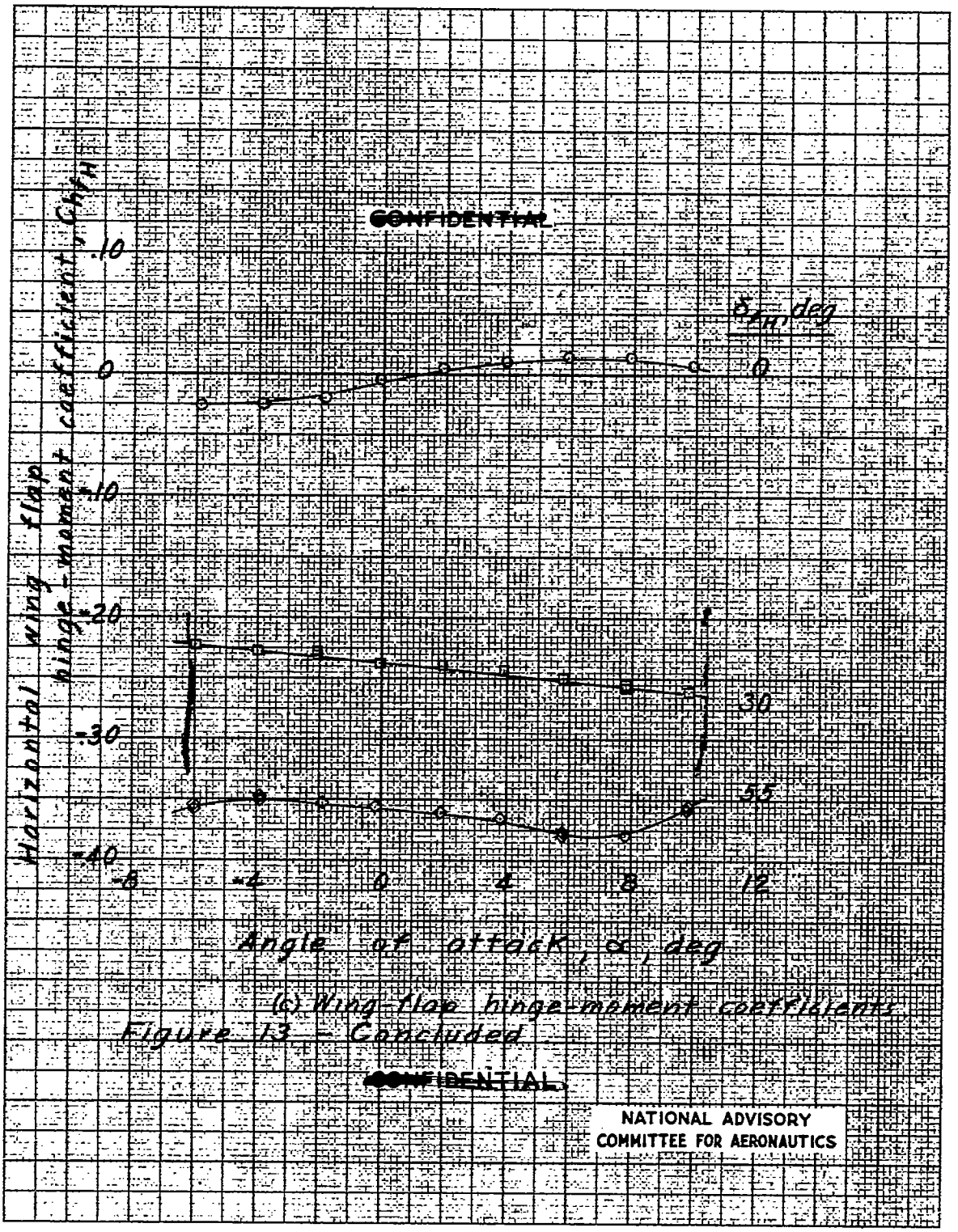


(c) Wing flap hinge-moment coefficients

Figure 13.- Concluded

CONFIDENTIAL

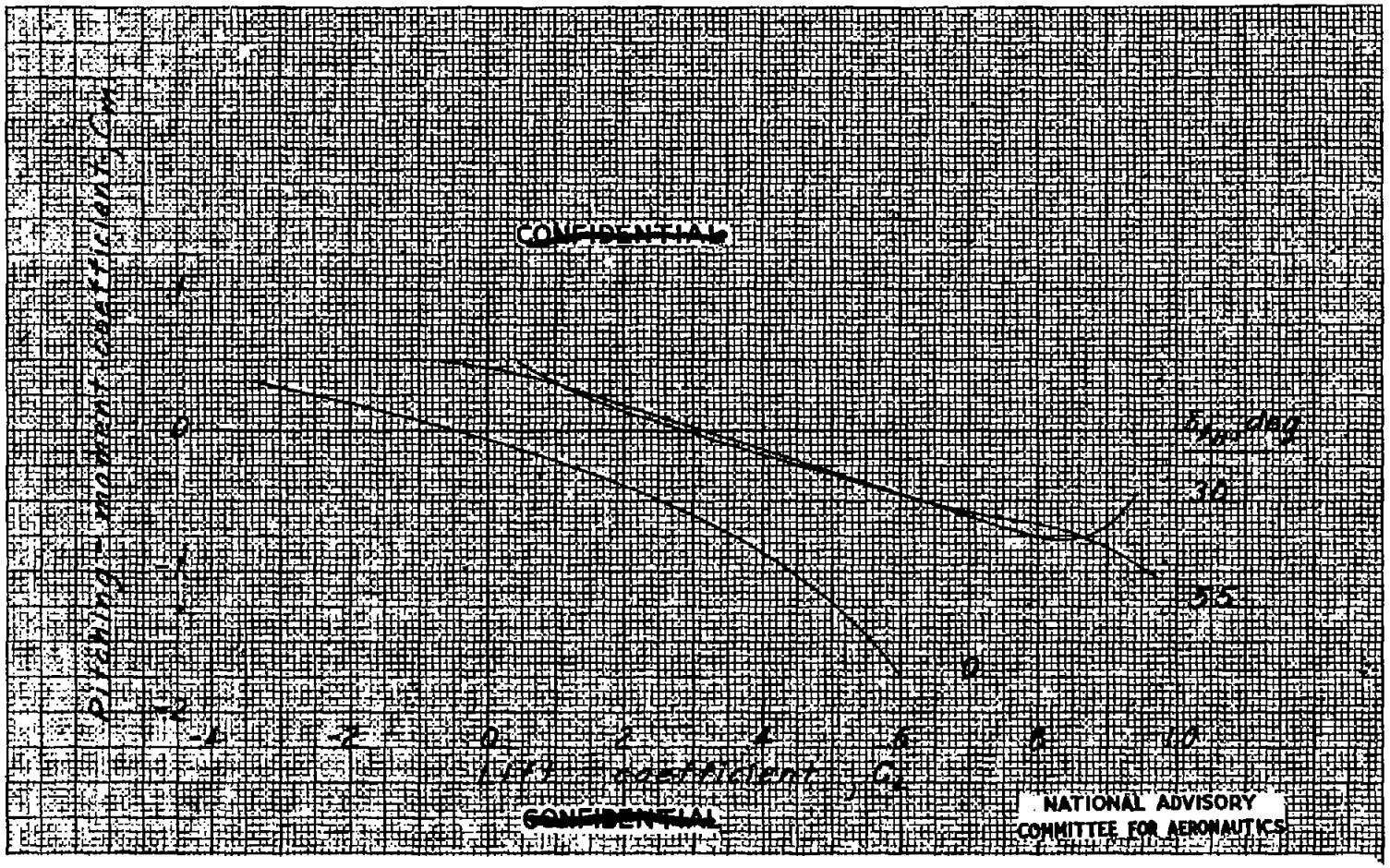


Figure 14.- Variation of pitching-moment coefficient with lift coefficient for the airplane with JATO units attached. Moment center at 19.8 percent M.A.C. aft of wing leading edge, 16.7 percent below fuselage center line. $\delta_e = 0^\circ$.

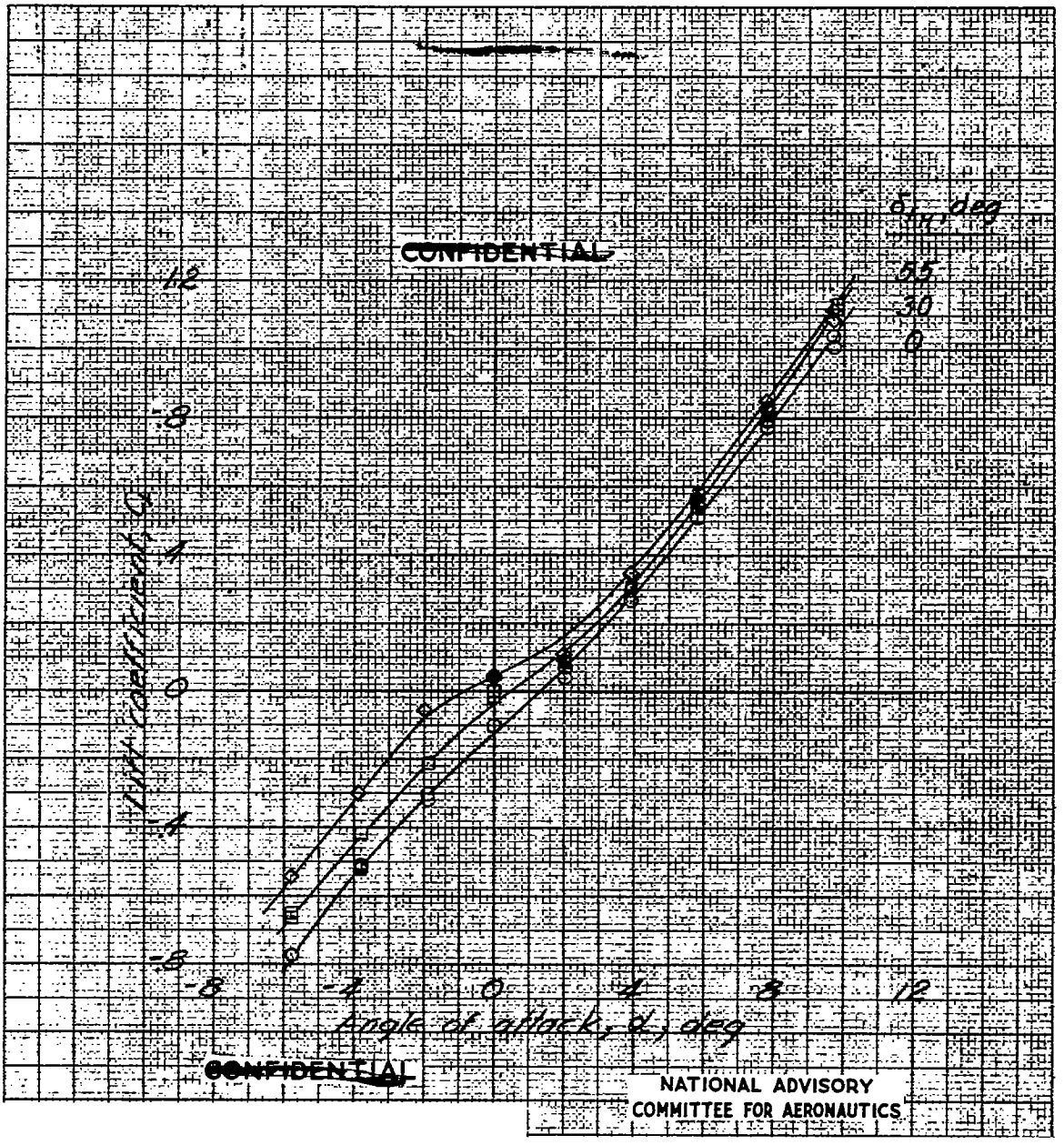


(a) $\delta_e = -20^\circ$.

Figure 15.- Aerodynamic characteristics of the airplane with rocket-booster assembly attached. Moment center at pivot point.

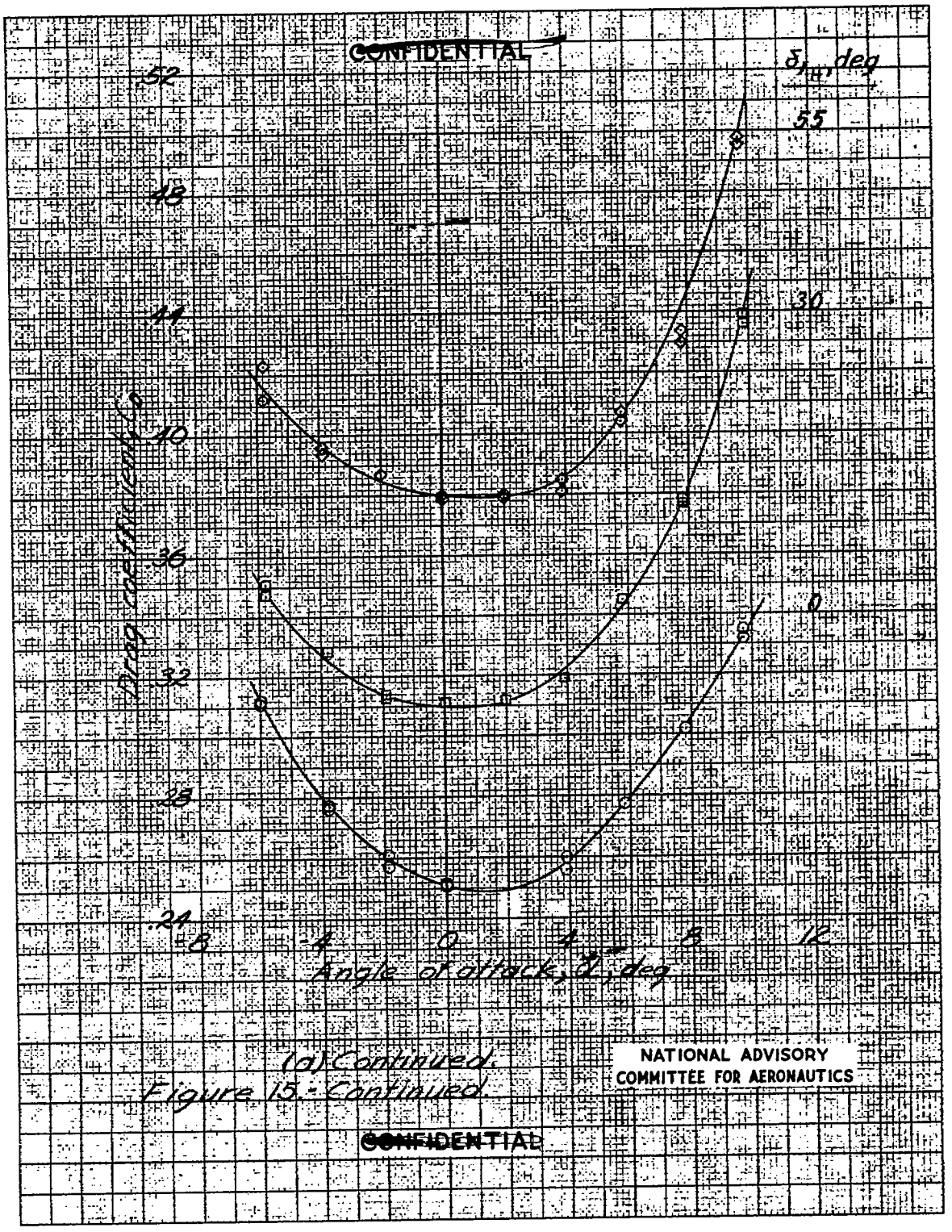


(a) Continued.

Figure 15.- Continued.

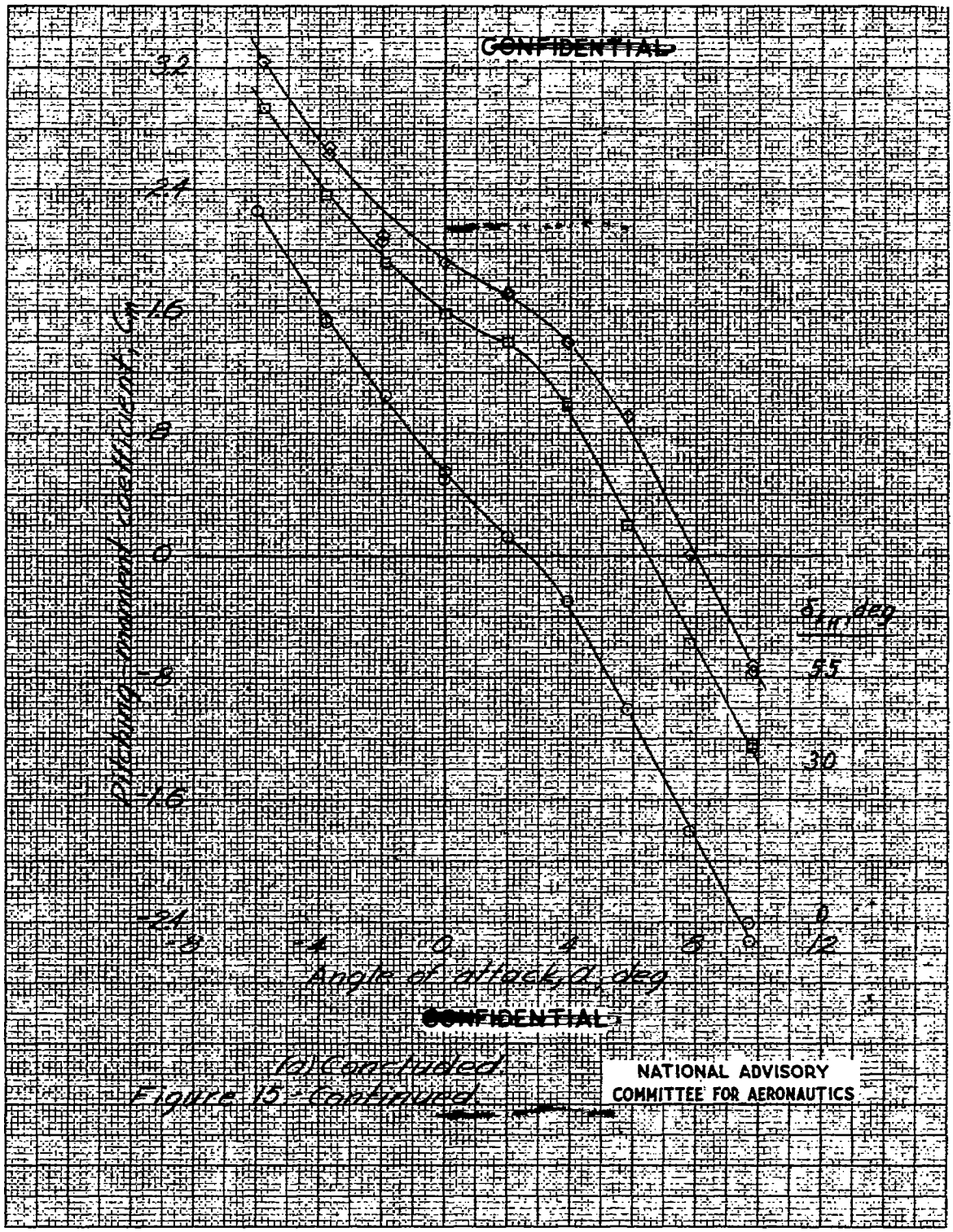


(c) Concluded

Figure 15.- Continued.

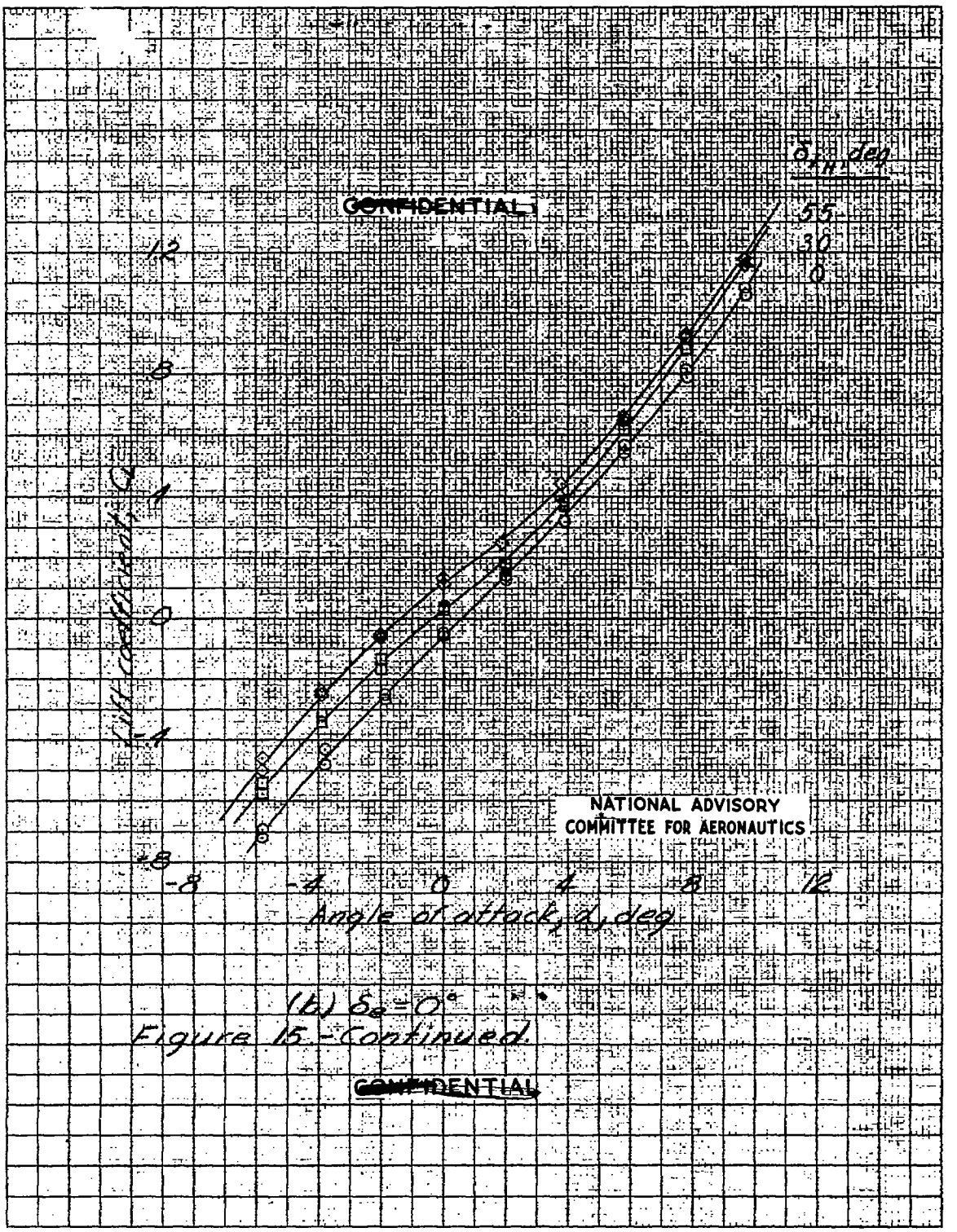


(b) $\delta_a = 0°$

Figure 15 - Continued.

Fig. 15b cont.

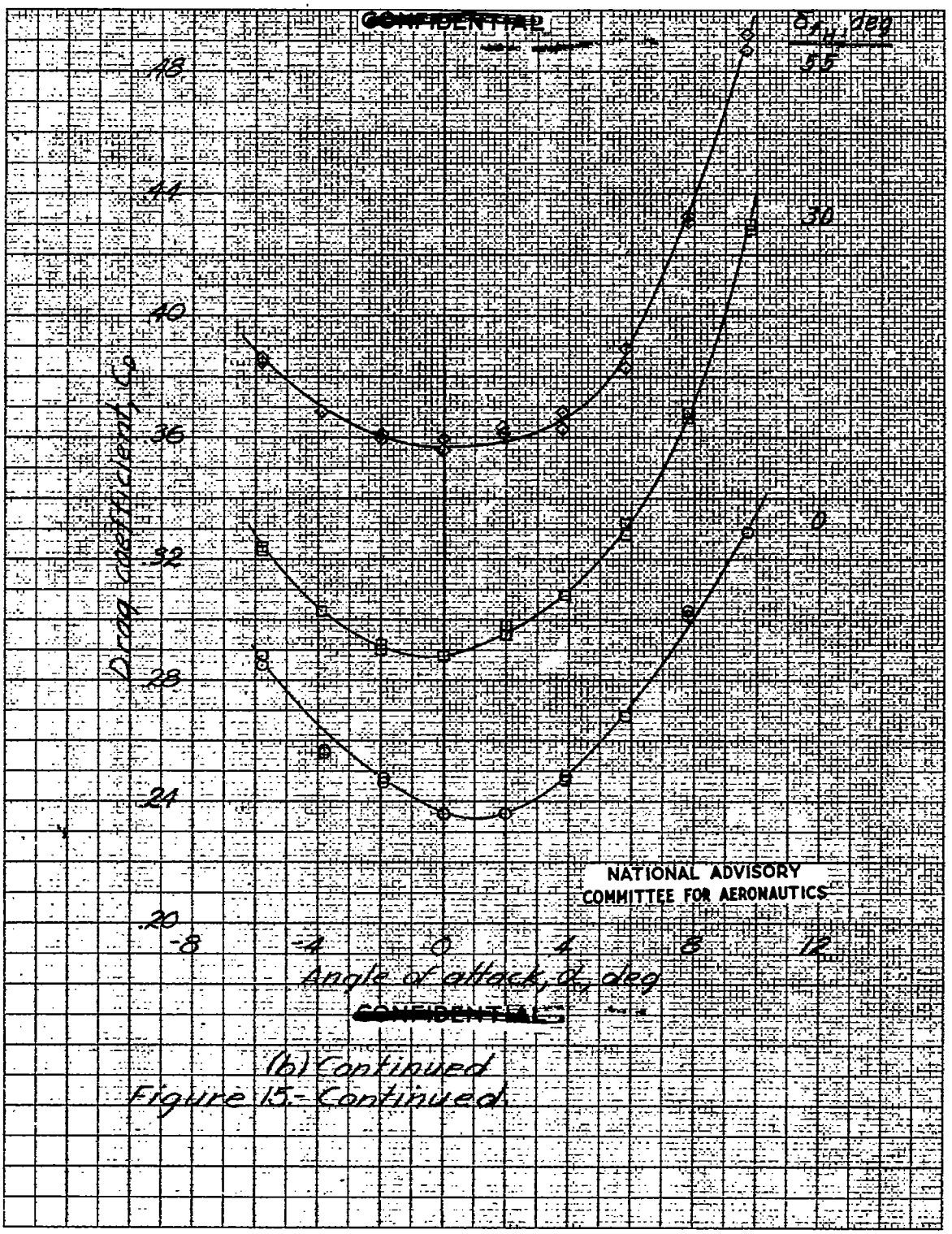


(b) Continued

Figure 15.- Continued.

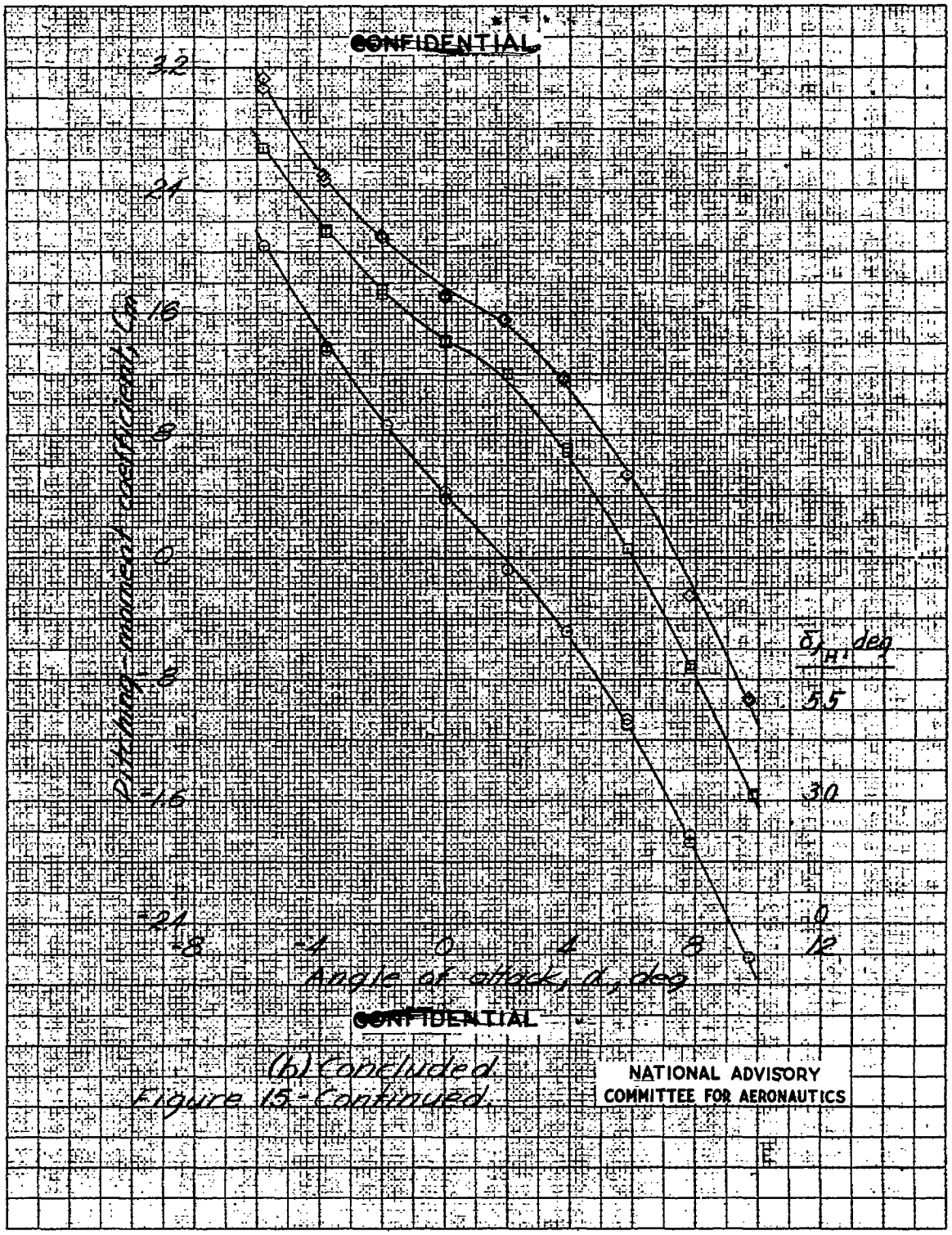


(b) Concluded

Figure 15.- Continued.

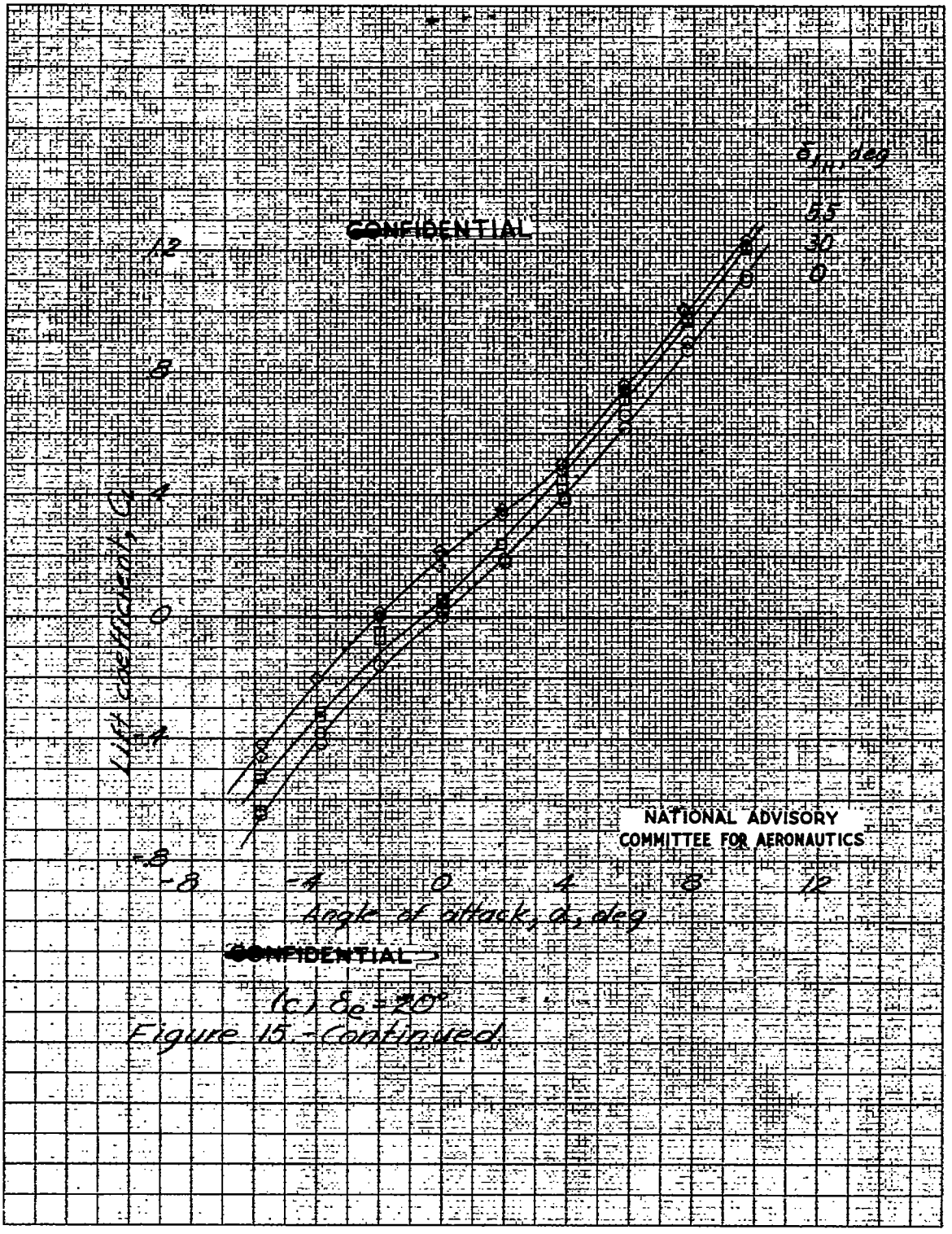


(c) $\delta_c = 20°$

Figure 15 - Continued.

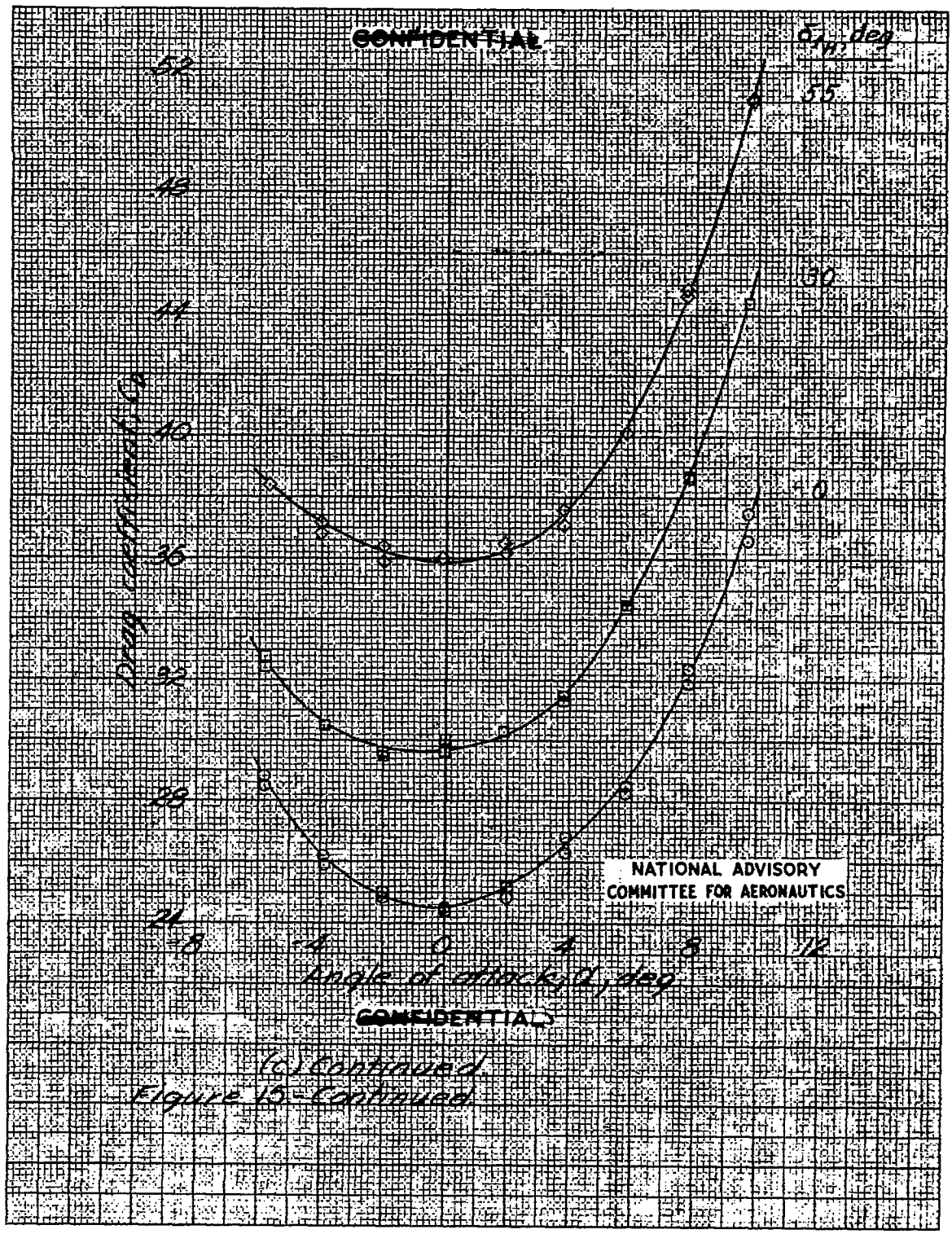


(c) Continued.

Figure 15- Continued.

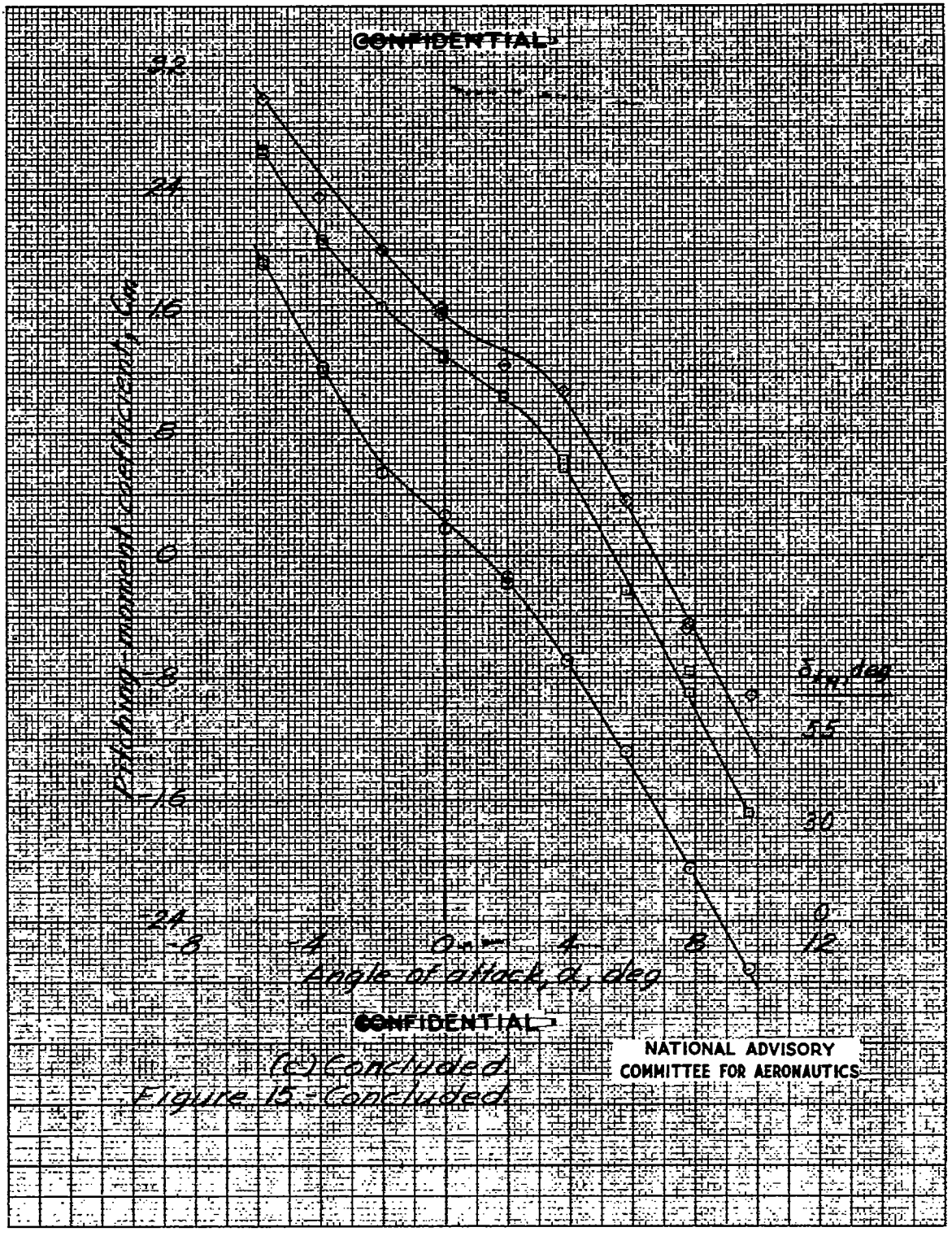


(c) Concluded

Figure 15.- Concluded.

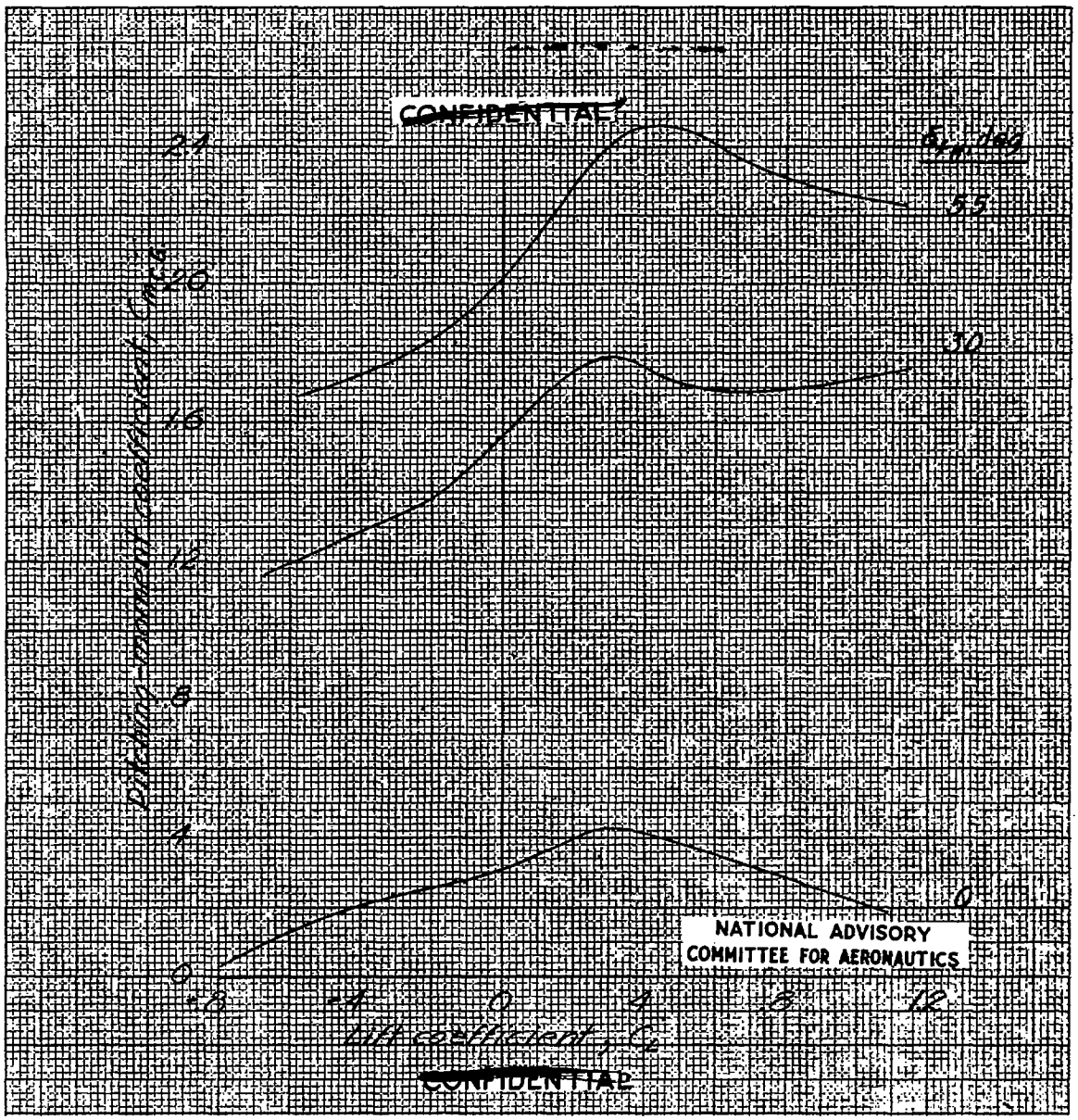


(a) $\delta_e = -20^\circ$.

Figure 16.- Variation of pitching-moment coefficient with lift coefficient for the airplane with rocket-booster assembly attached. Moment center at 251.4 percent M.A.C. aft of wing leading edge.

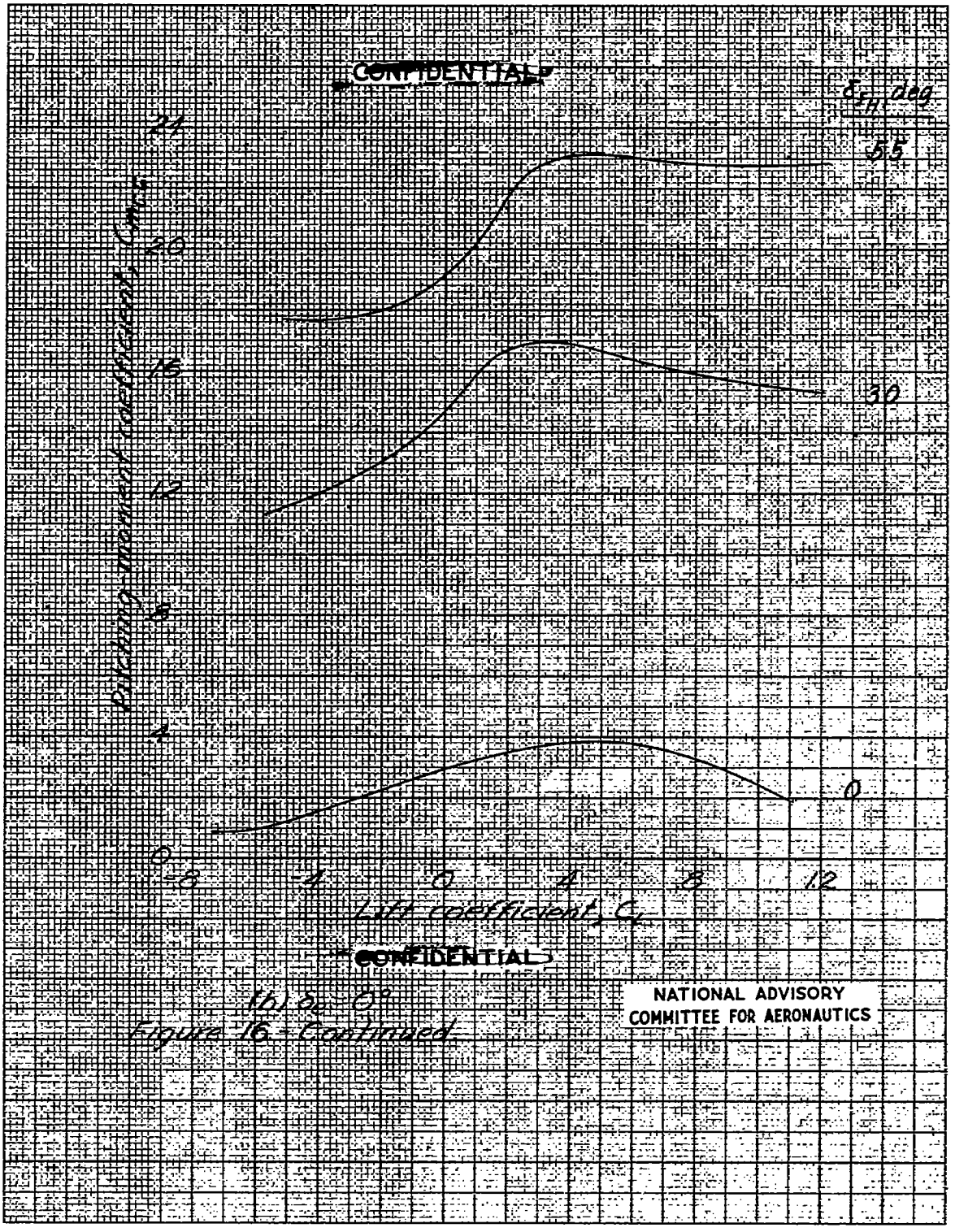


(b) $\alpha_e = 0°$

Figure 16.- Continued

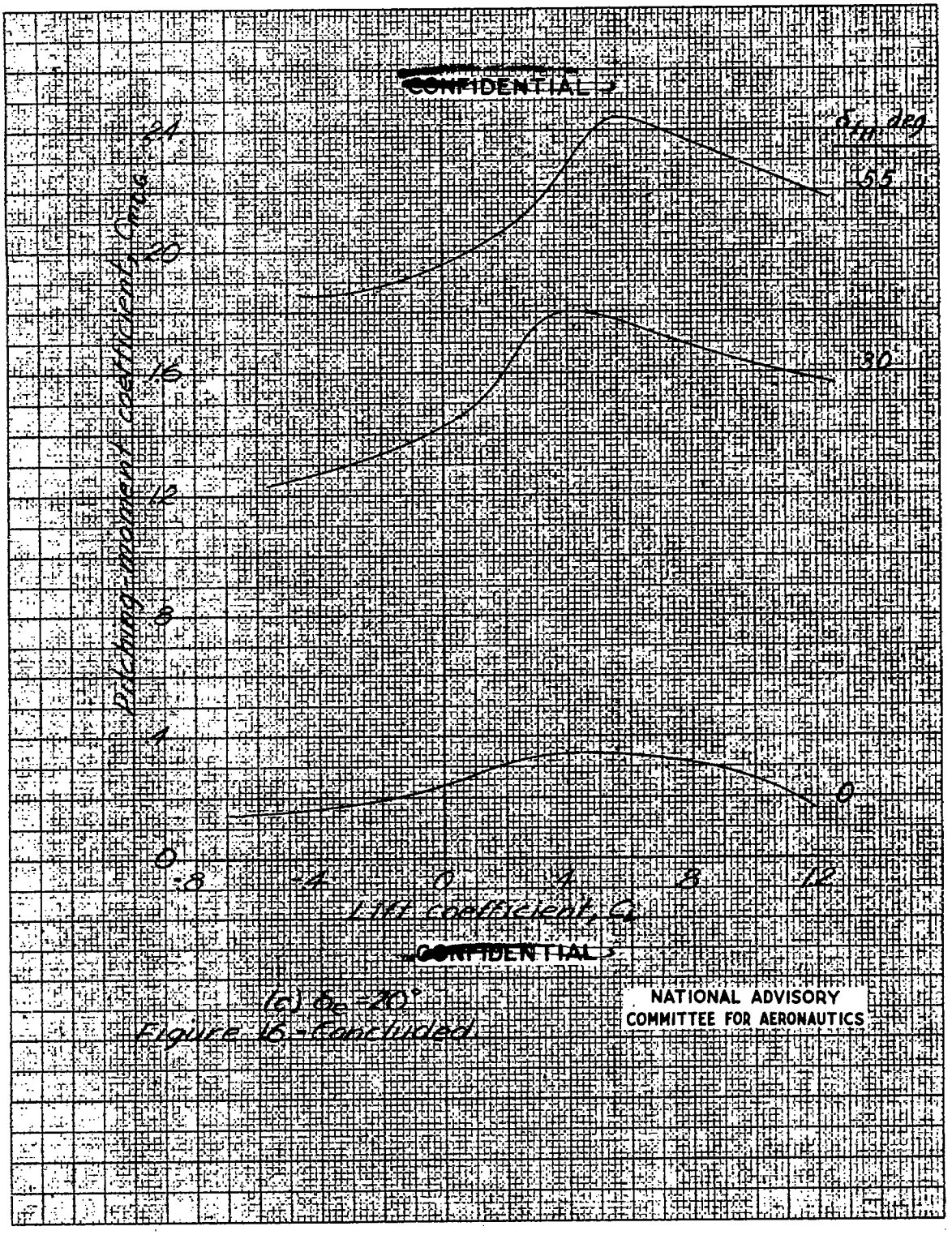


Figure 16.- Concluded.

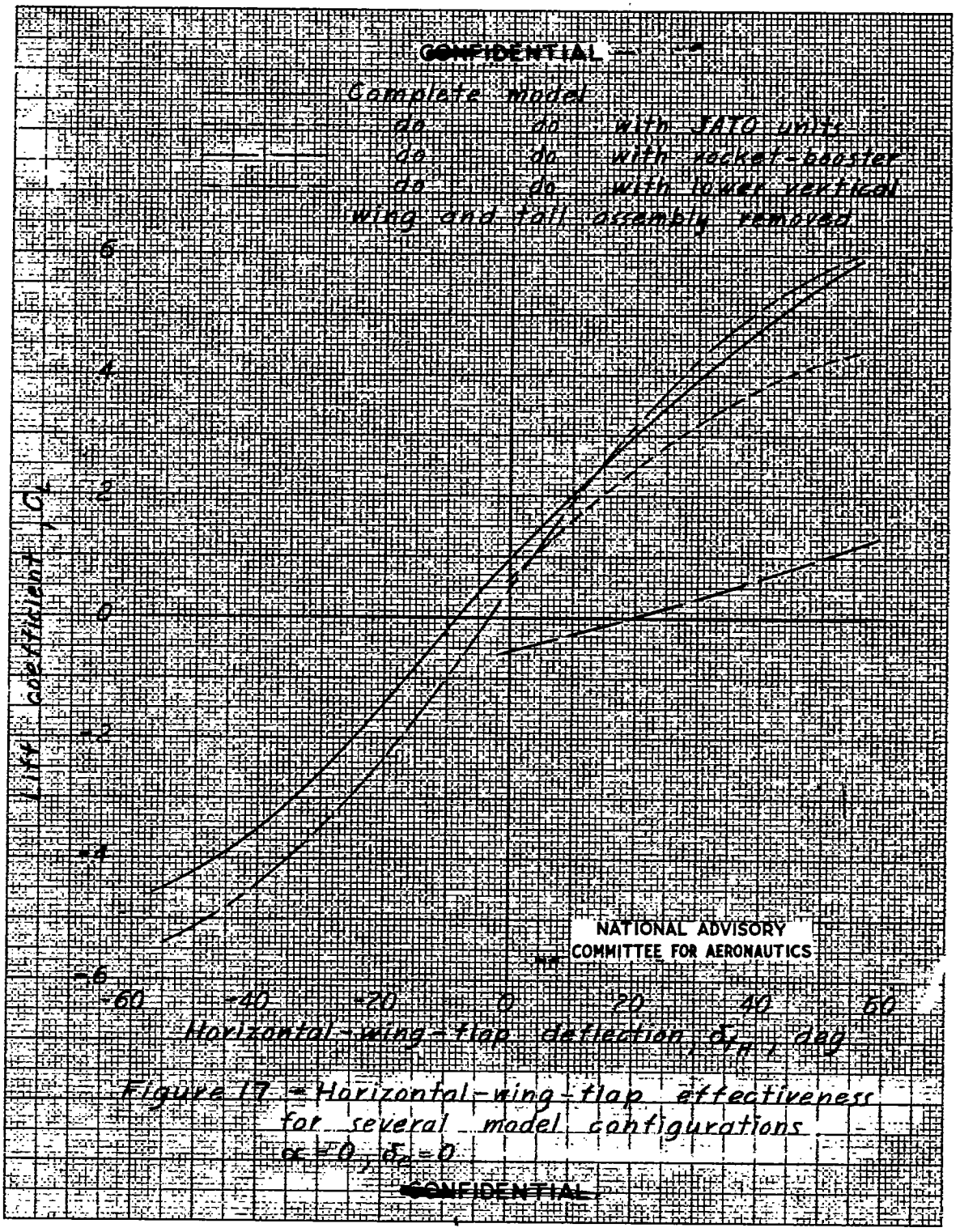


Figure 17 - Horizontal-wing-flap effectiveness for several model configurations. $\alpha = 0$, $\delta_a = 0$

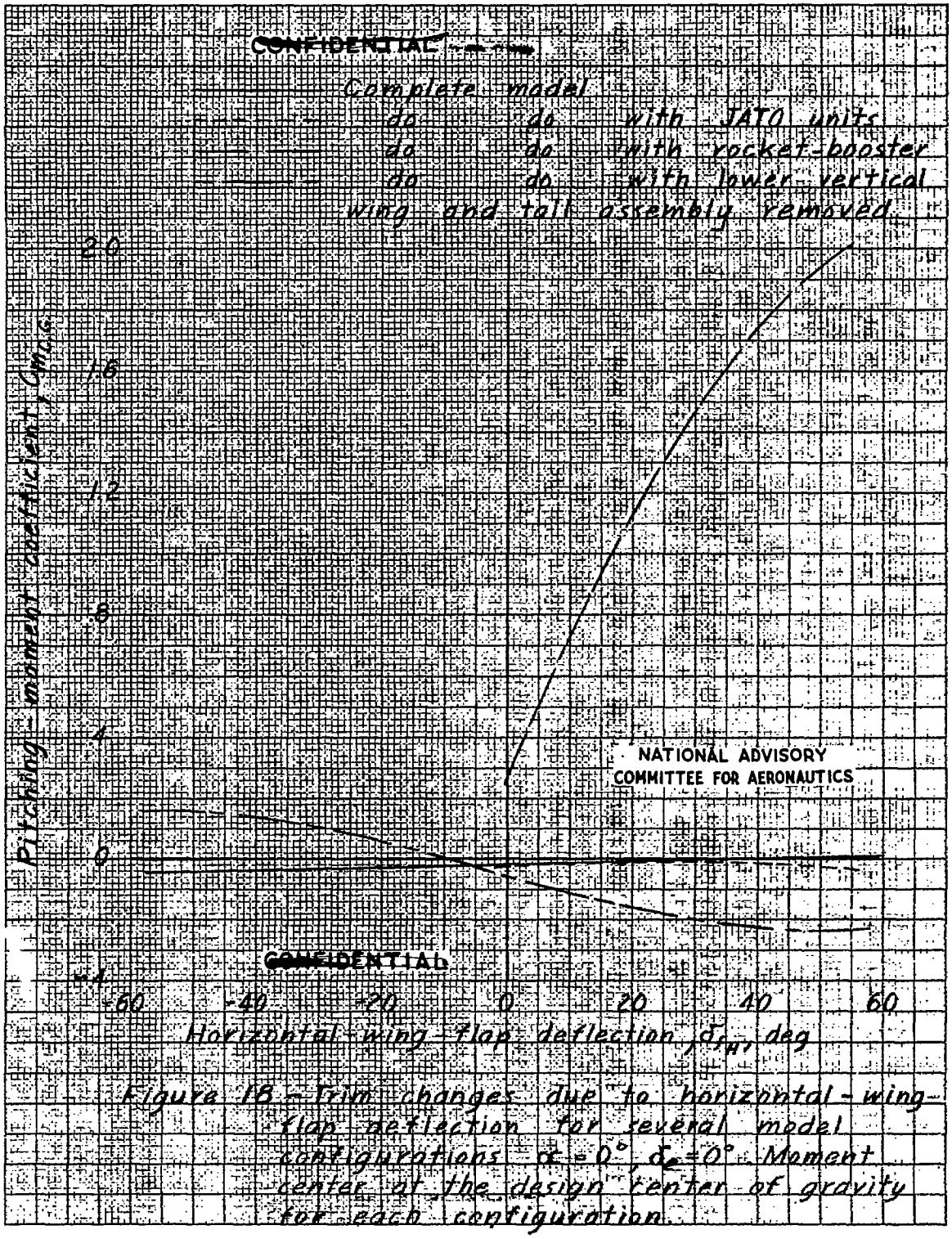


Figure 18.- Trim changes due to horizontal-wing-flap deflection for several model configurations. $\alpha = 0°$, $\delta_e = 0°$. Moment center at the design center of gravity for each configuration.

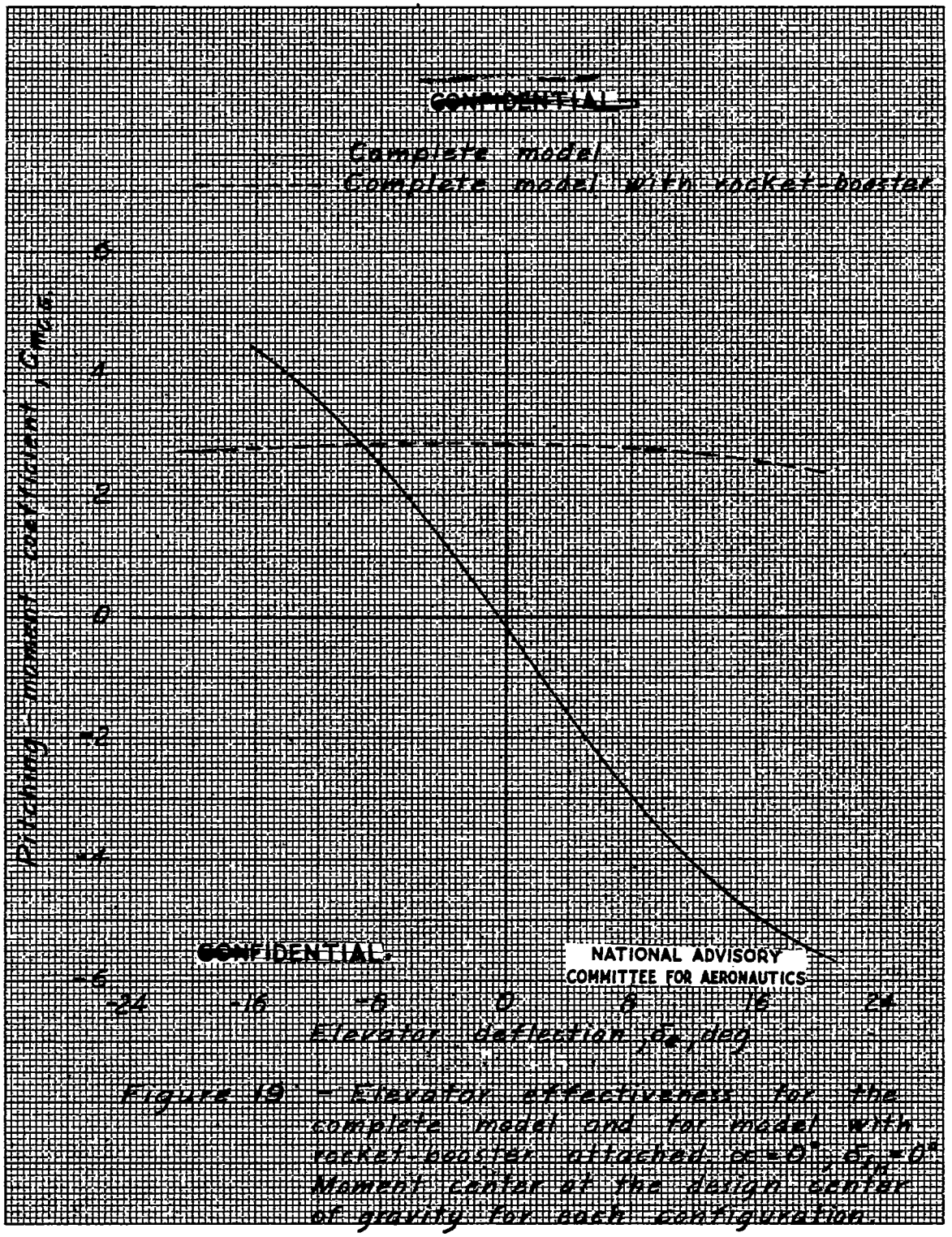


Figure 19 - Elevator effectiveness for the complete model and for model with rocket-booster attached. $\alpha = 0°$, $\delta_a = 0°$. Moment center at the design center of gravity for each configuration.

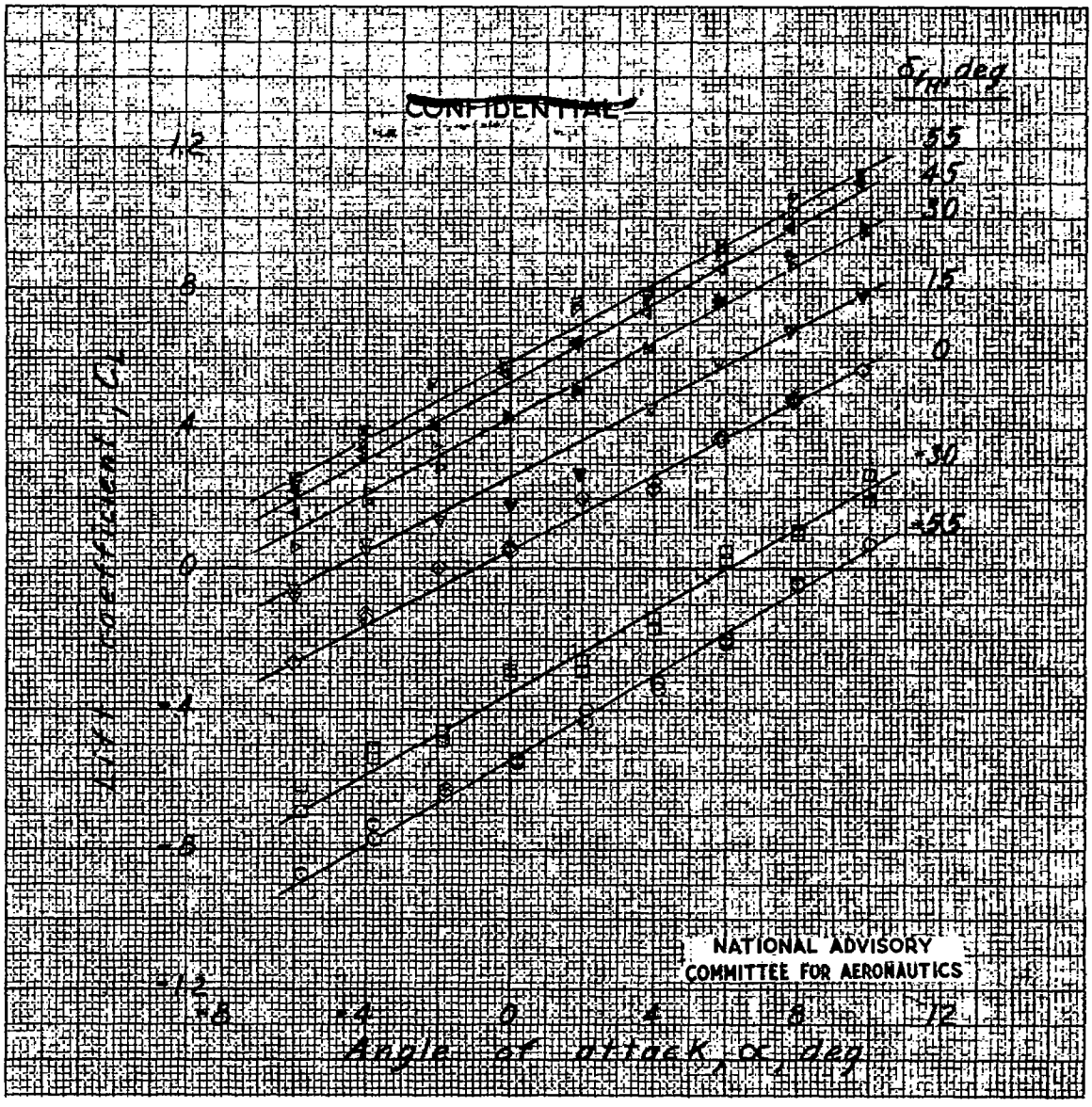


CONFIDENTIAL (a) Lift coefficients.

Figure 20.- Aerodynamic characteristics of the airplane with vertical wing and tail assembly removed. Moment center at pivot point.

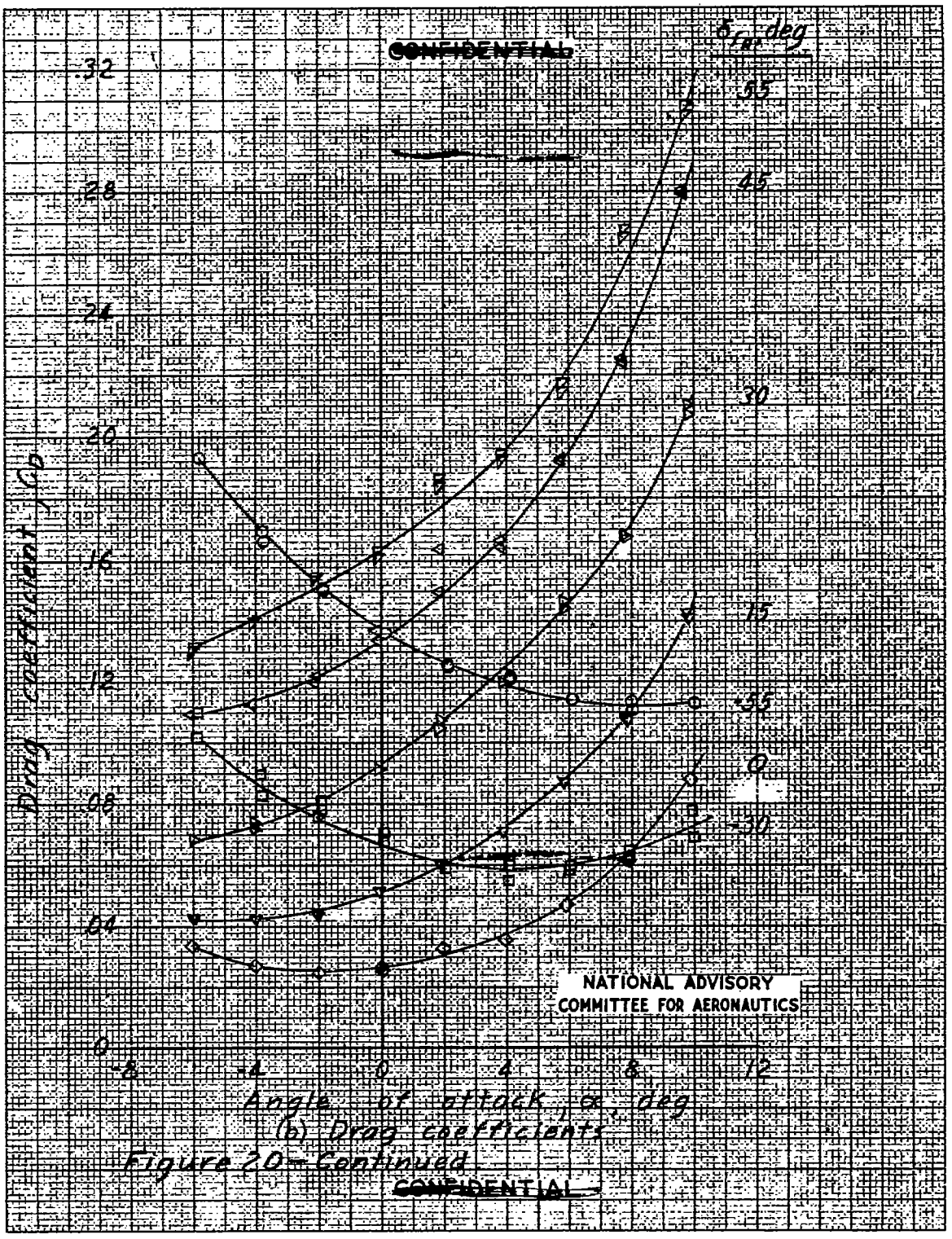


(b) Drag coefficients.

Figure 20- Continued.

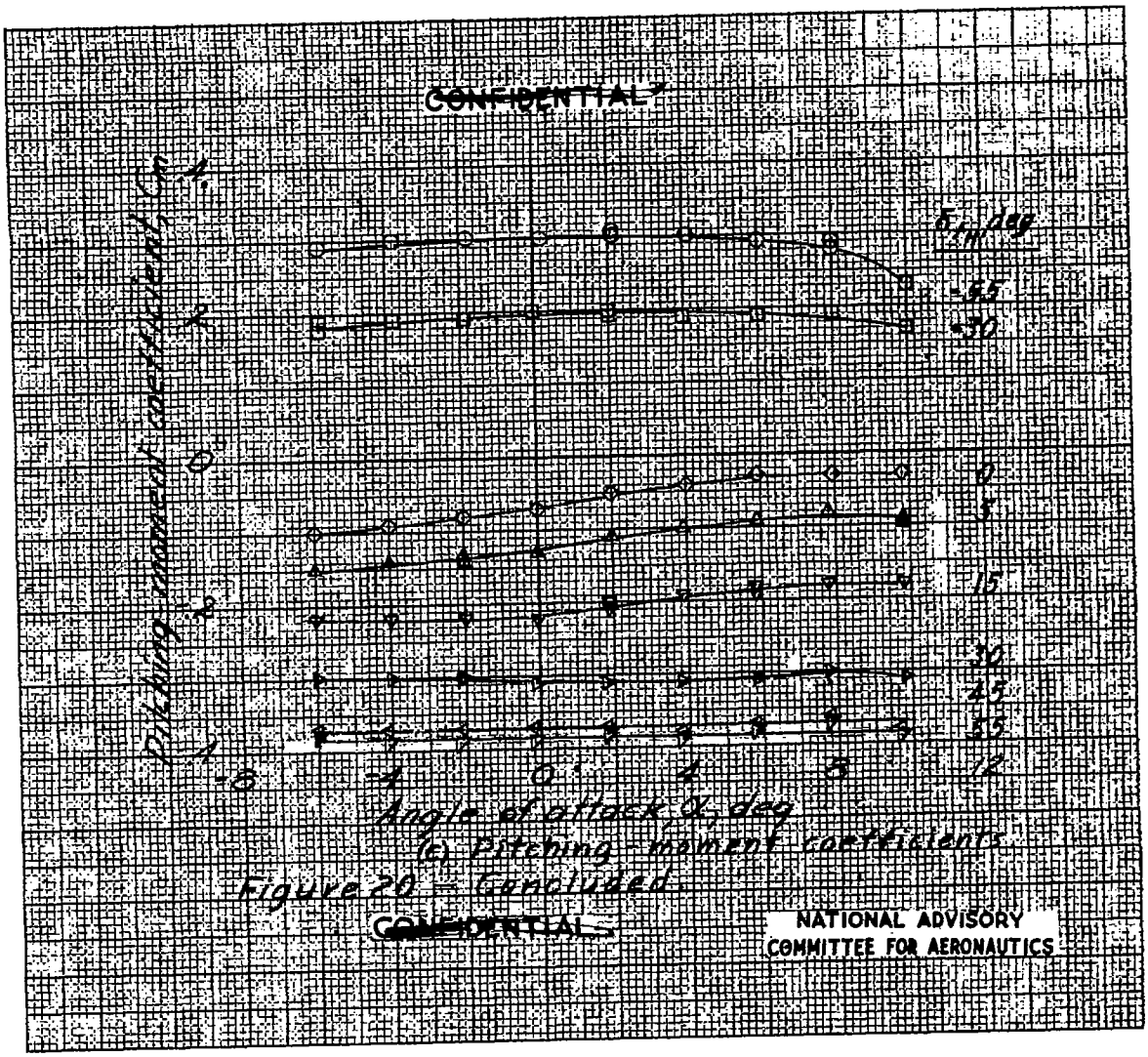


Figure 20 - Concluded

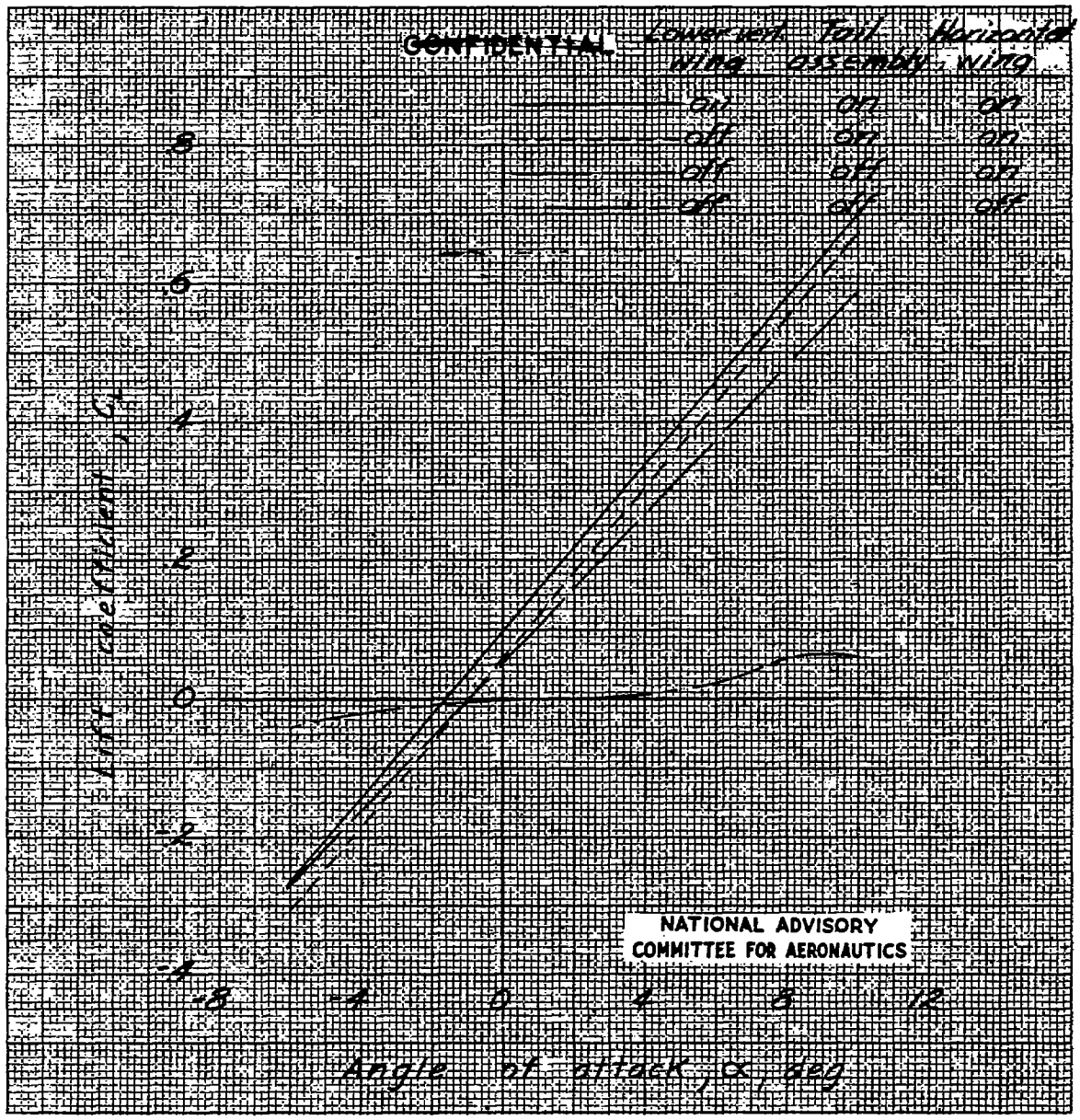


~~CONFIDENTIAL~~ (a) Lift coefficients.

Figure 21.- Contribution of components of the airplane to the aerodynamic characteristics; all control surfaces neutral; upper vertical wing removed. Moment center at 19.8 percent M.A.C. aft of wing leading edge.

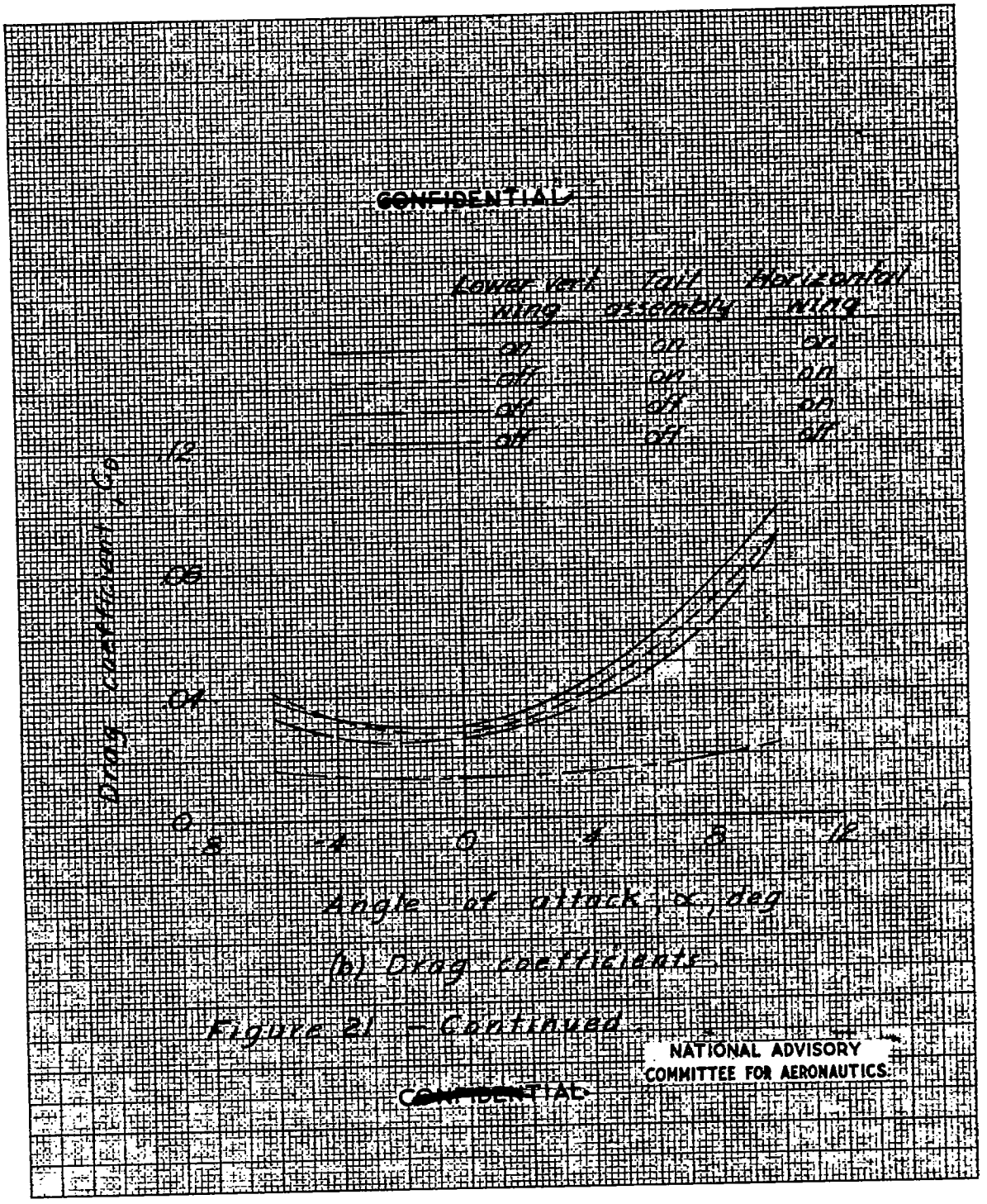


(b) Drag coefficients.

Figure 21 - Continued.

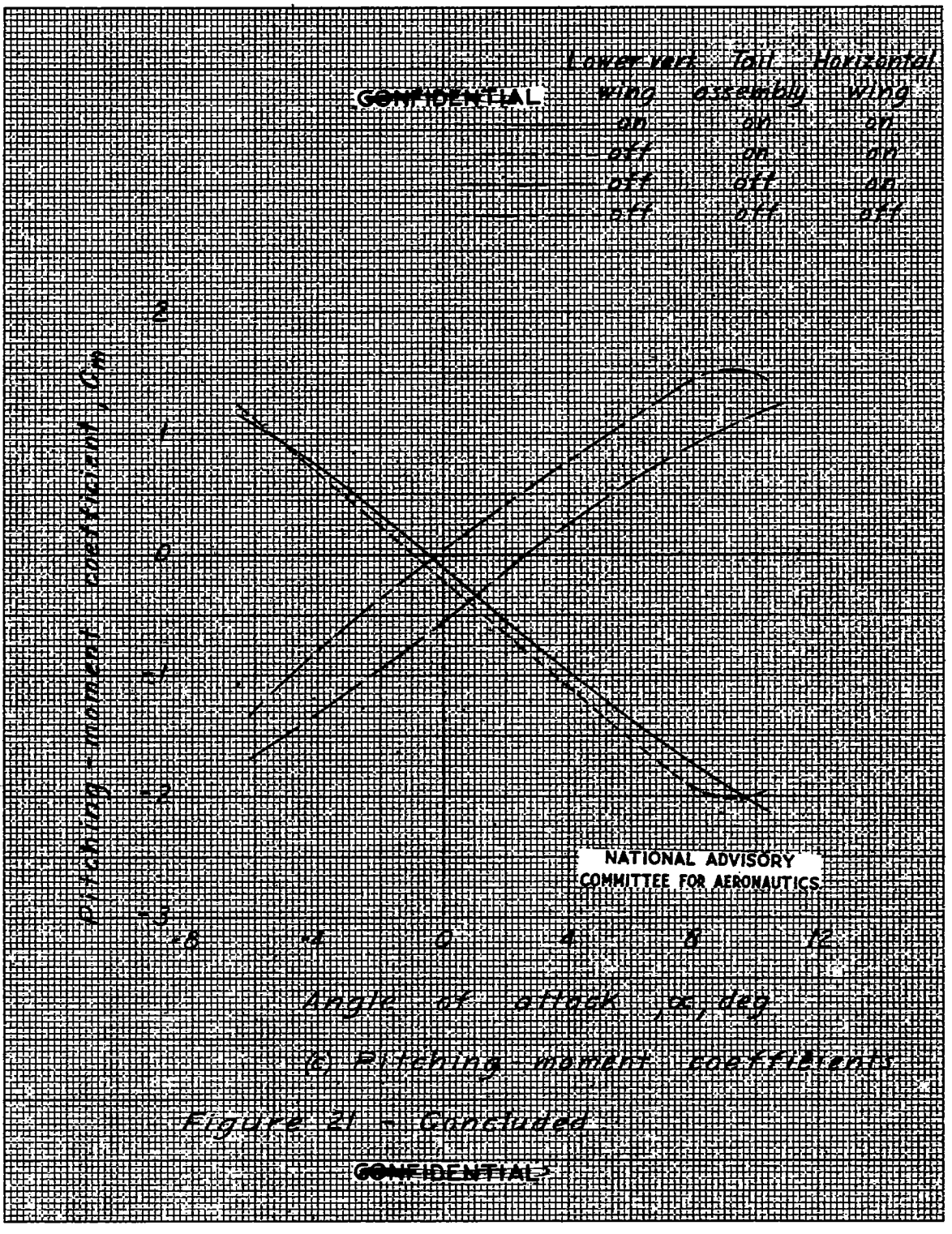


(c) Pitching-moment coefficients.

Figure 21.- Concluded.

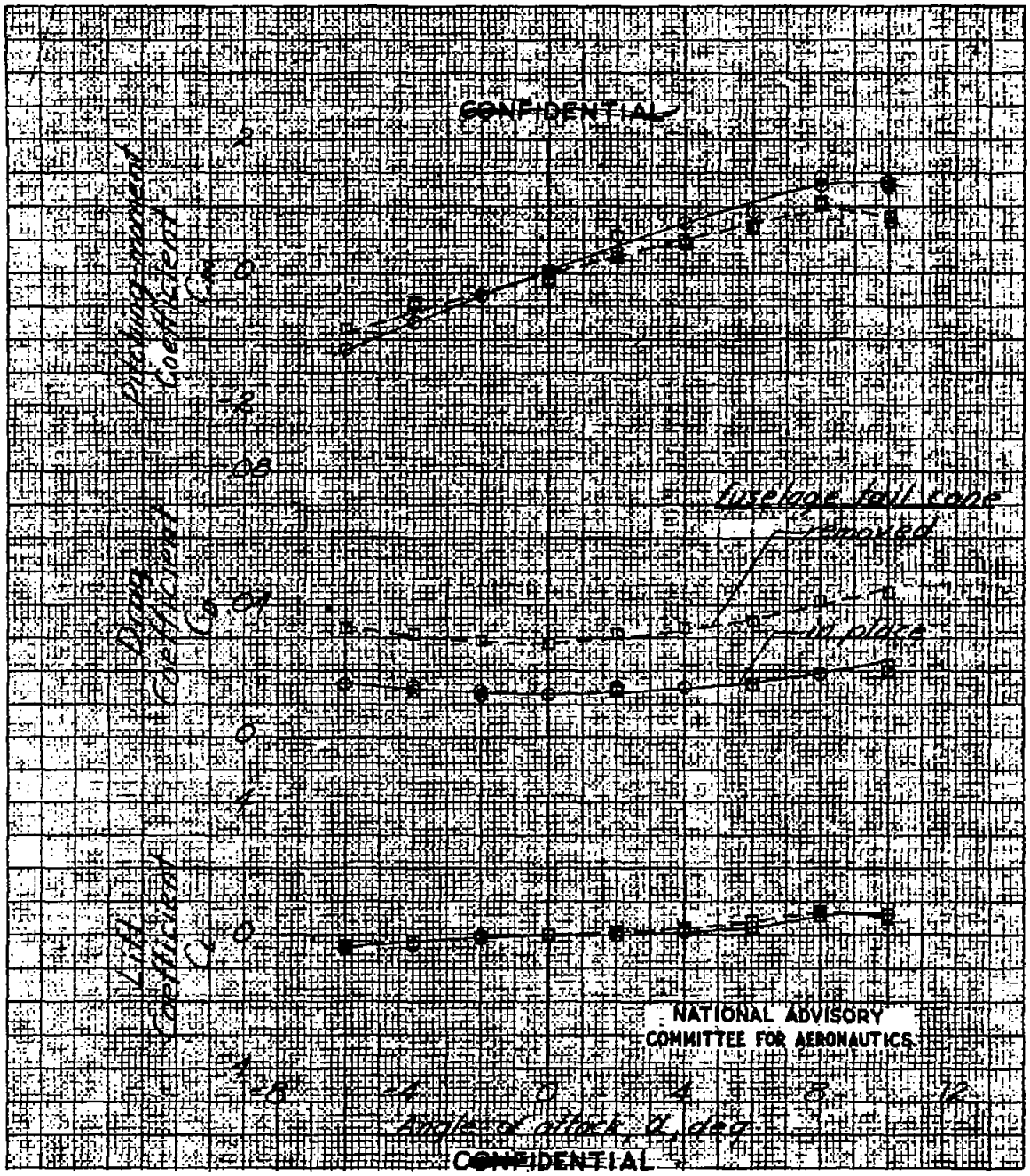


Figure 22.- Aerodynamic characteristics of the airplane, fuselage alone. Moment center at pivot point.

Fig. 23

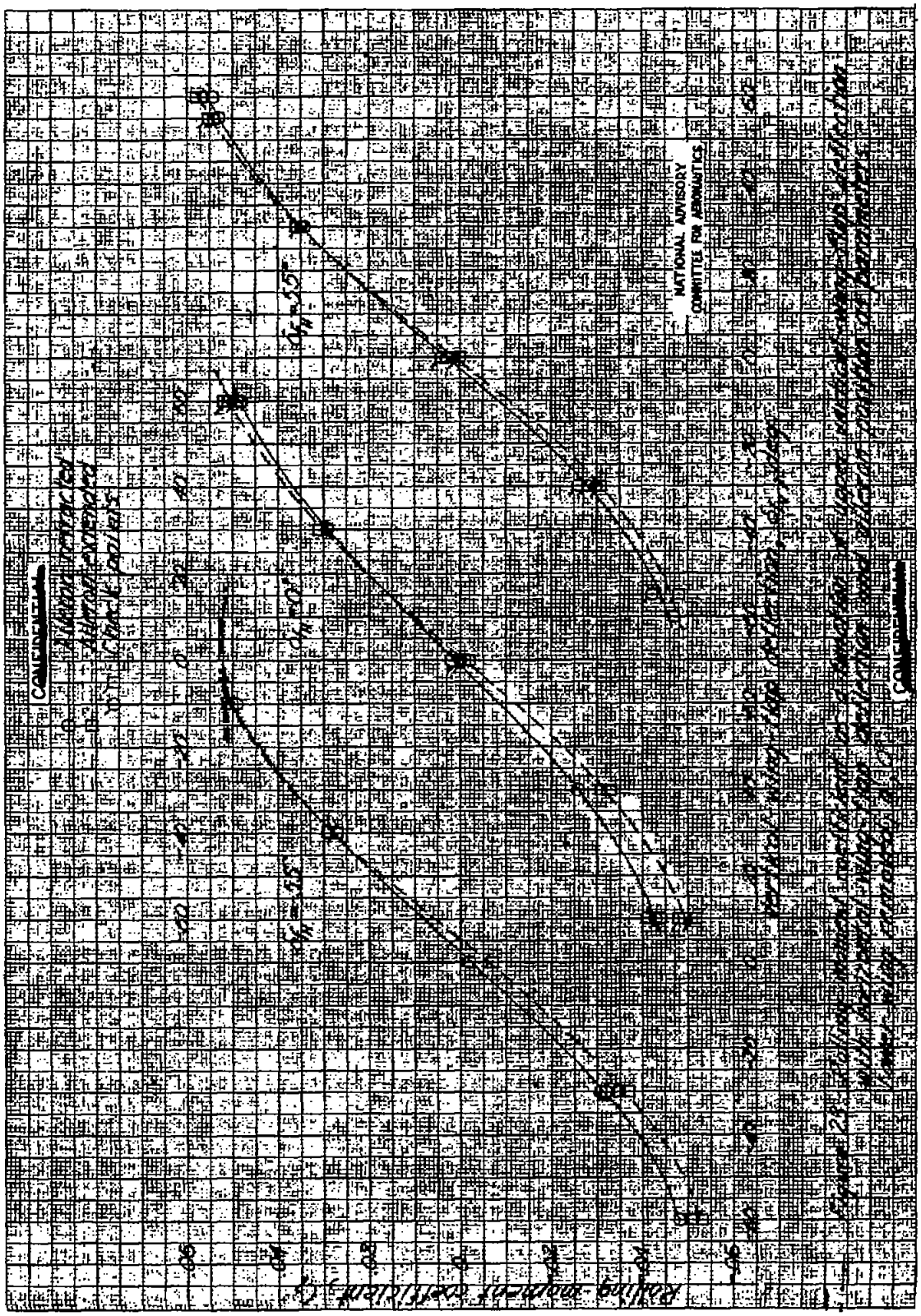
NATIONAL ADVISORY
COMMITTEE FOR AERONAUTICS
CONFIDENTIAL
CONFIDENTIAL

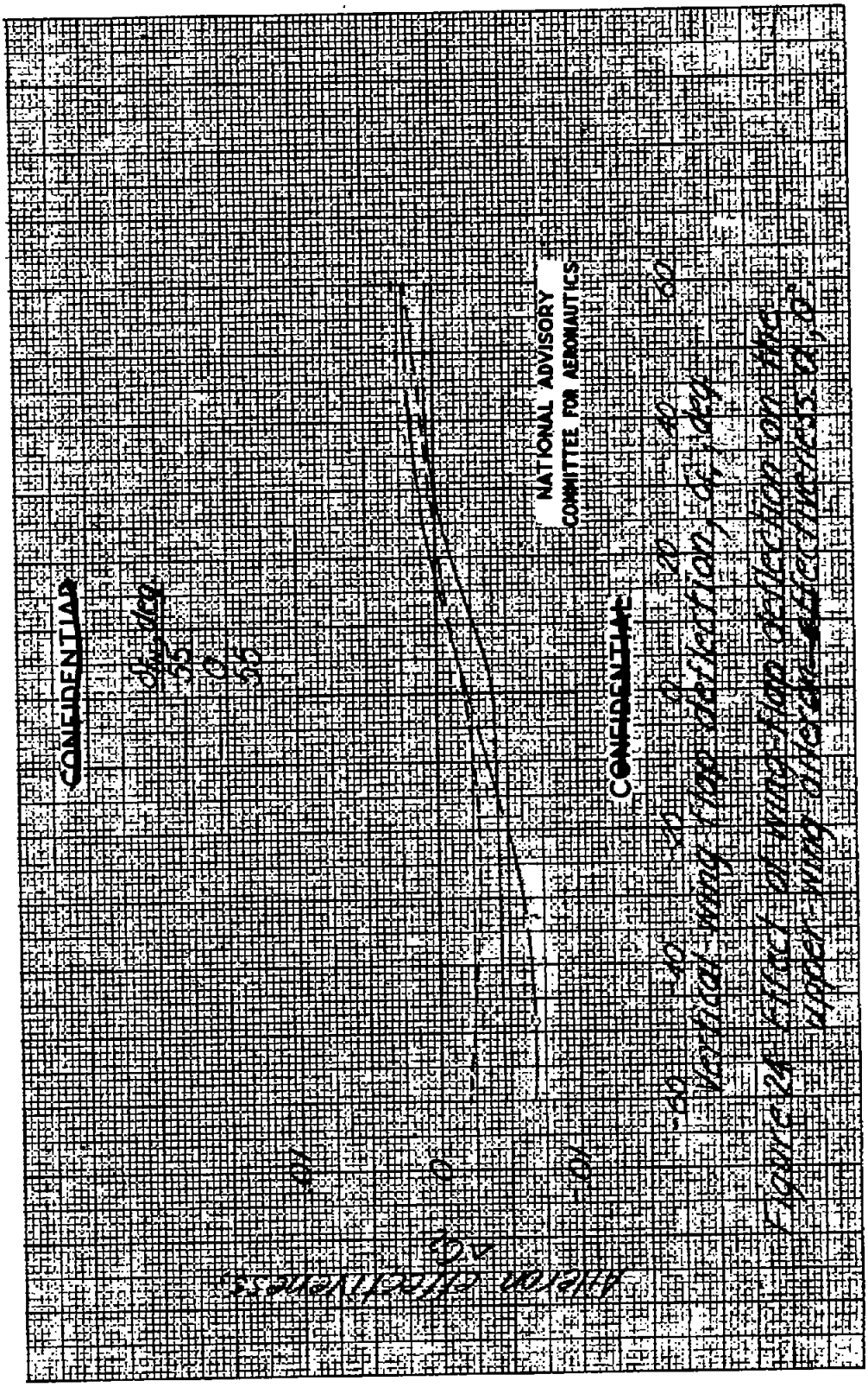
NATIONAL ADVISORY
COMMITTEE FOR AERONAUTICS
CONFIDENTIAL
CONFIDENTIAL

Fig. 25

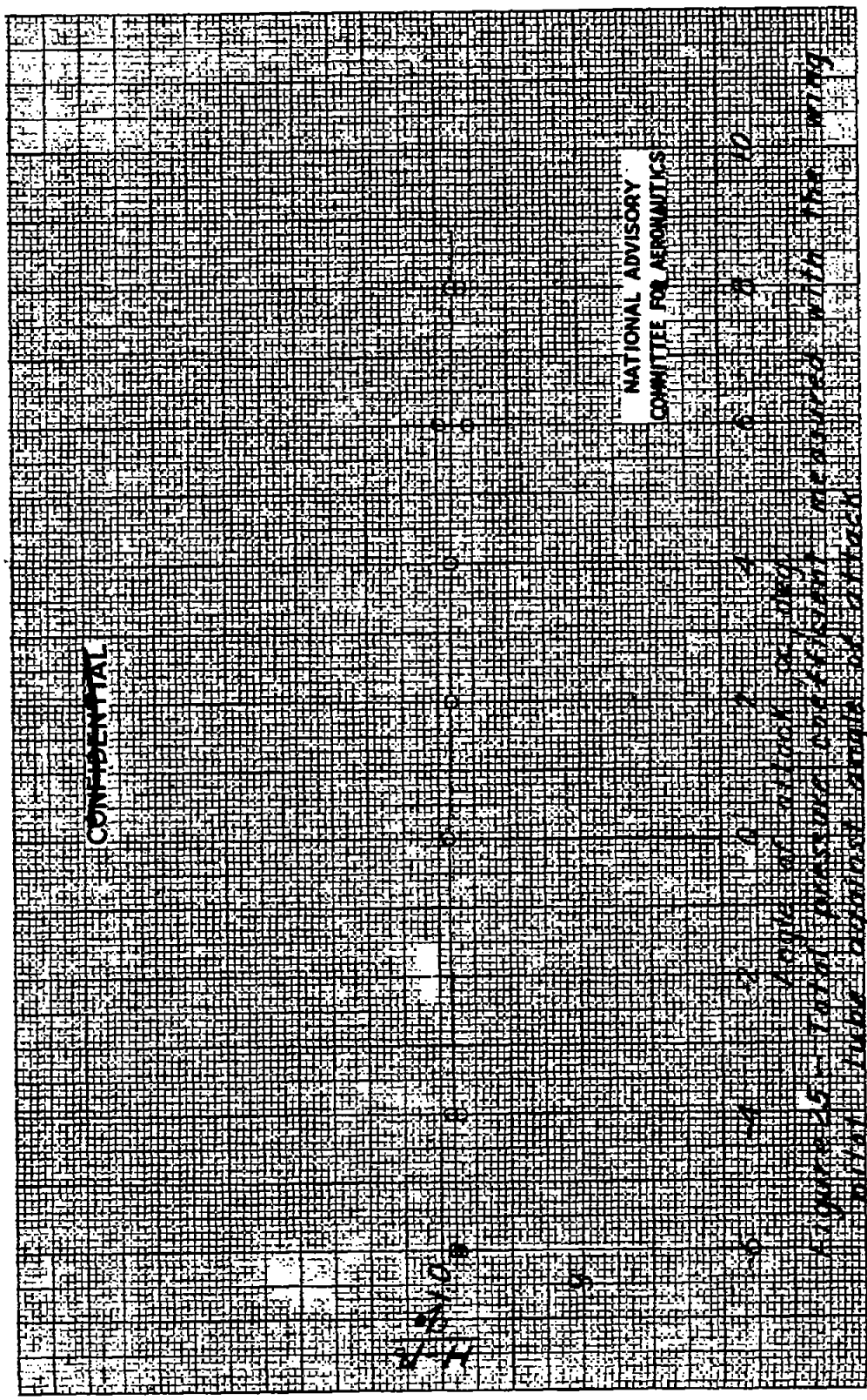
CONFIDENTIAL
NATIONAL ADVISORY
COMMITTEE FOR AERONAUTICS
CONFIDENTIAL

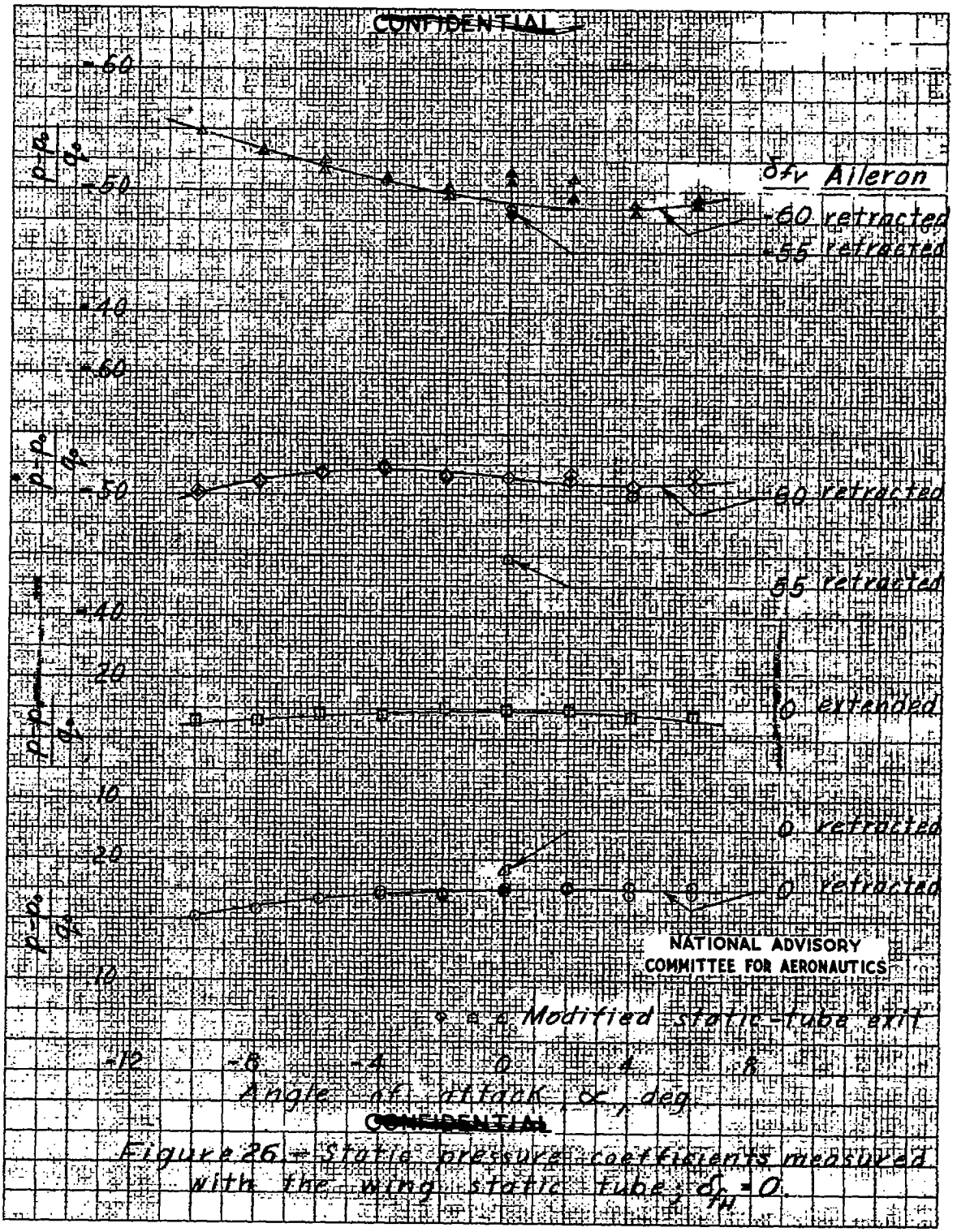


Figure 26.- Static pressure coefficients measured with the wing static tube; $\delta_{fu} = 0$.

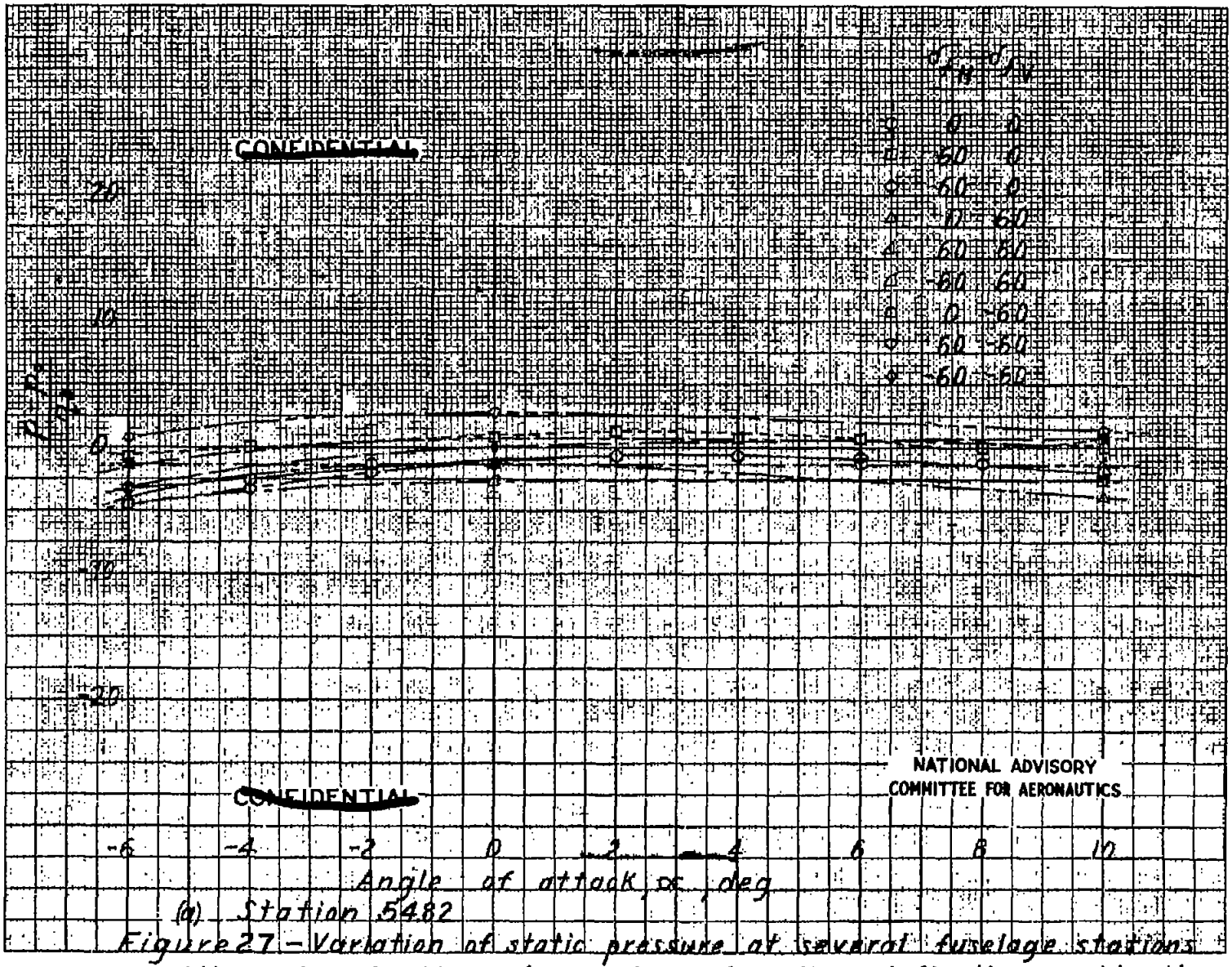


(a) Station 5482

Figure 27.- Variation of static pressure at several fuselage stations with angle of attack for various wing-flap-deflection combinations.

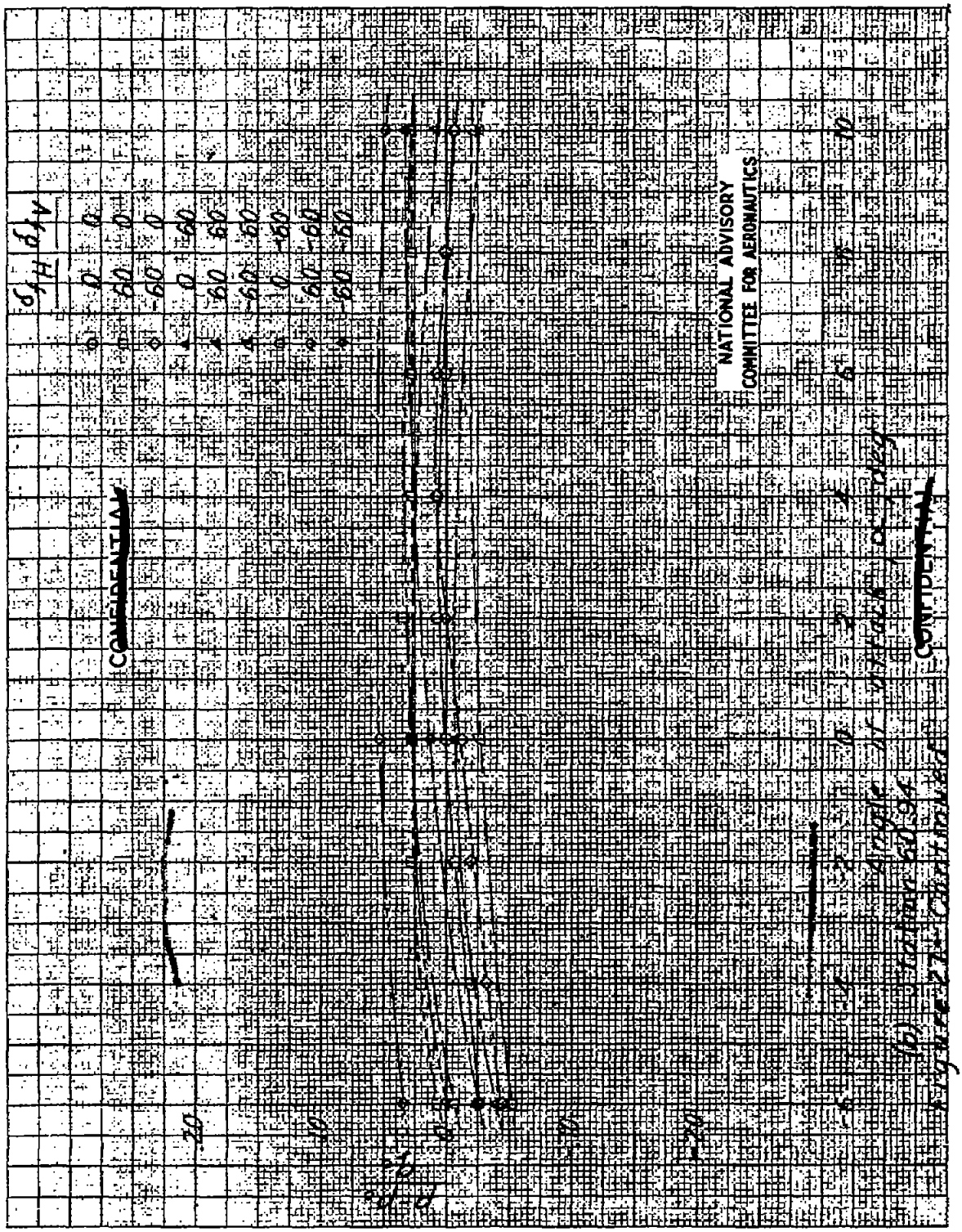
NATIONAL ADVISORY
COMMITTEE FOR AERONAUTICS
CONFIDENTIAL
CONFIDENTIAL

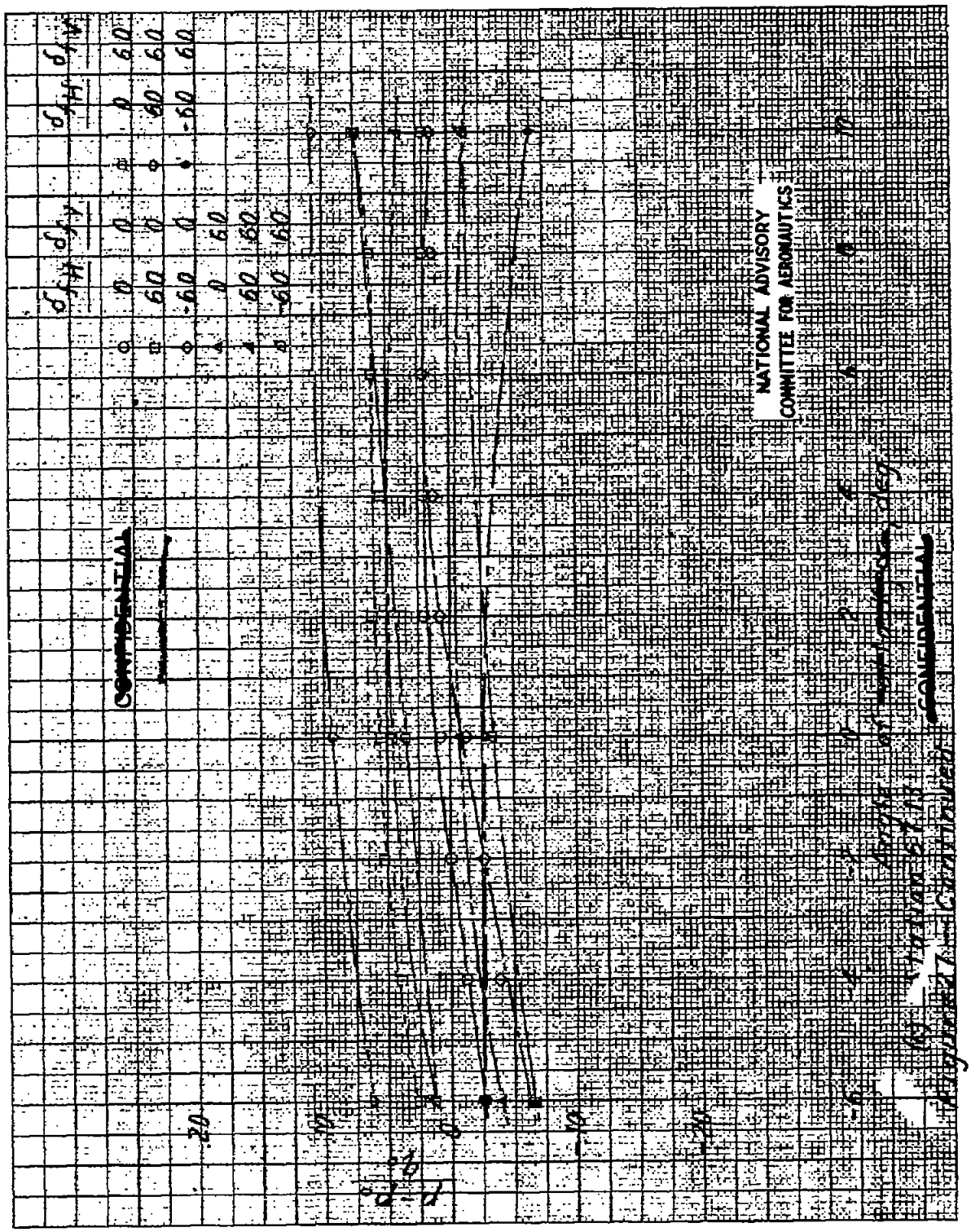
NATIONAL ADVISORY
COMMITTEE FOR AERONAUTICS
CONFIDENTIAL

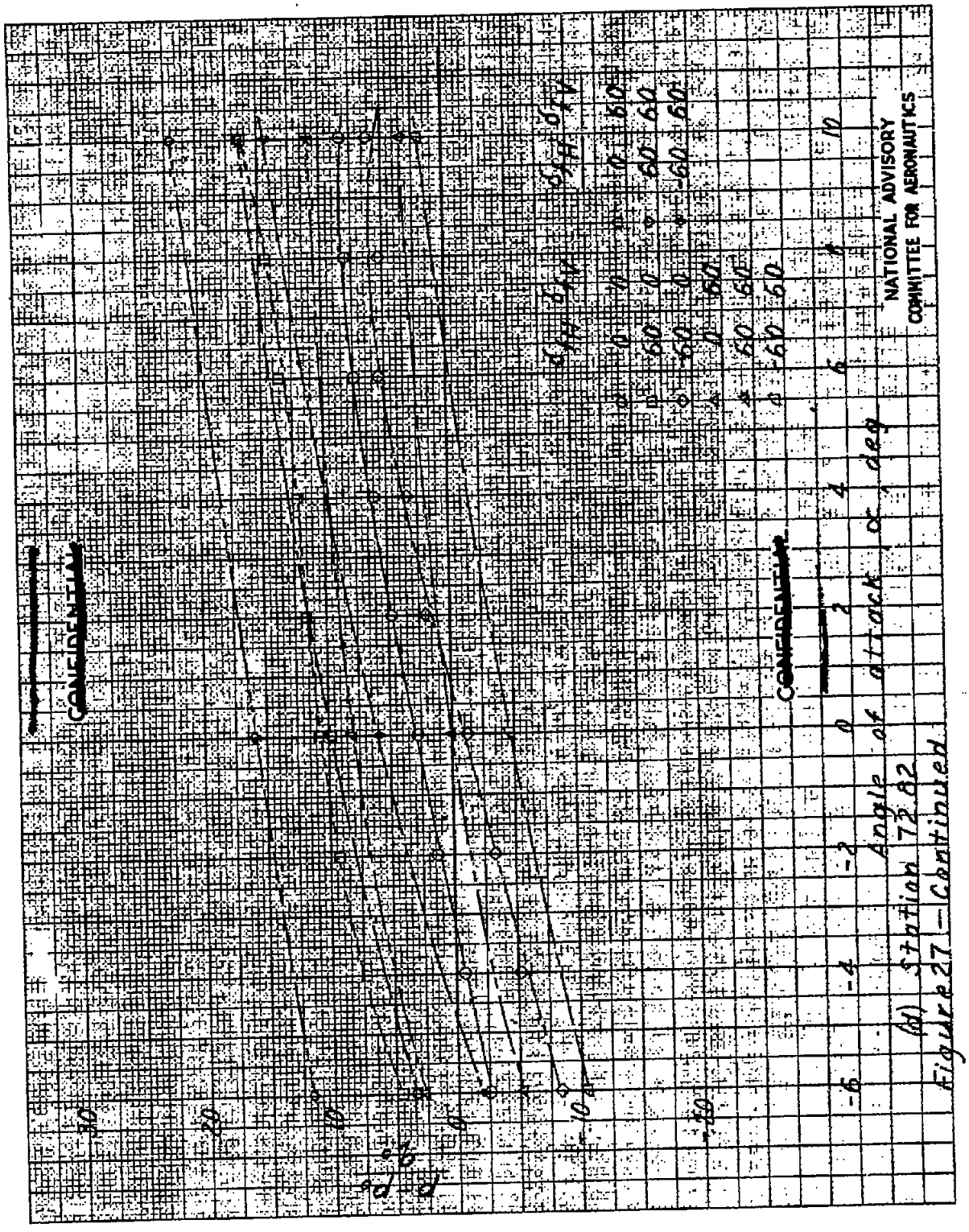
NATIONAL ADVISORY COMMITTEE FOR AERONAUTICS
CONFIGURATION
Angle of attack, α, deg
Station 72.82
(d) Figure 27.—Continued.

Fig. 27e

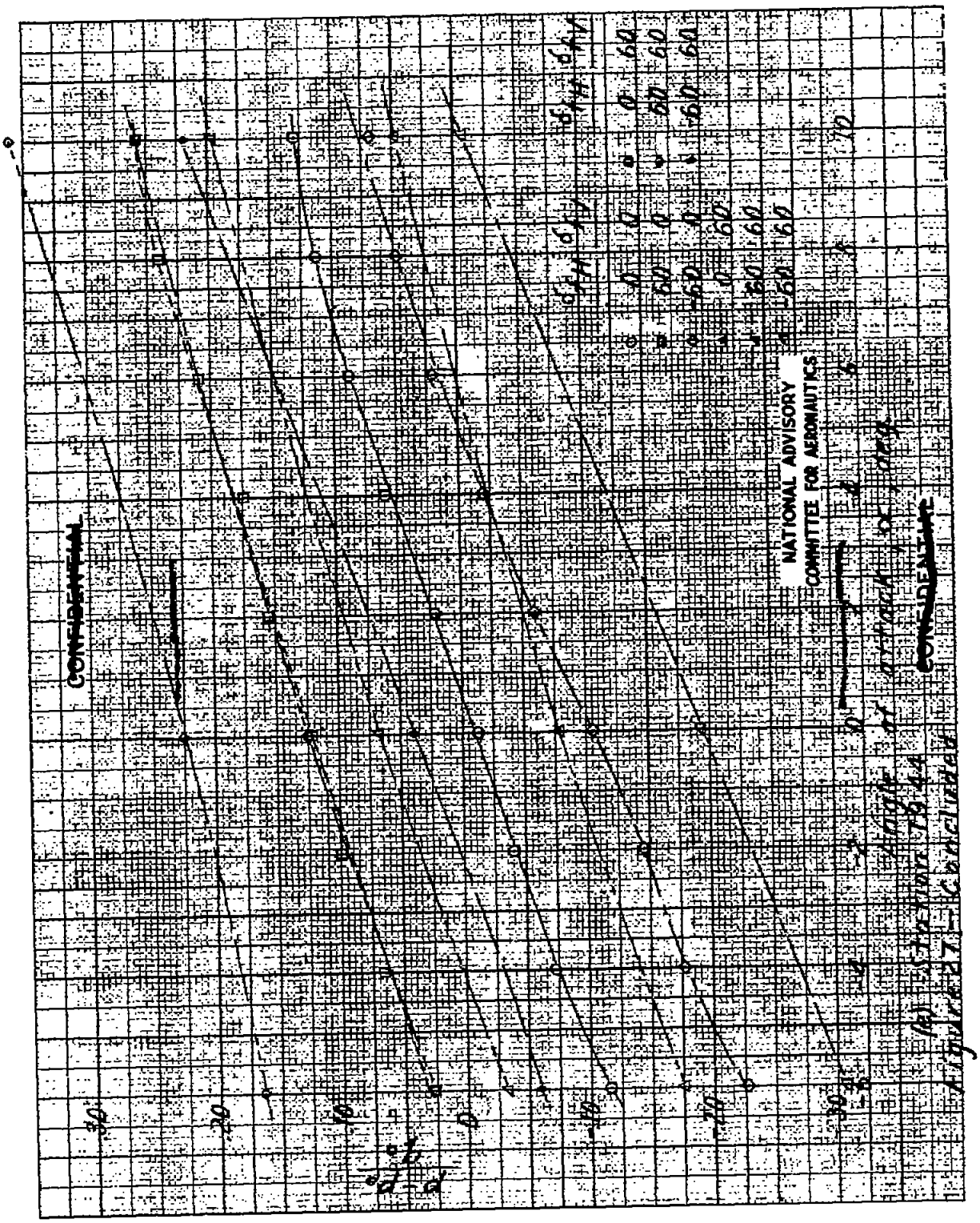
CONFIDENTIAL
NATIONAL ADVISORY
COMMITTEE FOR AERONAUTICS
CONFIDENTIAL

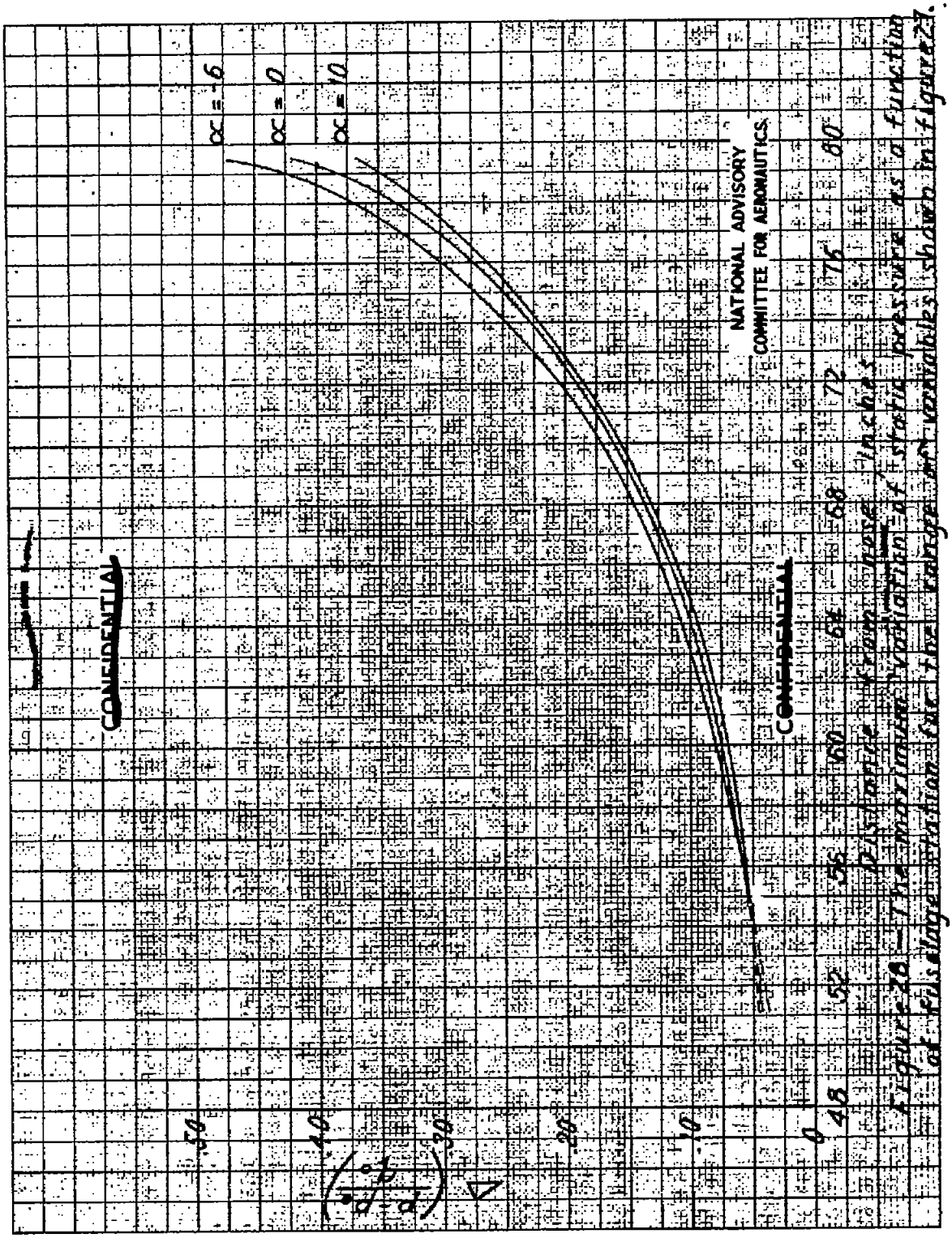
CONFIDENTIAL
NATIONAL ADVISORY
COMMITTEE FOR AERONAUTICS
CONFIDENTIAL
α = -6
α = 0
α = 10
-.20
-.10
0
.10
.20
.30
.40
0
48
52
56
60
64
68
72
76
80
Δ(p-p∞)/q
Pressure coefficient
Indicated Mach number
Figure 28.- The variation of pressure coefficient with indicated Mach number for various angles of attack at a station 0.25 inch behind the trailing edge of the wing on the fuselage with the nacelle shown in figure 27.

Figure 29.—Variation of static pressure at station 52.91 (a practical installation point) with angle of attack for various wing-flap deflection combinations.

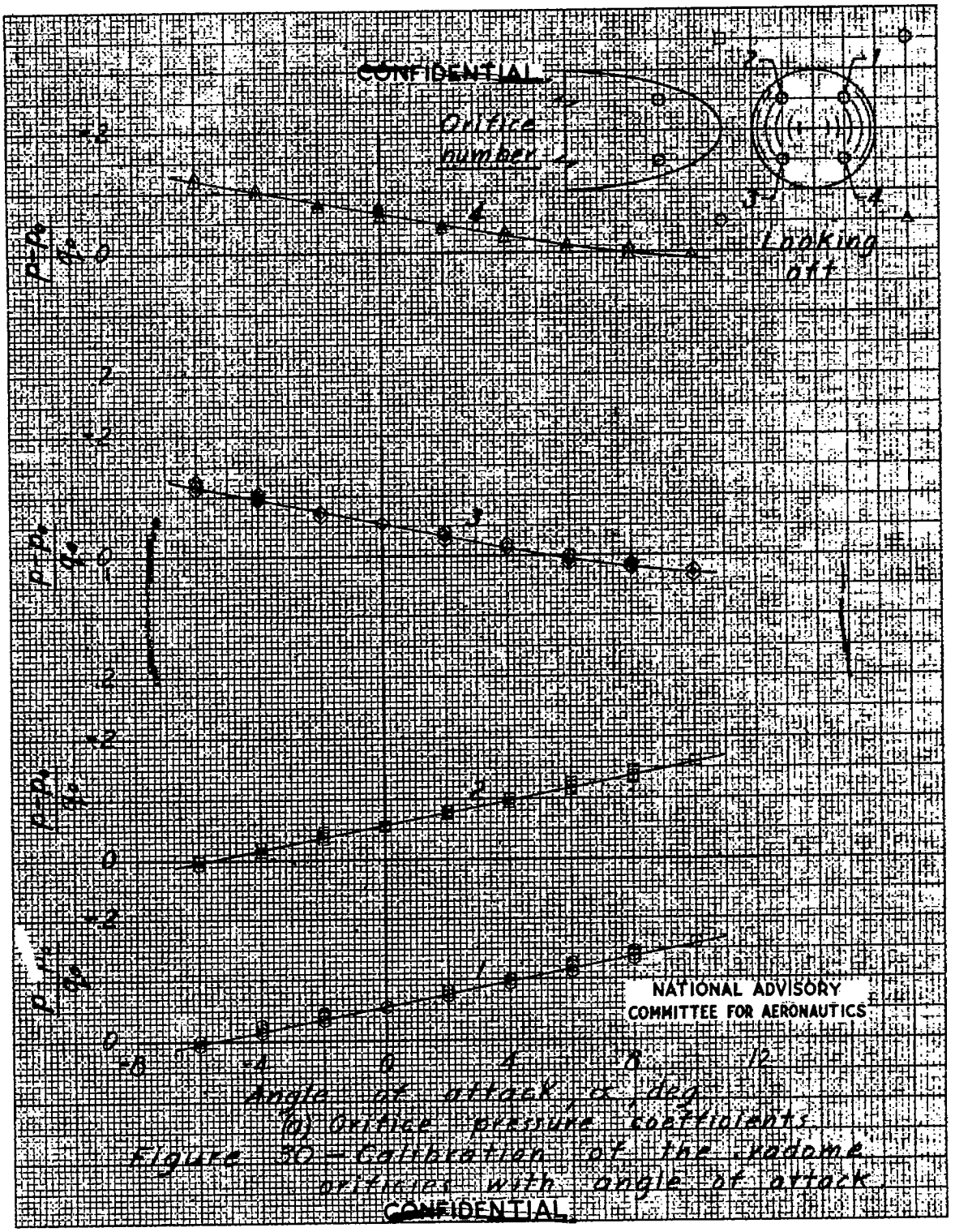


Figure 30 - Calibration of the radome orifices with angle of attack. (a) Orifice pressure coefficients.

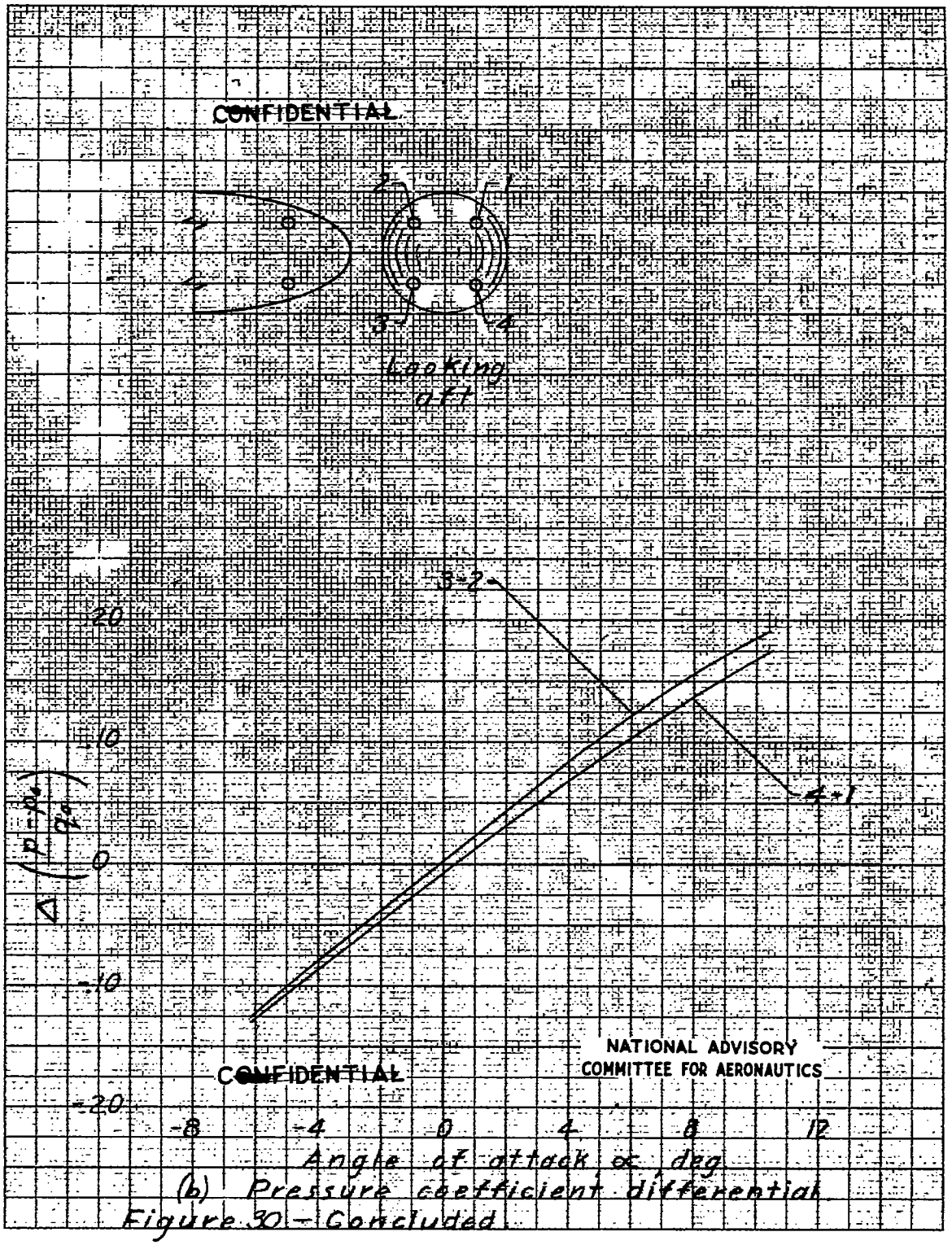


(b) Pressure coefficient differential

Figure 30 - Concluded